

## Oxidation of lignocellulosic platform molecules to value-added chemicals using heterogeneous catalytic technologies

Pedro L. Arias,<sup>a</sup> Juan A. Cecilia,<sup>b</sup> Iñaki Gandarias,<sup>a</sup> José Iglesias,<sup>c</sup> Manuel López-Granados,<sup>d</sup> Rafael Mariscal,<sup>d</sup> Gabriel Morales,<sup>c</sup> Ramón Moreno-Tost,<sup>b</sup> Pedro Maireles-Torres\*<sup>b</sup>

Received 00th January 20xx,  
Accepted 00th January 20xx

DOI: 10.1039/x0xx00000x

www.rsc.org/

Currently, much attention is being paid to the development of sustainable catalytic processes for the production of chemicals (biofuels, bioproducts, and so on) from lignocellulosic biomass. This minireview pursues to give an exhaustive overview about the heterogeneous catalytic technologies proposed for the oxidation of four key platform molecules (glucose, 5-hydroxymethylfurfural, furfural and levulinic acid) into important chemicals, such as gluconic acid and gluconates, glucaric and formic acids, 2-diformylfuran, 2,5-furandicarboxylic acid, maleic acid and anhydride, succinic acid, furanones, furoic acid, alkyl furoates, furan-2-acrolein, succinic acid, butanone and 3-hydroxypropanoic acid. The different mechanistic pathways will be highlighted, as well as the requirements in terms of catalytic sites and catalyst stability. The challenges and opportunities will be put forward for each type of oxidation process.

### Contents

#### 1. Introduction

#### 2. Oxidation of glucose

- 2.1. Production of gluconic acid and gluconates
- 2.2. Production of glucaric acid
- 2.3. Production of formic acid

#### 3. Oxidation of 5-hydroxymethylfurfural

- 3.1. Production of 2,5-diformylfuran
- 3.2. Production of 2,5-diformylfuran through integrated fructose dehydration and 5-hydroxymethylfurfural oxidation
- 3.3. Production of 2,5-furandicarboxylic acid
  - 3.3.1. Precious metal containing catalysts
  - 3.3.2. Base metal containing catalysts
  - 3.3.3. Alternative reactants to 5-hydroxymethylfurfural

#### 4. Oxidation of furfural

- 4.1. Production of C4 diacids and furanones
  - 4.1.1. Production of maleic anhydride in gas phase

using O<sub>2</sub> as oxidant

4.1.2. Production of maleic anhydride in liquid phase using O<sub>2</sub> as oxidant

4.1.3. Production of succinic acid and/or maleic acid in liquid phase using H<sub>2</sub>O<sub>2</sub> as oxidant

4.1.3.1. Production of succinic acid

4.1.3.2. Production of maleic acid

4.1.4. Production of furanones in liquid phase

4.2. Production of furoic acid and furoates

4.3. Production of furan-2-acrolein by oxidative-condensation of furfural

#### 5. Oxidation of levulinic acid

5.1. Production of succinic acid

5.2. Production of maleic anhydride

5.3. Production of butanone

5.4. Production of 3-hydroxypropanoic acid

#### 6. Conclusions and prospects

#### 7. List of abbreviations

#### Conflicts of interest

#### Acknowledgments

#### References

#### 1. Introduction

The depletion of fossil resources, and the serious environmental concerns associated with their use as sources of energy, chemicals and fuels, have driven the search and development of alternative renewable feedstocks. Among them, the use of biomass would help to reduce greenhouse gas emissions and mitigate climate change. However, special emphasis must be placed on avoiding competition for resources used for food, that is, non-edible biomass should be used. Lignocellulosic biomass appears as abundant, sustainable and cheap feedstock for the production of biofuels, energy and

<sup>a</sup> Chemical and Environmental Engineering Department, University of the Basque Country (UPV-EHU), Alameda Urquijo s/n, Bilbao, 48013, Spain.

<sup>b</sup> Universidad de Málaga, Departamento de Química Inorgánica, Cristalografía y Mineralogía (Unidad Asociada al ICP-CSIC, Facultad de Ciencias, Campus de Teatinos, 29071 Málaga (Spain).

<sup>c</sup> Chemical and Environmental Engineering Group, Universidad Rey Juan Carlos, Móstoles, Madrid, E28933, Spain.

<sup>d</sup> Institute of Catalysis and Petrochemistry (CSIC), C/Marie Curie, 2, Campus de Cantoblanco, Madrid, 28049, Spain

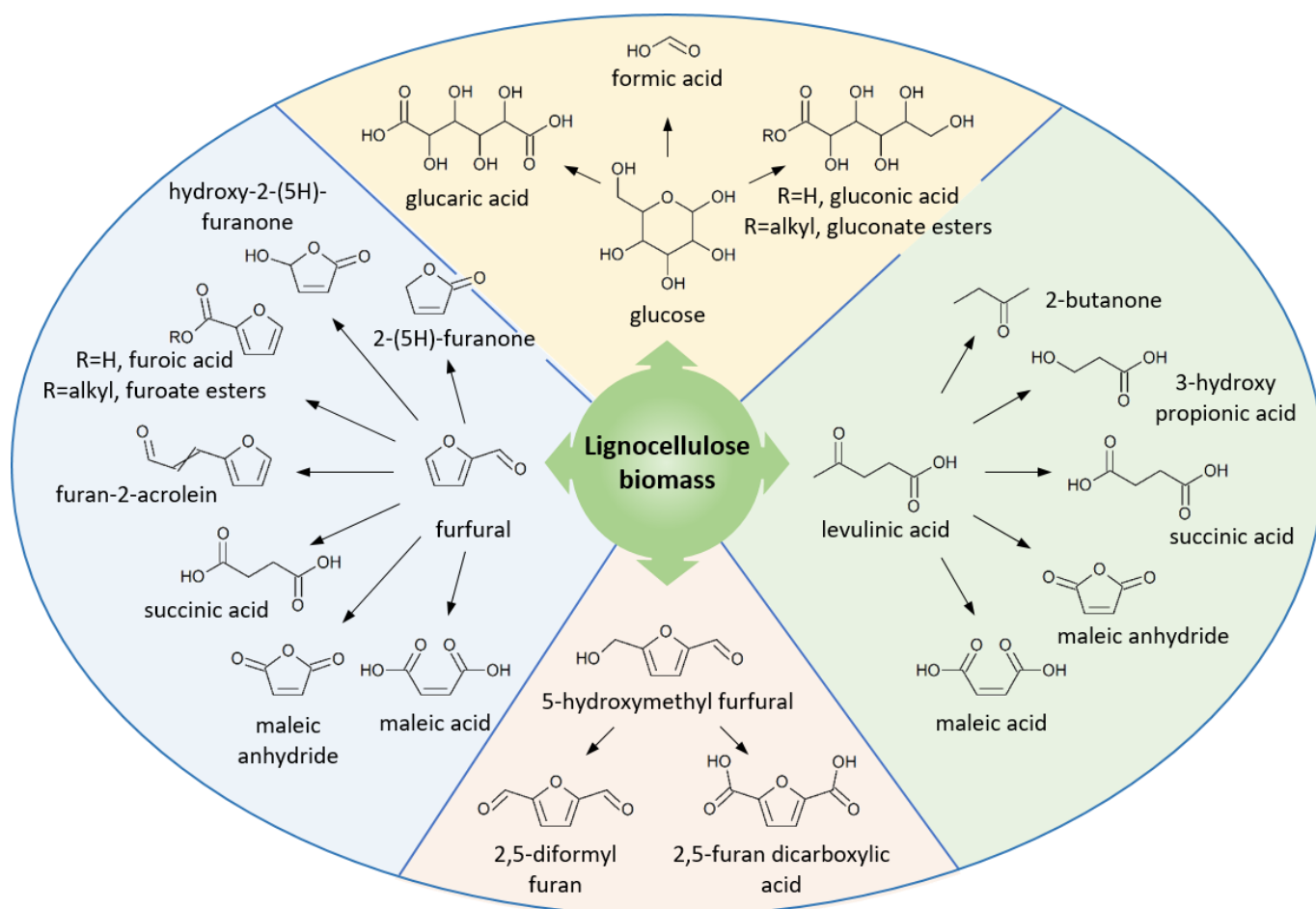
† Footnotes relating to the title and/or authors should appear here.

Electronic Supplementary Information (ESI) available: [details of any supplementary information available should be included here]. See DOI: 10.1039/x0xx00000x

renewable chemicals. The main constituents of lignocellulose are cellulose (40-50%), hemicellulose (25-35%) and lignin (15-20%), being the main components C5 and C6 sugars.<sup>1,2</sup>

The research aimed at the transformation of lignocellulose requires initial processing steps to make its different fractions accessible. In the case of cellulose and hemicellulose fractions, hydrolysis reactions generate C5 and C6 sugars, whose subsequent dehydration leads to platform molecules such as furfural (FUR) and 5-hydroxymethylfurfural (HMF). Levulinic acid is formed by the rehydration of HMF. These three platform chemicals can originate a large variety of chemicals through a wide spectrum of processes.<sup>3-6</sup> In the literature, several interesting reviews dealing with the catalytic conversion of biomass and derived chemicals by oxidation processes can be found,<sup>7-10</sup> including those summarizing the scientific works dealing with the oxidation of the lignin fraction.<sup>11,12</sup>

However, the present contribution has paid special attention to the transformation of the most important carbohydrate (glucose) and three relevant platform molecules (furfural, 5-hydroxymethylfurfural and levulinic acid) (Figure 1), mainly using heterogeneous catalytic technologies, covering the most recent scientific achievements focused on the oxidation of these important biomass-derived molecules into key chemicals. Besides showing the current research trends, the most relevant and singular features of this review are the discussion of the strengths and weaknesses of each catalytic process, and of the remaining challenges to be faced by the research community. Moreover, at the end of each section some alternative feedstocks, always obtained from lignocellulosic biomass, offering advantages in terms of higher yields from raw biomass and/or chemical stability will be presented.



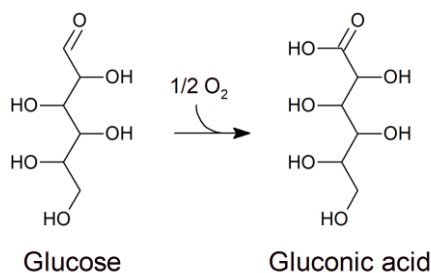
**Figure 1.** Simplified scheme of catalytic oxidation reactions addressed in this review

## 2. Oxidation of glucose

### 2.1. Production of gluconic acid and gluconates

The catalytic oxidation of glucose has attracted a great deal of attention in the last years because value-added chemicals, such as the gluconic and glucaric acids, can be obtained. In this sense, the worldwide annual production of gluconic acid reaches over more than 60000 tons,<sup>13</sup> with an average price of 1.5 to 8.5 \$/kg.<sup>14</sup> Gluconic acid and its derivatives find a wide range of applications as

food additive,<sup>15</sup> in the pharmaceutical industry,<sup>16</sup> cosmetics,<sup>17</sup> it is used as additive for cement,<sup>18</sup> and also in metallurgy.<sup>19</sup> Moreover, calcium and iron salts of gluconic acid are used as supplements,<sup>19,20</sup> to prevent calcium deficiency and anaemia, respectively.



**Figure 2.** Oxidation of glucose to gluconic acid

Currently, gluconic acid is industrially produced through fermentation of glucose by the *Aspergillus niger* fungus,<sup>20</sup> or *Gluconobacter suboxidans* bacteria.<sup>21</sup> Other methods for glucose oxidation have been evaluated, such as chemical oxidation using chlorine,<sup>22</sup> bromine,<sup>23</sup> nitric acid,<sup>24</sup> or electrochemical oxidation.<sup>25,26</sup>

Chemical routes produce wastewater, that must be treated and show a low selectivity towards gluconic acid, while electrochemical methods are hindered by the mass transfer on the electrode surface and by the cost of electricity. Noteworthy, raw materials other than glucose have been proposed for synthesizing gluconic acid, although mainly by biochemical methods, such as cellobiose,<sup>27,28,29</sup> cellulose,<sup>28,30,31</sup> and lignocellulosic materials.<sup>32,33,34</sup> Therefore, new routes are being investigated in order to use alternative environmentally friendly technologies based on heterogeneous catalysis for oxidizing glucose with oxygen or air under mild conditions (Figure 2).

The catalytic aerobic oxidation of glucose into gluconic acid has been extensively studied with catalysts based on noble metals, namely, Pt, Pd and Au (Table 1). Structural properties of catalysts and operational conditions have been evaluated for such catalysts.

**Table 1.** Summary of glucose oxidation to gluconic acid with different catalysts

Entry	Catalyst	Operating conditions					Catalytic properties		Ref
		[Glucose] (wt%)	Oxidant (O <sub>2</sub> )	pH	time (h)	Temp. (K)	X <sub>GLU</sub> (%)	Y <sub>Gluconic acid</sub> (%)	
1	Pt/C	0.90	0.02 MPa	9	6	323	75	67	35
2	Pd/C	27	0.05 L/min	n. r.	2	r.t.	100	98	17
3	Pt/HT	0.36	0.1 MPa	n. c.	12	323	99	83	36
4	Pt/C	11	0.01 L/min	9	7	333	85	66	37
5	Pd/C	11	0.01 L/min	9	7	333	95	91	37
6	Pd/C	0.18	0.0005 L/min	9	4	323	n. r.	50	38
7	PdBi/C	30	1.5 L/min (air)	9	2.5	313	100	100	39
8	PdBi/SiO <sub>2</sub>	18	1 L/min	9	2	333	100	80	40,41
9	PdBi/C	0.18	0.4 L/min	9	4	323	100	100	42,43
10	Au/C	3.2	0.02 L/min	n. c.	18	493	80	80	44
11	Au <sub>n</sub> (PET) <sub>m</sub>	5.4	0.04 L/min	9.5	0.6	333	100	100	45,46
12	Au/CMK-3	1.8	0.3 MPa	n. c.	2	383	92	81	47
13	Au/TiO <sub>2</sub>	1.8	0.5 L/min	9	2	313	100	98	48
14	Au/TiO <sub>2</sub>	0.36	0.3 MPa	n. c.	1	433	88	78	49
15	Au/CeO <sub>2</sub>	1.8	0.1 L/min	9	1	333	90	90	50
16	Au/Al <sub>2</sub> O <sub>3</sub>	3.6	0.02 L/min	n. c.	18	393	75	71	51
17	Au-Pd/MgO	9.0	0.1 MPa (air)	n. c.	24	323	62	62	52

n. c.: without pH control; n. r.: not reported; X: mol% conversion and Y: mol% yield in all Tables, unless indicated.

Thus, a strict pH control is required to maintain a high glucose conversion, which can be achieved by the addition of a sacrificial strong base, but keeping in mind that a strong alkaline solution (pH > 11) can promote side reactions such as retro-Claisen, Cannizzaro, condensation or isomerization.<sup>53</sup> In this context, Pt/C catalysts (Table 1, entry 1) were poisoned at pH < 7 by strong adsorption of reaction products on the catalyst surface.<sup>35</sup>

To avoid strong basic medium, Pt was supported on a basic hydrotalcite (Table 1, entry 3), attaining a similar glucose conversion and gluconic acid yield as Pt/Al<sub>2</sub>O<sub>3</sub> in the presence of Na<sub>2</sub>CO<sub>3</sub>.<sup>36</sup> The pH in the presence of Pt/HT catalyst was close to 9, which is reported as the optimum pH to carry out the reaction. Nikov *et al.* stated that the main factors governing the Pd(0.5%)/Al<sub>2</sub>O<sub>3</sub> catalyst deactivation were the concentration of O<sub>2</sub> in the liquid phase, being responsible for the formation of Pd-O species which deactivated the catalyst and the adsorption of reaction products.<sup>54</sup> Delidovich *et al.* (Table 1, entries 4 and 5) showed that the activity and selectivity depended on the noble metal, being Pt catalysts less active and selective to gluconic acid than Pd ones, with fructose as the main by-product of the reaction.<sup>37</sup> Moreover, they observed that the activity of both pre-reduced and non-reduced Pt catalysts was identical, whereas the activity of Pd catalysts increased in two-folds when the catalyst was pre-reduced. The authors stated that this different behavior was due to the capability of glucose to reduce the Pt<sup>2+</sup> ions, but not the Pd<sup>2+</sup> species. More interestingly, the authors showed that the TOF was irrespective of the Pt particle sizes, contrary to that observed regarding the catalytic activity of Pd catalysts, where the results evidence the possibility to tune the activity of catalysts by controlling the size of Pd particles. Those particles smaller than 3 nm were deactivated faster than particles larger than 6 nm. Indeed, Haynes *et al.* (Table 1, entry 6) found that the gluconic acid yield was strongly influenced by the Pd particle size, reaching the best results with an average particle size of 7 nm. Larger particles displayed much lower catalytic activity.<sup>38</sup> The explanation was the existence of a compromise between accessibility for sugar and oxygen coverage. In spite of the control of particle size, the catalysts showed a loss of activity with the course of reaction due to the formation of oxygen layers on Pd particles. The catalyst deactivation was not attributable to reaction product adsorption or Pd leaching.

In order to improve the activity, selectivity and stability of Pt and Pd catalysts, new catalytic formulations were developed by using heavy metals, like Bi, as promoters.<sup>39–43,55,56</sup> Besson synthesized BiPd catalysts (Table 1, entry 7), which were very active and could be reused 5 cycles without loss of activity, or changes in the selectivity pattern.<sup>39</sup> In addition, the Bi did not leach to the reaction medium and the active phase was formed by a bimetallic BiPd phase. More important, the Bi could stabilize Pd particles as small as 1 nm, avoiding the overoxidation of Pd since oxygen was adsorbed on Bi atoms instead of Pd ones. The formation of intermetallic BiPd compounds was also observed by Karski *et al.*<sup>40,41</sup> and Wenkin *et al.*<sup>42,43,55,56</sup> Thus, Pd supported on carbon catalysts

were promoted by Bi and the influence of the intermetallic BiPd phase as well as of the Bi leached on the catalytic activity were studied (Table 1, entry 9).<sup>43</sup> Bi<sub>2</sub>Pd was determined as the most active phase, whereas BiPd<sub>3</sub> resulted inactive. Furthermore, Bi was found to systematically dissolve in the reaction medium during the catalytic tests, due to both glucose and gluconate. Moreover, in further experiments, the authors proved that the leached Bi was also involved in the catalytic activity.<sup>55</sup> When recycling experiments were conducted, significant Bi losses were observed after the first and second runs, and then the leaching of Bi remained constant and lower than 2.5%. The recycling tests showed that gluconic acid yields remained constant (~40%), after normalization with respect to the mass of catalyst during 13 consecutive tests.

Au-based catalysts have been extensively studied since Haruta *et al.* demonstrated the surprising CO oxidation activity of gold catalysts at low temperature.<sup>57</sup> Moreover, from an environmental point of view, the gold catalysts exhibit the ability to oxidize glucose in the absence (or without pH control) of a base, yielding gluconic acid instead of gluconate.

Rossi *et al.* have extensively studied gold-based catalysts prepared by the immobilization of colloidal gold NPs on carbon.<sup>53,58,59</sup> They were very selective when operating under mild conditions (pH = 7 – 9.5, T = 323–373 K, PO<sub>2</sub> = 1–3 bar), comparable to commercial Pd or Pt catalysts, but with a higher selectivity.<sup>53</sup> Total glucose conversion was achieved at any assayed pH, although TOF was considerably decreased at pH 7. These catalysts were also very active without pH control, but, under those reaction conditions, the rate of glucose consumption rate was lower than that achieved under controlled pH, being necessary to increase the temperature up to 373 K and longer reaction times to attain complete glucose conversion. This high selectivity was explained by the great difference in the oxidation rate of the hydroxyl and aldehyde groups, the chemoselective ability of Au to selectively oxidize primary alcohols over secondary alcohols, and the operating pH under which the isomerization of glucose is avoided. Although Au-based catalysts were less sensitive to deactivation by adsorption of products, Au leaching was observed during reutilization tests, losing the 70% of Au after six runs and limiting its use from a practical viewpoint.

The influence of the metal-support interaction on the catalytic performance was evaluated with colloidal unprotected Au NPs of different sizes.<sup>58</sup> The catalytic activity increased for smaller particle diameter in the range of 2.5 to 4.5 nm, but particles larger than 10 nm were inactive, although the catalytic activity per Au atom was independent of the size. Similarly, Au NPs with size of 2 nm deposited onto cellulose showed a superior catalytic activity than particles of 7.7–14.5 nm.<sup>60</sup> However, the metal-support interaction did not affect to the gold intrinsic catalytic activity, as inferred from the similar activity of unsupported and supported gold NPs (3.6 nm) on carbon. Moreover, this work demonstrated that if the activity of Au catalysts was calculated based on theoretical surface Au atoms, the rate of reaction would be of the same order of magnitude as the enzymatic reaction.

Traditional methods for preparing supported Au catalysts, such as deposition-precipitation or impregnation, failed when the support has a low zero charge point (silica, carbon and organic polymer), and deposition-reduction (DR) and by solid grinding (SG) procedures appear as alternative. Thus, Haruta *et al.* have used the latter methods to deposit Au NPs onto cellulose,<sup>60</sup> inorganic oxides,<sup>61</sup> carbon,<sup>45,62,46</sup> and ion exchange resins,<sup>63</sup> from volatile organogold complexes. In particular, the SG technique was very effective to deposit Au NPs, with a mean diameter as small as 1.9 nm, on carbon.<sup>62</sup> Au NPs smaller than 10 nm exhibited appreciably high catalytic activity, regardless of the methods of Au deposition and the carbon support. Nevertheless, the TOF values obtained with Au NPs smaller than 3 nm were about one-third of those of Au NPs supported on metal oxides at 333 K and pH 9.5, thus demonstrating the influence of the support nature.<sup>61</sup>

Supporting Au NPs on metal oxides improved the long-term stability of catalysts. Haruta *et al.*, following the DR method, stabilized Au NPs on ZrO<sub>2</sub>, TiO<sub>2</sub>, CeO<sub>2</sub> and Al<sub>2</sub>O<sub>3</sub>.<sup>61</sup> They observed that the catalytic activity was influenced more significantly by the Au NPs size than by the nature of the support, at pH 9 and 323 K. The supported Au/MeO<sub>x</sub> catalysts showed an increase in TOF with a decrease in the size of Au particles.

Colloidal methods have been employed for the preparation of Au catalysts supported on CeO<sub>2</sub>, a very suitable support due to its ability to both favor the formation of small gold NPs (3.5 nm) and accumulate oxygen (Table 1, entry 15).<sup>50</sup> This would indicate that the NPs size not only depends on the synthetic procedure but also on the support type. This is one of the most active catalysts, and is completely recyclable after a simple washing with water. However, by immobilization of pre-formed colloidal Au NPs (4-20 nm) on carbon, a clear influence of the size on the catalytic performance was not observed (Table 1, entry 10).<sup>44</sup> Otherwise, when TOF was evaluated considering the Au dispersion and the actual Au loading, catalysts with NP sizes in the range 15-20 nm showed superior TOF values than samples with sizes lower than 10 nm, which is in contradiction with the previous reported data. The authors attributed this behavior to a different reaction mechanism from that operating under alkaline conditions.

The immobilization of Au<sub>x</sub>(PET)<sub>y</sub> clusters (PET= phenylethanethiolate, @SCH<sub>2</sub>CH<sub>2</sub>Ph) on activated carbon, annealed at 393 K in air, has been performed by Liu,<sup>45</sup> and Zang (Table 1, entry 11).<sup>46</sup> "Au(PET)" centers adsorb glucose by means of a strong interaction of its aldehyde group with S-Au-S motifs, allowing to be oxidized by reactive oxygen species (e.g. peroxides). Furthermore, the recyclability was excellent owing to its thermal robustness, without any appreciable loss of activity after 7 cycles, or aggregation to larger clusters. PVA (polyvinylalcohol) has also been incorporated on the surface of Au NPs supported on TiO<sub>2</sub> (Table 1, entry 14).<sup>49</sup> Both the metal NP size and the amount of PVA stabilizing surfactant used in the synthesis were key parameters influencing the catalytic activity. The most active catalyst did not have the smallest particle size (7.6 nm vs 2.1 nm), and was prepared by using the lowest PVA to metal ratio (0.1).

Au NPs have also been confined inside the channels of ordered mesoporous carbons (CMK-3) and tested under base-free conditions (Table 1, entry 12).<sup>47</sup> This catalyst can be reused for four runs, but conversion dropped to 70% due to catalyst deactivation the strong adsorption of carboxylic acids on the catalyst surface. However, the spent catalyst was fully recovered after treated with an aqueous NaOH solution at 363 K.

Au NPs supported on Al<sub>2</sub>O<sub>3</sub> were tested in a continuous stirred tank reactor for 70 days, at pH 9 and 313 K, without loss of activity or selectivity, converting 72 mol of glucose into sodium gluconate as a sole product by using 3.75 mg of Au.<sup>64</sup>

The influence of the support acidity has been studied by using gold NPs incorporated to different metal oxides (Al<sub>2</sub>O<sub>3</sub>, CeO<sub>2</sub> and mixed Al<sub>2</sub>O<sub>3</sub>-CeO<sub>2</sub>, ZrO<sub>2</sub>-CeO<sub>2</sub> and ZrO<sub>2</sub>-CeO<sub>2</sub>), in base-free glucose oxidation at 393 K (Table 1, entry 16).<sup>51</sup> All the tested catalysts were active, but the selectivity differed with the used support, being Au/Al<sub>2</sub>O<sub>3</sub> the most selective catalyst due to the lowest Lewis acidity of alumina, whereas a higher acidity favors the formation lactic acid. This catalyst was reused in 4 consecutive runs, but with a clear drop of the activity due to lixiviation of gold, which accounts for 10% of glucose conversion.

The use of a basic oxide (MgO) for supporting Au-Pd NPs (Table 1, entry 17) instead of a sacrificial base, or pH control, has also been proposed.<sup>52</sup> However, although the Au-Pd/MgO catalyst was active and selective, its reutilization was not possible due to the support leaching in the acid medium, although neither Au nor Pd were dissolved.

Au-containing bi- and tri-metallic colloidal NPs have also been thoroughly studied by Toshima *et al.*, including Ag/Au,<sup>65,66</sup> Au/Pt,<sup>66,67</sup> Au/Pd,<sup>68</sup> Au/Pt/Pd,<sup>69</sup> Au/Pt/Ag.<sup>66,70,71</sup> They examined their catalytic activity at 333 K, in alkaline medium (pH 9 – 9.5) and bubbling a flow of pure oxygen. The catalytic activity of such bi- and trimetallic particles was always higher than pure Au NPs. For example, Au/Pt/Pd with an average size of 1.7 nm showed the highest catalytic activity, which was 2.5 times higher than that of pure Au NPs, even though both had similar average particle sizes.<sup>69</sup> When Au/Pt/Ag was considered, its catalytic activity was 3.8 times higher than the corresponding Au NPs.<sup>70</sup> The main disadvantage of these colloidal particles was the isolation of the NPs for reutilization in consecutive runs. Thus, the long-time activity of NPs was investigated without the isolation of NPs by continuously withdrawing and adding new glucose solution after each 2 h of run, and they found that the 60% of the activity was maintained at least 8 h. The high catalytic activity of these NPS was ascribed to the presence of anionic Au atoms on the catalyst surface (and Pt when present) acting as catalytic centers. Those anionic Au atoms could activate the oxygen molecules by donating an excess of electronic charge to the antibonding orbital of oxygen, and the peroxy or superoxy-like oxygen promoted glucose oxidation.

Cellulose is the most abundant biopolymer present in lignocellulosic biomass and, at present, it is the unique meaningful alternative to fossil resources. Although some chemical transformations have been achieved regarding the catalytic conversion of cellulose to alcohols such as sorbitol, there are few bibliographic references

dealing with the oxidation of cellulose to valuable chemicals, like gluconic acid. Instead, there are several works focused on cellobiose oxidation.

The conversion of cellobiose requires the aid of a bifunctional catalyst to succeed in this cascade reaction, since this is a two-step process, in which, first, the cellobiose is hydrolyzed to glucose and later the glucose is oxidized to gluconic acid. The majority of the bifunctional catalysts consisted of an acid support, which promotes the hydrolysis reaction of cellobiose, and supported Au NPs for prompting the oxidation reaction. Besides the good catalytic activity and selectivity of Au NPs for primary alcohols oxidation, it should also be considered that they display lower activity in C-C bond scission, or C=C bond isomerization, in the presence of functional groups,<sup>72</sup> which should significantly reduce the number of side reactions in this cascade process. The role of the support is not limited to the hydrolysis of cellobiose, but it is also involved in the control of gluconic acid side reactions,<sup>28</sup> by regulating the oxidation capacity of Au NPs.<sup>73</sup> Indeed, the support modifies the electronic structure of Au NPs.<sup>74</sup> The cellobiose oxidation to gluconic acid proceeds under base-free conditions, although more severe conditions of temperature (373–433 K), oxygen pressure (3–5 bar) and reaction time (up to 24 hours) have to be used in order to obtain high gluconic acid yields. These conditions also cause a decrease in the gluconic acid yield and the formation of other by-products, such as fructose, glycolic acid, acetic acid, oxalic acid, glyceric acid, glucaric acid, succinic acid, formic acid, sorbitol and ethylene glycol.<sup>73–76</sup>

Another example of bifunctional catalysts is the one formed by Au NPs supported on polyoxometalates. An *et al.* attained a gluconic acid yield of 97% by using Au/Cs<sub>1.2</sub>H<sub>1.8</sub>PW<sub>12</sub>O<sub>40</sub>, with a mean Au particle size of 2.7 nm, at 418 K for 3 h.<sup>28</sup> The catalysts with a Cs ratio between 1.2–1.6 displayed lower gluconic acid yields (47–60%), after 11 h, at 418 K. They examined the reusability of the catalyst showing a slightly decrease in both cellobiose conversion and gluconic acid selectivity after 5 runs, but remaining the yield higher than 90%.

A gluconic acid yield as high as 96.4% at 418 K, after 3 h, was attained from cellobiose oxidation, in the presence of a Au/Cs<sub>2</sub>HPW<sub>12</sub>O<sub>40</sub> catalyst.<sup>73</sup> Its reusability was evaluated, and after six sequential reactions, the catalyst remained stable with cellobiose conversion and gluconic acid yield of 93.4% and 76.4% respectively.

Recently, Amaniampong *et al.* reported a 72% yield of gluconic acid using Au/TiO<sub>2</sub> catalyst, at 418 K after 2 h.<sup>74,77</sup> The doping with a second transition metal (Au-Cu, Au-Ru, Au-Co and Au-Pd) allowed improving the catalytic performance.<sup>29</sup> Thus, a complete conversion of cellobiose with a gluconic acid selectivity of 88.5%, at 418 K within 3 h, was attained with Au-Cu/TiO<sub>2</sub>, whereas a conversion of 98.3% with a gluconic acid selectivity of 86.9% at 418 K within 9 h was observed for reactions performed over a Au-Ru/TiO<sub>2</sub> catalyst. It was found that the reaction mechanism depended on the catalyst nature; and cellobiose is converted to cellobionic acid, from which gluconic acid is formed through the cleavage of the β-1,4 glycosidic bond over Cu–Au/TiO<sub>2</sub> catalysts. On the other hand, over the Ru–

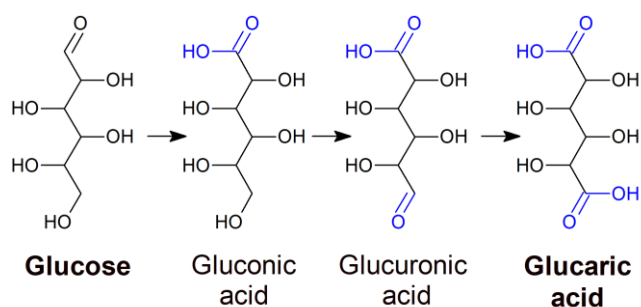
Au/TiO<sub>2</sub> catalyst, glucose was observed as the reaction intermediate and gluconic acid resulted from glucose oxidation. However, the kinetics of the conversion of cellobiose to gluconic acid over Ru–Au/TiO<sub>2</sub> was slower than that over Cu–Au/TiO<sub>2</sub>.

The heterogeneous catalytic technologies for the oxidation of glucose to gluconic acid have shown their potential to substitute the enzymatic route, currently developed in industry. However, much research effort is needed to overcome the main hurdles found in the previous works, such as those related to the reutilization of the catalyst (leaching of the active phase), the necessity of an exhaustive control of the reaction pH, leading to a post neutralization step to isolate the gluconic acid instead its salt and move from glucose to other sugars such as cellulose. For this purpose, bifunctional catalysts have to be deeply explored, where acid and metallic functionalities would allow to transform cellulose as raw material. Moreover, there is a lack of techno-economic studies of the different catalytic routes and the comparison with the enzymatic pathway.

## 2.2. Production of glucaric acid

The oxidation of gluconic acid yields glucaric acid, the corresponding polyhydroxy dicarboxylic acid with both terminal oxidized groups. It has been included in the report of US Department of Energy” as a “*Top value-added chemical from biomass*” due to its wide range of applications.<sup>78</sup> The global glucaric acid market size was estimated at 550.4 million \$ in 2016 on account of increasing demand from detergents, soaps, food ingredients, corrosion inhibitors, and de-icing applications.<sup>79</sup> The potential uses vary for new formulations of phosphate-free detergents and metal complexation agents,<sup>80</sup> as monomer in the preparation of a variety of polymers,<sup>80–82</sup> and intermediate in the production of biobased adipic acid,<sup>83</sup> which is conventionally obtained from fossil-fuel feedstocks. Its derivatives have also been studied as cholesterol reducing agent,<sup>84</sup> antitumor agent,<sup>85</sup> and for diabetes treatment.<sup>86</sup> Traditionally, glucaric acid is industrially produced by glucose oxidation with nitric acid with moderate yields (c.a. 40%).<sup>86</sup> Recently, Rivertop Renewables Company has improved the process,<sup>87</sup> reducing the amount of chemical inputs and consumption, so the production of waste is minimized and a commercial pilot-scale production of glucarate products was launched. The current processes of glucaric acid production relies on the use of concentrated nitric acid, or bleaching agents, processes that generate significant amounts of toxic substances and waste products. Therefore, from a green chemistry viewpoint, it would be more sustainable to use catalytic methods employing heterogeneous catalysts in the presence of air, molecular oxygen or hydrogen peroxide (Figure 3).

Some representative catalytic systems for the oxidation of glucose and gluconic acid to glucaric acid are gathered in Table 2.



**Figure 3.** Pathways for oxidation of glucose to glucaric acid

Dirkx *et al.* studied the production of glucaric acid from both gluconic acid and glucose, using oxygen as oxidant, over Pt/C catalyst (Table 2, entry 1).<sup>88</sup> The product distribution was studied at pH 8–11 and 318–338 K. The highest yield of glucaric acid was 50–55 % and it was obtained from both glucose and gluconic acid. These authors demonstrated the detrimental effect of a high concentration of oxygen on the catalytic activity. If the catalyst was saturated with oxygen before the experiment, the authors observed the consumption rate of gluconic acid was relatively low compared with an experiment in which the catalyst suspension was first heated in nitrogen flow and then contacted with the gluconic acid solution prior to change the atmosphere to oxygen. Therefore, the authors seem to demonstrate the detrimental effect of oxygen excess on the catalytic performance, since oxygen occupied the active sites, saturating the catalyst, although they did not provide a conclusive evidence of this phenomenon. Besides, they evaluated the side reactions, observing that the selectivity to glucaric acid was affected by C–C cleavage of gluconic acid, yielding mono and dicarboxylic acids, irrespective of the reactant. The product distribution was not strongly influenced by the temperature, but

increasing the pH, the amount of tartronic, tartaric, and xylaric + arabinaric acids strongly increased, whereas the amount of arabinonic acid diminished.

Besson *et al.* studied the effect of Bi and Au addition on the activity of Pt/C catalysts for the oxidation of glucose and gluconate solutions, with air at 333 K and pH 7 (Table 2, entries 2 and 3).<sup>89</sup> The Pt/C catalyst showed higher activity than the Pd analogues, which was ascribed to the higher redox potential of platinum, and hence to its lower affinity for oxygen. Glucose was initially converted into gluconate, with small amounts of glucuronate. After reaching 80% yield of gluconate at total glucose conversion, gluconate was converted to glucarate and to lower molecular weight acids and diacids, such as tartaric and oxalic acids. After 24 h of reaction, the glucarate selectivity was 50%. When gluconate solution was used as feedstock, the initial rate of gluconate oxidation was about four times lower than that of glucose under similar experimental conditions. This would explain the fact that, in glucose oxidation experiments, gluconate starts to oxidize only when glucose is completely converted. The maximum selectivity achieved was of 56.6% at 97.2% conversion. The initial specific reaction rates with PtBi/C were larger than that of the parent Pt/C catalyst. The addition of Au on platinum was intended to decrease the catalyst deactivation. The initial reaction rate on PtAu/C was hardly larger than on the parent Pt/C, but, after 24 h of reaction, the conversion was 91% on the former compared to 67% on the latter. The promoter effect of Au might be related to a decrease in the poisoning of the metal surface, either by oxygen or by acidic by-products, probably because the surface Pt–Au alloy has lower affinity for oxygen than pure Pt.

**Table 2.** Summary of glucose (or gluconic acid) oxidation to glucaric acid with different catalysts

Entry	Catalyst	Operating conditions				Catalytic properties		Ref.	
		[S] <sup>a</sup> (wt%)	Oxidant (O <sub>2</sub> )	pH	time (h)	Temp. (K)	X <sub>S</sub> (%)		Y <sub>Glucaric acid</sub> (%)
1	Pt/C	3.9 (GLA)	1 L/min	10	5.1	328	94	53	88
2	Pt/C	36 (GLU)	1.5 L/min (air)	7	24	333	97	50	89
3	Pt/C	39 (GLA)	1.5 L/min	7	24	333	97	56.6	89
4	AuBi/AC	5.0 (GLU)	1 MPa	n. r.	24	333	100	31	90
5	Pt <sub>1</sub> Cu <sub>3</sub> /TiO <sub>2</sub>	11 (GLA)	0.1 MPa	n. r.	4	318	76	29	91
6	Pt <sub>1</sub> Cu <sub>3</sub> /TiO <sub>2</sub>	10 (GLU)	0.1 MPa	n. r.	24	318	100	25	91
7	PtPd/TiO <sub>2</sub>	5.0 (GLU)	0.1 MPa	n. r.	24	318	100	40.4	92
8	Pt/C	10 (GLU)	1.38 MPa	n. r.	10	353	100	74	93

n. r.: not reported; <sup>a</sup> substrate: glucose (GLU) or gluconic acid (GLA);

In the study of glucose oxidation to glucaric acid over Au/C, without pH control,<sup>90</sup> it was found that small Au NPs were very effective to convert glucose, but poorly selective, since side reactions leading to degradation products of the gluconic acid intermediate were enhanced. The best catalytic results were found for a bimetallic AuBi/C catalyst. Concerning the glucaric acid yield, it was 29% after 3 h of reaction at 333 K and under 10 bar O<sub>2</sub> pressure (Table 2, entry 4). When the AuBi catalyst was reused in successive runs, it was observed that the glucaric acid selectivity declined after each reutilization test, although the gluconic acid selectivity was not noticeably modified. The deactivation was ascribed to both the sintering of Au nanoparticles and the strong adsorption of heavy compounds.

A bimetallic PtCu catalyst, immobilized on TiO<sub>2</sub>, was also used for the oxidation of both glucose and gluconate to glucaric acid (Table 2, entries 5 and 6).<sup>91</sup> They achieved a TOF of 3542 h<sup>-1</sup> with a glucaric acid selectivity of 46% at 318 K, and 0.1 MPa of O<sub>2</sub> pressure for the gluconate oxidation. These results were higher than those obtained with the monometallic catalysts, and besides, these results remarked that the reaction was sensitive to the surface morphology of Pt nanoparticles. The reaction mechanism from sodium gluconate points out that the PtCu alloy promoted more significantly the C-C cleavage reactions by retro-aldol condensation than the monometallic phases. This further confirmed that Cu species on Pt improved the oxidation rates of hydroxyl functionalities to carboxylic groups, increasing the oxidation rates of sodium gluconate on the bimetallic catalyst. Accordingly, this catalyst was tested in the glucaric acid synthesis from glucose, reaching a selectivity of 25.4% at complete glucose conversion after 24 h of reaction. The catalyst was reused in three consecutive runs, without remarkable loss of activity or selectivity to glucaric acid.

Jin *et al.* prepared PtPd nanoparticles as alloy, core-shell, and cluster-in-cluster structures, and immobilized then on TiO<sub>2</sub> support (Table 2, entry 7).<sup>92</sup> The PtPd alloy structure displays better oxidation performance than the others. Moreover, the use of a bimetallic PtPd catalyst enhanced both the catalytic activity and glucaric acid selectivity compared to the monometallic Pt and Pd catalysts. Thus, a complete conversion of glucose was achieved after 10 h, with a TOF 2404 h<sup>-1</sup>. With respect to product distribution, monometallic catalysts gave high selectivity toward gluconic acid (S= 57-76%) with negligible glucaric acid formation (S~ 4%) during 12 h reaction time. In contrast, the glucaric acid selectivity attained 31% on bimetallic catalyst. These differences highlighted that the bimetallic PtPd catalyst had higher oxidation activity for gluconic to glucaric acid, while this reaction was disfavored on monometallic Pt and Pd catalysts. In addition, other products, tartronic, oxalic, glyceric, glycolic and lactic acids, were

also detected on the bimetallic catalyst, while the selectivity toward these products was low on monometallic catalysts. These authors observed that the formation of aldarcic acids was negligible until the starting glucose consumption was complete, suggesting a glucose inhibition effect in secondary oxidation reactions. This would indicate that glucose might be strongly adsorbed on the bimetallic PtPd surface, thus preventing the side reactions such as C-C cleavage of glucose, being highly possible that C-C cleavage occurs significantly from gluconic acid. The catalyst stability was also evaluated after three runs, without significant modifications.

The influence of the pH and the nature of support was evaluated over Pt supported on activated carbon, SiO<sub>2</sub> and Al<sub>2</sub>O<sub>3</sub>.<sup>93</sup> The Pt/C catalyst showed the highest glucaric acid yield (74%) in water, with a TOF of 879 h<sup>-1</sup> (Table 2, entry 8). The effectiveness of catalysts decreased in the order: Pt/C > Pt/SiO<sub>2</sub> > Pt/ Al<sub>2</sub>O<sub>3</sub>. The effect of pH was studied, finding that the selectivity of glucaric acid was higher under base-free and mild basic conditions than in high base or acid conditions. It is found that in an acid solution, gluconic acid was the major product, while in a highly basic solution, selectivity to glucaric acid is poor due to C-C bond cleavage, leading to low carbon chain carboxylic acids, such as tartronic and oxalic acids. The catalyst was stable after five recycling tests, and no Pt leaching was observed.

The hydrolysis of lignocellulosic biomass, after separation of each fraction, i.e. hemicellulose, cellulose and lignin, produces a hydrolysate which can be used as a low-cost source of sugars for the production of glucaric acid. Thus, Derrien *et al.* evaluated the possible inhibition effect of impurities present in such hydrolysates on the oxidation of glucose over AuPt/ZrO<sub>2</sub>.<sup>94,95</sup> The oxidation process was performed at 373 K, under 40 bar of air and a glucose/metal ratio of 80. Under these experimental conditions, the oxidation of commercial glucose (free of impurities) produced a yield of glucaric acid of 50%, after 10 h, and it was completely reusable. These authors studied separately the effect of each type of impurity, demonstrating that acids (sulfuric or acetic acid) did not influence on the gluconic acid production concentration, but the major effect was found on the yield of glucaric acid, which was slightly lower. These results indicate that these acids are prone to cause some side reactions of glucaric acid. The inhibitory effect of furanic compounds was more evident, the maximum production of gluconic acid was delayed 3h, and the glucaric acid yield was 40% at the end of the reaction. When cellobiose was present as a disaccharide residue, the oxidation of gluconic to glucaric acid was not complete after 24 h, being the glucaric acid yield slightly lower after 8 h of reaction. However, the formation of glucose from cellobiose surprisingly involved no positive effect on the final yield of glucaric acid. Guaiacol, a model molecule of phenolic residue,



caused an abrupt decrease in the oxidation rate of glucose, yielding less than 10% glucaric acid.

The glucaric acid production through greener routes, as heterogeneous catalysis, is still in its infancy and much effort has to be devoted to substitute the current technology based on the use of inorganic oxidants. The main pitfall to overcome is related to the low selectivity of proposed catalysts and their stability in reutilization tests. Once those barriers are overwhelmed when glucose is the starting point, it should be convenient exploring the lignocellulose residues as raw material for the production of glucaric acid.

### 2.3. Production of formic acid

Formic acid (FA) is a very interesting commodity finding a wide variety of applications in different industrial sectors, ranging from hydrogen donor and C1 feedstock in chemical industry,<sup>96</sup> to liquid hydrogen storage material in the energy field, all along with preservative and additive in animal feeding, or tanning additive in leather and textile industry.<sup>97</sup>

The industrial production of FA has been tackled throughout different processes, including direct hydrocarbon oxidation, hydrolysis of formamide, and acidolysis of formate salts.<sup>98</sup> However, the most extended process, with a larger installed production capacity, is that developed by BASF in early 80s, specifically dedicated to the production of formic acid, with no undesirable by-products.<sup>99</sup> This process consists of the hydrolysis of methyl formate, and it is based on a sequential multi-stage conversion process, involving the production of methanol (oxidation of methane to syngas, followed by conversion to methanol, through a high pressure process) and its subsequent carboxylation to methyl formate. Finally, this last is hydrolysed to yield formic acid and methanol, which is recycled to the carboxylation step.<sup>97</sup> This process involves serious drawbacks, such as starting from a non-renewable fossil feedstock like natural gas, or a cascade of reactions operating in the presence of different catalysts: Ni-based catalysts for natural gas reforming, Cu-based materials for syngas conversion, and sodium methoxide for methanol carboxylation. Finally, the needing to apply harsh reaction conditions in most of the stages (up to 533 K and 8 MPa) to get proper intermediate product yields, is a strong drawback of this industrial methodology for the production of formic acid.

As alternative to traditional methods, interesting options for the production of FA can be found,<sup>100,101</sup> including the use of biomass as feedstock.<sup>97,102,103</sup> Hydrolysis and oxidation pathways are the most reported procedures for the production of FA from biomass, because of the high versatility of these two alternatives, being applicable to the conversion of a wide variety of feedstock, from single molecules, like glucose, to complex mixtures, like pyrolysis bio-oils. Nevertheless, though FA is obtained as a hydrolysis by-product, its productivity is usually quite low compared to oxidation, so that the latter seems to be more feasible at an industrial scale.

Oxidation of glucose has been widely reported as a very interesting alternative for the selective production of FA,<sup>104–107</sup> because of the high potential of sugars in this reaction pathway. The most reported

routes for glucose oxidation to formic acid include wet alkaline, and catalytic oxidations. From them, although the former provides FA yields over 50%, depending on the substrate, it also involves several drawbacks,<sup>108,109</sup> hampering its applicability at high scale, such as the use of strong soluble bases, and harsh temperature (393–523 K) and pressure conditions, which cause high FA decomposition. These disadvantages hamper the applicability of wet alkaline glucose oxidation at high scale. On the other hand, catalytic oxidation has been reported to be more productive and selective towards the formation of FA, compared to wet alkaline oxidation, mainly because the use of catalysts allows decreasing the operation temperature, thus reducing the extent of FA decomposition. The most successful oxidation pathway (OxFA process)<sup>97</sup> is based on the use of polyoxometalates,<sup>110</sup> including vanadium salts,<sup>107</sup> and heteropolyacids,<sup>111</sup> as catalysts, which operate under 2–3 MPa O<sub>2</sub> to provide high FA yields, under certain conditions above 90%. However, despite its very high selectivity, since only FA and CO<sub>2</sub> appear as main reaction products, and bulk side products formation is avoided, the homogeneous nature of catalysts and their complexity hinder the scale up of this process to industrial production. In addition, attempts to get heterogeneous counterparts of these catalytic systems have not been completely successful,<sup>112</sup> so that different alternatives have been explored.

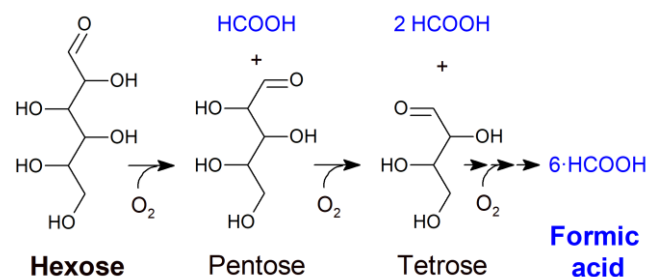
An interesting approach for the catalytic oxidation of lignocellulose biomass into formic acid was reported by Xue *et al.*,<sup>113</sup> based on micrometer-sized metal oxides as heterogeneous catalysts. These authors used CeO<sub>2</sub>, Al<sub>2</sub>O<sub>3</sub>, ZrO<sub>2</sub> and TiO<sub>2</sub> as catalysts for the oxidation of powdered corncob (35% cellulose) in water, under an oxygen atmosphere (1.2 MPa). Results revealed the superior catalytic performance of CeO<sub>2</sub> in the oxidation test, as compared to the rest of the tested metal oxides, in terms of substrate conversion and selectivity towards small organic acids (lactic, acetic and formic acids). The higher catalytic activity of CeO<sub>2</sub> was attributed to its better oxygen-storage properties, which, in turn, also displayed poor selectivity towards formic acid, as the obtained FA yield was always below 18%. The reaction mechanism was postulated to proceed through the formation of acetic acid, which was subsequently oxidized to FA and, finally, to CO<sub>2</sub>. The partial poisoning of active sites of CeO<sub>2</sub> allowed tuning its intrinsic catalytic activity to provide increasing FA yields together with a lower production of CO<sub>2</sub>.

Further steps in the transformation of glucose into FA in the presence of metal oxides as catalysts were taken by using hydrogen peroxide as oxidant. This chemical, though not as benign as oxygen, can also be considered as a clean oxidant as it provides excellent FA yields and the reduction product is just water. In this context, Ebitani *et al.* studied a MgO-supported CTAB-capped copper oxide catalyst in the transformation of glucose into FA.<sup>114</sup> Copper oxide is known to be an excellent catalyst in selective oxidation reactions with H<sub>2</sub>O<sub>2</sub> as oxidant, so it was proved to be in the oxidation of glucose to FA, as it provided 65% FA yield, in water at 393 K. More recently, the same authors have tested a huge variety of solids as oxidation catalysts under similar experimental conditions, finding out that Mg–Al hydrotalcites displayed a quite good catalytic

performance in FA production in aqueous media (37% FA yield). This was much enhanced when using ethanol as reaction solvent (78% FA yield), a quite high improvement which was attributed to the decrease in the extent in non-oxidative H<sub>2</sub>O<sub>2</sub> consumption (decomposition), thus increasing the efficiency in the use of this oxidant, a crucial parameter to scale up this process to industrial level.<sup>115</sup>

An alternative pathway in the search for efficient procedures for the selective transformation of glucose into FA using heterogeneous systems is photocatalysis. Within this context, the reported catalytic systems are based in promoted and unpromoted TiO<sub>2</sub>. This was employed by Palmisano *et al.* in the oxidation of aqueous solutions of glucose into FA, at room temperature, under natural pH, using UV radiation.<sup>116</sup> No oxygen was bubbled into the system, but the reaction media was open to air. Under these conditions, bare TiO<sub>2</sub> provided good yields towards intermediate oxidation products, such as arabinose and erythrose, but scarce production of formic acid. The promotion of TiO<sub>2</sub> by surface impregnation with heteropolyacids (Keggin-type clusters H<sub>3</sub>PW<sub>12</sub>O<sub>40</sub> and K<sub>7</sub>PW<sub>11</sub>O<sub>39</sub>), which demonstrated a poor activity under homogeneous conditions, enhanced the catalytic activity of TiO<sub>2</sub> towards the formation of FA. It was postulated that the presence of supported heteropolyacids favored the product desorption from the catalyst surface, especially in presence of H<sub>3</sub>PW<sub>12</sub>O<sub>40</sub> clusters, thus avoiding overoxidation. Under these conditions, the sequential transformation of monosaccharides was postulated, starting from the anomeric centre (C1 in glucose), and the oxidation attack to the adjacent carbon (C2), causing the  $\alpha$ -scission (C1-C2 cleavage) and the evolving of a formic acid molecule together with a one-carbon-less monosaccharide. This reaction pathway (Figure 4) is similar to that proposed in the presence of homogeneous heteropolyacid

clusters in the OxFA process,<sup>97,107,110,111</sup> allowing a theoretical production of a number of formic acid molecules equal to the number of carbons of the starting monosaccharide, that is, a high FA productivity.



**Figure 4.** Sequential oxidation of glucose to minor monosaccharides and formic acid

High FA production values (up to 35% FA yield) have been reported when using UV irradiated TiO<sub>2</sub> under basic conditions (30 mM NaOH), operating at room temperature.<sup>117</sup> Under these conditions, sodium hydroxide seems to exert a crucial role in the reaction, as it favors the production of oxidative radicals, such as O<sub>2</sub><sup>-</sup> and OH, while preventing FA mineralization by reducing the affinity of the TiO<sub>2</sub> surface for this acid. In this way, high glucose conversion was achieved together with moderate FA yields. Other authors have used metal promoted TiO<sub>2</sub>-based photocatalysts, such as Pd/TiO<sub>2</sub>,<sup>118</sup> and Ag/TiO<sub>2</sub> catalysts.<sup>119</sup> Nevertheless, the requirements of these processes involve the use of quite energy intense radiation (UV), as well as low substrate concentration (1-20 mM), and these provide quite low FA production values, reducing the possibilities for the scale up to industrial production.

**Table 3.** Formic acid production from biomass through heterogeneous catalytic oxidation

Entry	Substrate	Catalyst	Operating conditions & catalytic properties						Ref.
			Cat load (g/g) <sup>a</sup>	[subs] (wt%) <sup>b</sup>	Oxidant <sup>c</sup>	Temp. (K)	time (h)	Y <sub>FA</sub> <sup>d</sup> (%)	
1	Corn cobs	nanosized CeO <sub>2</sub>	0.03	2.5	O <sub>2</sub> (1.7 MPa)	453	3	18	113
2	Glucose	CuO-CTAB / MgO	1	1.8	H <sub>2</sub> O <sub>2</sub> (4:1)	393	12	65	114
3	Glucose	Mg-Al Hydrotalcites	1	4.6	H <sub>2</sub> O <sub>2</sub> (9:1)	343	5	78	115
4	Glucose	H <sub>3</sub> PW <sub>12</sub> O <sub>40</sub> / TiO <sub>2</sub>	100	1.8·10 <sup>-3</sup>	air + hv	298	6	60	116
5 <sup>e</sup>	Glucose	nanosized TiO <sub>2</sub>	30	0.18	air + hv + NaOH	298	12	33	117

<sup>a</sup> catalyst to substrate weight ratio; <sup>b</sup> substrate concentration; <sup>c</sup> Oxidant, in brackets when available: pressure in MPa for O<sub>2</sub>-based processes; oxidant:substrate molar ratio for other oxidants; <sup>d</sup> Product yield is quantified as the moles of produced formic acid referred to the maximum moles of formic acid liable to be produced from the used feedstock attending to the carbon content; <sup>e</sup> NaOH:substrate=3:1 molar ratio.

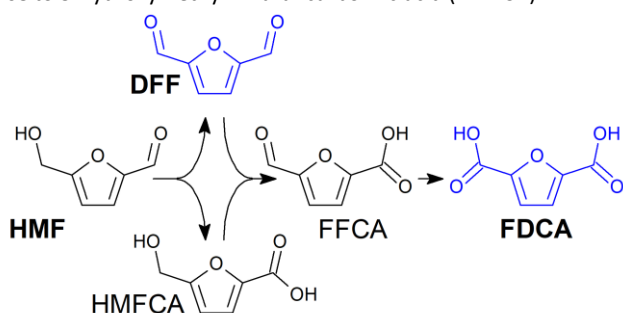
### 3. Oxidation of 5-hydroxymethylfurfural

HMF is a versatile building block that can be converted to a wide range of chemicals with applications as monomers for bioplastics, biofuels or precursors of macromolecules.<sup>120</sup> Two reviews were recently published on this topic. The first one deals with those

catalytic systems only containing non-precious metal sites,<sup>121</sup> while the second one is only focused on those studies carried out in aqueous phase.<sup>122</sup> An earlier review by Tong *et al.*<sup>123</sup> covered works using stoichiometric reagents, with little environmental sustainability, as oxidants. In this section, the goal is to provide an

overview of the main results obtained by the scientific community in the HMF aerobic oxidation using heterogeneous catalysts.

The HMF oxidation can take place through two parallel routes. The selective oxidation of the hydroxyl group (Figure 5) yields 2,5-diformylfuran (DFF),<sup>124</sup> whereas the oxidation of the aldehyde gives rise to 5-hydroxymethyl-2-furancarboxylic acid (HMFCFA).



**Figure 5.** Reaction routes for the selective oxidation of HMF.

The further oxidation of either DFF or HMFCFA produces 5-formyl-2-furancarboxylic acid (FFCA), which is the final intermediate in the 2,5-furandicarboxylic acid (FDCA) production.

Each one of the following sections summarizes the state of the art on the HMF selective transformation into the two chemicals with the wider market prospects i.e. DFF and FDCA. There are few papers dealing with the selective production of FFCA; however, as this chemical has no relevant applications, its role as a reaction intermediate will only be considered.<sup>125,126</sup>

### 3.1. Production of 2,5-diformylfuran

2,5-diformylfuran (DFF) is a very promising building block, with a wide range of uses in various fields. For instance, the DFF condensation with nonlinear diamines yields resins showing high thermal stability and applications as energy storage or gas adsorption materials.<sup>127,128</sup> It is also the starting material for the synthesis of pharmaceuticals,<sup>129</sup> poly Schiff bases,<sup>130</sup> and cross-linking agents of poly(vinyl alcohol) for battery applications.<sup>131</sup> As depicted in the Figure 5|Error! No se encuentra el origen de la referencia., the production of DFF requires a catalyst that selectively activates the primary hydroxyl group of HMF, without affecting the  $\alpha,\beta$ -unsaturated aldehyde group, which would otherwise yield 5-hydroxymethyl-2-furancarboxylic acid (HMFCFA). Heterogeneous catalysts containing Ru as active metal sites have been extensively utilized in this transformation. In carbon supported catalysts, Ru provided higher activity and DFF selectivity compared to other precious metals, such as Pt, Pd, Rh or Au.<sup>132,133</sup> Ru proved to be the active site in a trimetallic Co-Ce-Ru mixed oxide catalyst, as the catalyst gave no activity in the absence of this precious metal.<sup>134</sup> Ru plays a key role in the H-abstraction of the dissociatively adsorbed alcohol,<sup>135</sup> which is the kinetically relevant step of the reaction.<sup>132</sup> Concerning the support, Ru on basic, i.e.  $Mg_2AlO_x$  and  $MgO$ , or acidic materials, i.e.  $Al_2O_3$  and ZSM-5, yielded DFF in low selectivities, due to the promotion of degradation and resinification reactions.<sup>132</sup> Moreover, the stability of basic catalysts, such as hydrotalcites, is compromised due to the strong adsorption

of reactants and products on the catalyst surface.<sup>133</sup> In this sense, neutral supports, such as  $C$ ,<sup>132,133</sup> or C nanotubes<sup>136</sup> have provided the highest productivities, i.e.  $> 3 h^{-1}$ , and prominent DFF yields (Table 4, entries 3 and 4).

Ru-based catalysts containing iron oxide<sup>137,138</sup> possess the advantage of being magnetically separable, nonetheless, reported activities are lower than those supported on carbon (Table 4, entries 6 and 7). With regards to the catalyst stability, the Ru leaching phenomenon has not been reported regardless of the support,<sup>133,134,137</sup> and the loss of activity relates to the presence of insoluble furanic compounds that block the active sites.<sup>134,139</sup>

Vanadium-based catalysts are the second relevant family of materials used for this transformation. The interest relies on their relatively low cost as compared to the catalytic systems containing precious metals. Pioneering work by the Du Pont company<sup>140,141</sup> showed the suitability of vanadium phosphate oxides (VPO) to selectively produce DFF from HMF.

Grasset *et al.* studied the introduction of alkylmethylammonium into a  $VOPO_4 \cdot 2H_2O$  material, finding that the formation of side products decreased as compared to the unmodified  $VOPO_4 \cdot 2H_2O$ ,<sup>142</sup> and this improvement in DFF selectivity was related to the generation of mesostructured phases that moderate the oxidation properties of the catalyst. Unfortunately, the catalyst was not stable due to the leaching of intercalated ammonium ions. Stability problems were also an issue in different zeolite-supported vanadia catalyst, i.e. H-beta, H-ZSM-5, H-Y and H-modernite.<sup>143</sup> Indeed, more than fifty percent of the catalyst activity came from the contribution of the lixiviated species. Nie *et al.* studied the effect of the  $VO_x$  surface densities on different supports.<sup>144</sup> Two dimensional polyvanadates and  $V_2O_5$  nanoclusters, favored at surface densities near the monolayer capacity, combined with a reducible support, promoted the selective production of DMF. This correlation between reducibility and reactivity suggests a Mars-van-Krevelen redox mechanism, where the surface atoms of the  $VO_x$  domains take part on the HMF oxidation to DFF.

An interesting strategy to increase the catalytic activity was the isolation of the active sites, by immobilizing vanadium complexes in polyaniline.<sup>145</sup> Nonetheless, this catalytic system was unstable, as vanadium leached from the catalyst. In this regard, immobilization of cupric ions together with vanadyl on sulfonated carbon not only improved the selectivity towards DFF, but also suppressed the leaching of the active phase.<sup>146</sup>

Concerning other active metals, silver was loaded on manganese oxide octahedral molecular sieves (K-OMS) and tested in HMF oxidation.<sup>147</sup> Both HMF conversion and DFF selectivity increased with the silver content. Silver plays a role in the Mars-van Krevelen redox mechanism: the catalytic cycle starts with the reduction of  $Ag^{2+}$  into  $Ag^+$  and the oxidation of  $Mn^{3+}$  into  $Mn^{4+}$ . Next, the oxidation of HMF to DFF takes place together with the reduction of  $Mn^{4+}$  to  $Mn^{3+}$ . The cycle closes by the re-oxidation of  $Ag^+$  by molecular oxygen. A similar mechanism was suggested for a  $Mn_{0.70}Cu_{0.05}Al_{0.25}$  catalyst,<sup>148</sup> with the participation of the  $Cu^{2+}$  and  $Cu^+$  species instead of silver ones.

**Table 4.** Summary of HMF oxidation reactions into DFF with different catalysts in batch reactors.

Entry	Catalyst	Operating conditions				Catalytic properties			Ref.
		Solvent	Temp. (K)	Pressure (MPa)	time (h)	[HMF] (wt%)	X <sub>HMF</sub> (%)	Y <sub>DFF</sub> (%)	
1	Ru/Hydrotalcite	DMF	393	0.1 (O <sub>2</sub> )	6	4.5	95	97	133
2	CoCeRu	MIBK	373	0.1 (O <sub>2</sub> )	24	4.1	100	80	134
3	Ru/C	Toluene	383	2.0 (O <sub>2</sub> )	n. r.	1.4	100	96	132
4	Ru-PVP/CNT	DMF	393	2.0 (O <sub>2</sub> )	12	1.3	100	94	149
5	Ru/γ-Al <sub>2</sub> O <sub>3</sub>	Toluene	403	0.27 (O <sub>2</sub> )	4	1.4	100	97	139
6	γ-Fe <sub>2</sub> O <sub>3</sub> @HAP-Ru	4-Chlorotoluene	383	0.1 (O <sub>2</sub> )	2	1.6	100	81	138
7	ZnFe <sub>2-x</sub> Ru <sub>x</sub> O <sub>4</sub>	DMSO	383	0.1 (O <sub>2</sub> )	4	1.9	100	94	137
8	VO <sub>x</sub> /TiO <sub>2</sub>	Toluene	363	1.6 (air)	n. r.	0.3	n. r.	n. r.	144
9	VO <sup>2+</sup> -Cu <sup>2+</sup> /CS	MeCN	413	4 (air)	4	1.3	100	98	146
10	Polyaniline-VO(acac) <sub>2</sub>	4-Chlorotoluene	383	0.1 (O <sub>2</sub> )	12	1.2	100	86	145
11	Ag-OMS-2	2-Propanol	438	1.5 (O <sub>2</sub> )	4	1.0	100	99	147
12	Mn <sub>0.70</sub> Cu <sub>0.05</sub> Al <sub>0.25</sub>	Water	363	0.8 (O <sub>2</sub> )	24	1.3	90	78	148
13	MgO-CeO <sub>2</sub>	Water	373	0.9 (O <sub>2</sub> )	15	1.8	97.8	96	150
14	CS-Ti	water	343	0.9 (O <sub>2</sub> )	8	0.6	91	88	151

n. r.: not reported; <sup>a</sup> The productivity was estimated as an average value at HMF conversions near 100 %.

In terms of operating conditions, the O<sub>2</sub> partial pressure and the temperature have similar effects. They promote catalyst activity and DFF selectivity until a certain value, above which, over oxidation of DFF to FFCA or FDCA occurs.<sup>132,134,138,147,149</sup> As observed in Table 4, initial HMF concentrations were always below 5 wt%, even though higher values are required seeking for industrial viability.<sup>152</sup> Higher concentrations of HMF are problematic because of its prone to polymerize, consequently diluted HMF solutions have been explored so far. As regards the productivity values, they range between 0.11 and 8.7 mol<sub>DFF</sub> (mol<sub>active phase</sub> · h)<sup>-1</sup>, being the best data achieved with a VO<sup>2+</sup>-Cu<sup>2+</sup>/CS catalyst (Table 4, entry 9).

Much effort has been devoted for establishing the role of the reaction solvent. It is well known that solvent features, such as polarity, steric hindrance, acid-base properties, or dielectric constant, affect the chemical reactions.<sup>153</sup> For instance, if the reaction is carried out in aqueous phase, HMF is mainly converted into HMFFCA<sup>135</sup> (*vide infra*), which can further react to form FFCA (Figure 5). Hence, the vast majority of the research works dealing with DFF production use organic solvents. Nonetheless, the reported results are contradictory and trends in terms of solvent dielectric constant or polarity effect have not yet been established. Zhang *et al.* observed that solvents containing N, O or S heteroatoms, such as N,N-dimethylformamide (DMF), methyl-

isobutyl-ketone (MIBK), ethanol or dimethyl sulfoxide (DMSO) resulted in lower DFF yields due to the strong interaction of the solvent and Ru centers.<sup>138</sup> Solvents with weaker interactions, such as toluene,<sup>139,144,149,154</sup> or 4-chlorotoluene,<sup>132,138,145</sup> provided higher selectivities. However, other authors have claimed that strong polarity solvents, such as DMSO and DMF, promote HMF oxidation due to the stabilization of the intermediate carbocation, which is formed after the removal of the secondary H-atom.<sup>155</sup> In DMSO, the selectivity towards DFF significantly improved when the solvent was dried before the reaction.<sup>137</sup> 1,4-dioxane should be avoided due to the lack of stability under conventional operating conditions.<sup>139,149</sup> Recently, very promising results were published using a MgO-CeO<sub>2</sub> catalyst in water.<sup>150</sup> The catalyst suffered deactivation due to the hydration of MgO into Mg(OH)<sub>2</sub>, however, as there was no leaching, the catalyst recovered the activity after a calcination step. Despite the relatively low productivity of the catalyst (Table , entry 13), the results are promising, as high yields could be obtained in water, which is the solvent used for HMF production from biomass.

### 3.2. Production of 2,5-diformylfuran through integrated fructose dehydration and 5-hydroxymethylfurfural oxidation.

The HMF production from hemicellulosic biomass faces two significant issues: (i) in the aqueous acid medium in which is produced, HMF further reacts to yield levulinic acid, formic acid and humins, and (ii) as a hydrophilic and low volatility compound, it is difficult to isolate HMF from the aqueous medium through liquid extraction or steam stripping. Hence, it is hard to envision a future chemical market in which HMF is readily available and at competitive costs. An interesting alternative is to produce DFF from carbohydrates without the intermediate HMF purification. Fructose, which is obtained from the isomerization of glucose, is an interesting starting molecule for this integrated process.

In terms of catalytic requirements, the process needs an acid catalyst to transform fructose into HMF, and a redox catalyst to oxidize HMF into DFF. As observed in Table , entries 1-4, several combinations of heterogeneous acids and redox catalysts have been reported: Dowex-type cation-exchange resin + V<sub>2</sub>O<sub>5</sub>,<sup>141</sup> Amberlyst-15 + polyaniline-VO(acac)<sub>2</sub>,<sup>145</sup> CrCl<sub>3</sub>·6H<sub>2</sub>O/NaBr + NaVO<sub>3</sub>·2H<sub>2</sub>O,<sup>156</sup> Amberlyst-15 + Ru/HT.<sup>133</sup> In order to obtain DFF yields higher than 50%, the reaction must take place in two steps. In the fructose dehydration step, only the acid catalyst must be present, because the redox catalysts promote fructose oxidation reactions into undesired products. The presence of the acid catalyst in the HMF oxidation step has also been reported to be detrimental and to decrease the DFF yields.<sup>136,141,145</sup>

In order to make simpler the separation of heterogeneous catalysts between the dehydration and the oxidation step, magnetically separable catalysts, such as Fe<sub>3</sub>O<sub>4</sub>@SiO<sub>2</sub>-SO<sub>3</sub>H + γ-Fe<sub>2</sub>O<sub>3</sub>/HAP-Ru,<sup>138</sup> and Fe<sub>3</sub>O<sub>4</sub>-SBA-SO<sub>3</sub>H + K-OMS-2, have been employed.<sup>155</sup> Moreover, they reported prominent DFF yields (ca. 80%, see Table , entries 3 and 4).

From an integrated point of view, the use of a bifunctional catalyst capable of carrying out the dehydration and the oxidation steps would be desirable. Graphene oxide prepared with sulfuric acid presents acid sites from the sulfonic groups and redox catalytic properties from the carboxylic acid groups and the unpaired electrons at the edge defects.<sup>157</sup> This bifunctional material was tested in the fructose transformation into DFF with a 72.5% reported yield. The initial dehydration step was carried out under N<sub>2</sub>, because the coexistence of O<sub>2</sub> and the redox sites induced fructose oxidation and the subsequent formation of undesired products. A similar effect was observed with a bifunctional protonated vanadium-doped graphitic carbon nitride catalyst (V-g-C<sub>3</sub>N<sub>4</sub>(H<sup>+</sup>), which yielded DFF in 45% from fructose when the dehydration step was performed in N<sub>2</sub>.<sup>136</sup> Keggin heteropolyacids, which exhibit Brønsted acidity and redox potential, have also been used as bifunctional catalysts for the direct transformation of fructose into DMF.<sup>158</sup> A problem with the heteropolyacids is that they dissolve in most liquids. Zhao *et al.*<sup>159</sup> tried to solve this problem by encapsulating the heteropolyacids into chromium terephthalate metal-organic framework (MIL-101). Unfortunately, the catalyst was not stable due to the leaching of Mo from the catalyst. Molybdenum leaching was also reported by the same authors when utilizing a MoO<sub>3</sub>-containing protonated nitrogen-doped carbon.<sup>160</sup>

Another method to avoid the leaching of heteropolyacids consisted in a partial substitution of H<sup>+</sup> by Cs<sup>+</sup>, obtaining a Cs<sub>0.5</sub>H<sub>2.5</sub>PMo<sub>12</sub> heterogeneous catalyst.<sup>161</sup> Besides reporting a high DFF yield (69.3%) (Table , entry 7), the whole process was carried out in air, which simplifies a future possible industrial operation. Moreover, the catalyst did not show a significant activity lost upon reuse. Regarding the solvent, DMSO is ubiquitous used in reported works. DMSO, as a dipolar aprotic solvent,<sup>162</sup> acts as a catalyst in the dehydration of fructose into DMF.<sup>163</sup> Nonetheless, under conventional operating conditions, DMSO disproportionation occurs, yielding MeS and MeSO<sub>2</sub>, together with an unpleasant odor. The formation of these impurities complicates the final product purification.<sup>141</sup>

**Table 5.** Summary of fructose transformation into DFF with different catalysts in batch reactors.

Entry	Catalyst	Operating conditions					Catalytic properties		Ref.
		Solvent	Temp. (K)	Pressure (MPa)	time (h)	[Fructose] (wt%)	Y <sup>a</sup> (%)		
1	Dowex ion exchange resin	DMSO	383	0.1 (air)	5	17	85 (HMF)	141	
	V <sub>2</sub> O <sub>5</sub>		423	0.1 (air)	13	-	43 (DFF)		
3	Amberlyst-15	DMSO + 4-Chlorotoluene	383	0.1 (air)	2	n. r.	92 (HMF)	145	
	Polyaniline-VO(acac) <sub>2</sub>		383	0.1 (O <sub>2</sub> )	12	-	71 (DFF)		
3	Fe <sub>3</sub> O <sub>4</sub> -SBA-SO <sub>3</sub> H	DMSO	383	0.1 (air)	2	5.2	81 (HMF)	155	
	K-OMS-2		383	0.1 (O <sub>2</sub> )	6	80 (DFF)			
4	Fe <sub>3</sub> O <sub>4</sub> @SiO <sub>2</sub> -SO <sub>3</sub> H	DMSO + 4-Chlorotoluene	383	0.1 (air)	2.5	2.6	90 (HMF)	138	
	γ-Fe <sub>2</sub> O <sub>3</sub> /HAP-Ru		383	0.1 (O <sub>2</sub> )	24	79 (DFF)			
5	Graphene Oxide	DMSO	413	0.1 (N <sub>2</sub> )	2	7.6	93 (HMF)	157	
			413	0.1 (O <sub>2</sub> )	22	73 (DFF)			
6	V-g-C <sub>3</sub> N <sub>4</sub> (H <sup>+</sup> )	DMSO	403	0.1 (N <sub>2</sub> )	2	8.3	45 (DFF)	136	
			403	1 (O <sub>2</sub> )	6				
7	C <sub>50.5</sub> H <sub>2.5</sub> PMo <sub>12</sub>	DMSO	433	0.1 (air)	4	3.9	69 (DFF)	161	
8	Mo-HNC	DMSO	423	0.1 (O <sub>2</sub> )	9	3.5	77 (DFF)	160	

<sup>a</sup> Yield from fructose. <sup>b</sup> Due to the bifunctional nature of the active phase, productivity is calculated based on total catalyst/s weight.

Taking all this into account, the future research on DFF production should allow establishing the structure-activity relationships of the oxidation catalysts, and enable a rational design of bifunctional catalysts for the direct conversion of fructose into DFF. These catalysts should provide higher yields and activities than the current ones, as most of them show values below the industrial viability window (i.e. productivity > 0.1 g<sub>DFF</sub> g<sub>cat</sub><sup>-1</sup> h<sup>-1</sup>; DFF yield > 70%; see Table ).<sup>152</sup> Studies on long-term stability in continuous operation are also lacking. Finally, glucose is a more abundant and cheaper six-carbon sugar than fructose. Hence, direct transformation of glucose into DFF would be preferable, although very low DFF yields were reported so far, with a best result being 55%.<sup>156</sup>

### 3.3. Production of 2,5-furandicarboxylic acid.

FDCA is one of the top-12 value-added chemicals from biomass by the U.S. Department of Energy.<sup>164</sup> DuPont, Corbion and Synvina (a BASF–Avantium joint venture) tested the quality of the 2,5-FDCA derived polyethylene furan (PEF) plastic in food and beverage containers, automotive applications and textile fibers. PEF bottles show superior barrier properties towards water, oxygen, carbon

dioxide, and have higher glass transition temperature and tensile strength as compared to polyethylene terephthalate (PET) based bottles.<sup>165</sup> Hence, FDCA is a representative biorefinery product with large potential as a replacement for a petroleum-based product, i.e. terephthalic acid.

Water is the preferred solvent for this transformation, as it takes part in the reaction mechanism, being the solvent used for HMF production (Figure 5). In aqueous phase, the aldehyde group of HMF reacts with water to generate HMFCa. The next step of the reaction, the oxidation of the remaining alcohol group into aldehyde, is the rate-controlling step of the reaction, and requires OH<sup>-</sup> concentrations clearly above the HMFCa stoichiometric one.<sup>166</sup> The final oxidation of the aldehyde group into acid, i.e. the FFCA conversion into FDCA, is usually fast and selective. The reaction mechanism seems to be independent of the reaction medium pH: the oxygen inserted comes from the water molecules and the oxygen is proposed to act as an electron scavenger from the catalyst surface, closing the cycle.

As in the previous section, only those works that report activity tests using heterogeneous catalysts, and molecular oxygen as the only oxidizing agent will be considered. In this case, however, most

of the works report the use of a homogeneous base in order to increase the concentration of OH<sup>-</sup> that plays a role in the alcohol activation. Nonetheless, recent researches dedicated to substitute the homogeneous base effects by other strategies, such as the use of other precious metals (or a combination of them), different promoters and/or basic solids as supports, are also included.

### 3.3.1. Precious metal containing catalysts

Gold-based catalysts are active and selective when HMF must be oxidized to FDCA under high pH conditions. Their main drawback deals with their stability. Even if no Au lixiviation associated to usual high pH is detected, an important increase of the Au particle size along the reaction time is the main cause of deactivation. Different

strategies to avoid or minimize this problem have been tried. Several supports, such as TiO<sub>2</sub>, CeO<sub>2</sub>, Al<sub>2</sub>O<sub>3</sub>, hydrotalcite, Y-zeolites and C have been tested. Using nano-particulate ceria as support, better activity and selectivity results were obtained compared to titania or carbon supported catalysts (Table 6, entry 1) associated to more stable Au particles.<sup>167</sup> However, the activity of ceria-supported catalysts is strongly related to a good interaction between Au particles. For example, if the surfactant used to generate Au nanoparticles is not totally eliminated, it reduces the ceria-gold interaction and the catalyst behavior deteriorates.<sup>168</sup> Some interesting results were also obtained using alumina as support, if Au was incorporated by the direct anionic exchange procedure.<sup>169</sup>

**Table 6.** Summary of HMF transformation into FDCA with different precious metals containing catalysts in batch reactors.

Entry	Catalyst	Operating conditions					Catalytic properties			Ref.
		Temp. (K)	Pressure (MPa)	time (h)	[Fructose] (wt%)	NaOH/HMF molar ratio	Y <sup>a</sup> (%)	Productivity (mol <sub>FDCA</sub> (mol <sub>act. phase</sub> h) <sup>-1</sup> )		
1	Au/CeO <sub>2</sub>	403	1 (air)	5	1.8	4	84	107.5		167
	Au/TiO <sub>2</sub>									
2	Au/CeO <sub>2</sub> -TiO <sub>2</sub>	368	1 (O <sub>2</sub> )	4	n. r.	4	91	22.7		168
	AuCu/CeO <sub>2</sub> /TiO <sub>2</sub>									
3	Au/Al <sub>2</sub> O <sub>3</sub>	303	1 (O <sub>2</sub> )	4	1	4	99	24.7		169
4	Au/SiO <sub>2</sub>	353	1 (O <sub>2</sub> )	4	0.3	2 <sup>c</sup>	50	>15		170
5	Au/CeO <sub>2</sub>	343	1 (O <sub>2</sub> )	4	1	4	92	18		171
6	Au/C	363	1 (O <sub>2</sub> )	4	0.36	2	75	13		172
7	Au/Y-zeolite	333	0.3 (O <sub>2</sub> )	4	6.9	4	100	18.3		173
8	Ru(OH) <sub>x</sub> /CeO <sub>2</sub>	413	0.25 (O <sub>2</sub> )	6	0.63	n. r.	35	1.2		174
9	Ru(OH) <sub>x</sub> /MgAl <sub>2</sub> O <sub>4</sub>	413	0.5 (O <sub>2</sub> )	18	0.63	n. r.	55	0.6		175
10	Ru/ZrO <sub>2</sub>	393	0.5 (O <sub>2</sub> )	18	0.63	n. r.	97	2.5		176
11	Ru/ZrP <sup>b</sup>	423	0.1 (O <sub>2</sub> ) flow	12	1.4	10 eq. <sup>d</sup>	31/34	1.7		177
12	Ru/AC	373	0.4 (air)	48	0.67	4 <sup>c</sup>	93	2		178
13	Ru/AC	423	0.4 (air)	48	1.26	2.4 wt, HT	78.2	n. r.		179

Solvent: water; n. r.: not reported; <sup>a</sup> All the yields are provided at HMF conversions near 100%; <sup>b</sup> Solvent: p-chlorotoluene; <sup>c</sup> base: NaHCO<sub>3</sub>; <sup>d</sup> base: KOH

**Table 6.** Summary of HMF transformation into FDCA with different precious metals containing catalysts in batch reactors (continuation).

Entry	Catalyst	Operating conditions					Catalytic properties			Ref.
		Temp. (K)	Pressure (MPa)	time (h)	[Fructose] (wt%)	NaOH/HMF molar ratio	Y <sup>a</sup> (%)	Productivity (mol <sub>FDCA</sub> (mol <sub>act.phase</sub> h) <sup>-1</sup> )		
14	Ru/MnCo <sub>2</sub> O <sub>4</sub>	393	2.4 (air)	10	1.26	n. r.	99	3.5		180
15	Pt/ZrO <sub>2</sub>	373	4 (air)	12	1.26	2 <sup>b</sup>	95	7.7		181
16	Pt/Fe-C	363	O <sub>2</sub> flow	4	0.2	0.2 mmol <sup>c</sup>	100	1.7		182
17	Pt(Bi)/C	373	4 (air)	6	1.25	2 <sup>c</sup> 4 <sup>b</sup>	98	16		183
18	Pt/Ce-BiO <sub>x</sub>	333	1 (O <sub>2</sub> )	0.5	1.9	4	98	400		184
19	Pt/Ce-BiO <sub>x</sub>	363K	1 (O <sub>2</sub> ) flow	10	0.3	2 <sup>b</sup>	>99	1.1		185
20	Pt/C	343	0.69 (O <sub>2</sub> )	4	1.9	2	2.6	n. r.		186
21	Pt/ZrO <sub>2</sub>	373	0.4 (O <sub>2</sub> )	12	0.5	n. r.	97	19		187
22	Pt/CeO <sub>2</sub> -NC	383	0.4 (O <sub>2</sub> )	8	0.1	n. r.	100	40		188
23	Pd/ZrO <sub>2</sub> -La <sub>2</sub> O <sub>3</sub>	363	0.1 (O <sub>2</sub> ) flow	8	0.35	NaOH flow	90	11.2		189
24	Pd/C-Fe <sub>3</sub> O <sub>4</sub>	353	0.1 (air) flow	4	0.63	0.5 <sup>d</sup>	92	0.05		190
25	γ-Fe <sub>2</sub> O <sub>3</sub> @HAP-Pd	373	0.1 (O <sub>2</sub> )	6	0.63	0.5 <sup>d</sup>	93	2.5		191
26	PdNP	373	0.1 (air) flow	7	0.25	NaOH flow	90	0.25		192
27	Fe <sup>III</sup> -POP-1	373	1 (air)	10	1.9	n. r.	79	7.8		193
28	NNC	353	0.1 (O <sub>2</sub> )	48	0.79	n. r.	80	0.006		194
29	MnO <sub>x</sub> -CeO <sub>2</sub>	383	2 (O <sub>2</sub> )	6	0.63	0.25 <sup>b</sup>	84	0.091 <sup>e</sup>		195
30	CuO-MnO <sub>2</sub> -CeO <sub>2</sub>	403	2	12	0.19	n. r.	71	0.042 <sup>f</sup>		196

Solvent: water; n. r.: not reported; <sup>a</sup> All the yields are provided at HMF conversions near 100%; <sup>b</sup> base: NaHCO<sub>3</sub>; <sup>c</sup> base: Na<sub>2</sub>CO<sub>3</sub>; <sup>d</sup> base: K<sub>2</sub>CO<sub>3</sub>; <sup>e</sup> Mn is taken as the active metal; <sup>f</sup> Cu is taken as the active metal

Mesoporous supports have also been used to avoid or limit the Au particles sintering, as an alternative to a strong interaction with the support. Mesoporous silica,<sup>170</sup> ceria<sup>171</sup> or supercage Y zeolite<sup>173</sup> have been tested, proving the interest of this approach. Basic carbon materials with a low density of functional groups show a better behavior as Au supports than acidic carbons<sup>172</sup>. In order to avoid the use of NaOH addition, basic supports, like hydrotalcites, have also been tested<sup>197,198</sup>, but a fraction of those supports is

almost stoichiometrically leached, and used in the reaction as a substitute of NaOH, provoking the catalyst degradation. A similar behavior was observed when MgO was used as support: excellent activity results, but Mg ions leaching.<sup>199</sup> A possible solution for this problem is to dilute the basic MgO within the inert and inactive MgF<sub>2</sub>. Lower but interesting activities were measured, and no Mg leaching was detected.



Similar to other catalytic applications, Ru has been tested in the HMF oxidation to FDCA looking for active and stable catalysts avoiding, if possible, the operation at high pH values. Different supports have been studied, such as titania, alumina, zirconia, ceria, magnesia, lanthana, hydrotalcite, hydroxyapatite, spinels and active carbon. As in the case of Au-based catalysts, ceria supported ones showed higher activities and selectivities than those supported on titania.<sup>174</sup>

Hydrotalcite, magnesia and  $\text{MgAl}_2\text{O}_4$  spinel were also tested as supports for  $\text{Ru}(\text{OH})_x$  species. All these catalysts proved to be active in the HMF oxidation to FDCA, but, even if Ru leaching was almost negligible in all three systems, only the spinel support generated quasi-stable catalysts.<sup>175</sup> Zirconia is an interesting Ru support for the base-free oxidation of HMF to FDCA.<sup>176</sup> However, high Ru contents (around 5 wt.%) are required to obtain full yield to FDCA in acceptable reaction times, and the best results were obtained when nanoparticles of Ru were formed on  $\text{ZrO}_2$  prepared using  $\text{SiO}_2$  aerogel templates (Table 6, entry 10).

Zirconium phosphate was also used as support for Ru oxidation catalysts, but suitable results were only obtained if high amounts of a base ( $\text{K}_2\text{CO}_3$ ) were added to the reaction mixture.<sup>177</sup> When activated carbons were used as Ru supports, the pretreatment of the carbon surface clearly modified the final activities of the Ru supported catalysts.<sup>60</sup> The introduction of acidic groups by an oxidative treatment was detrimental, but no influence could be detected when basic functionalities were generated. Another limitation of carbon-supported catalysts is associated to the balance between the activation procedure to guarantee a good Ru dispersion and the loss of hydrophobicity generated by the O-containing groups that appear on the carbon surface. If a commercial activated carbon is used as Ru support, high HMF conversions and FDCA selectivities can be obtained. but adding a base.<sup>179</sup> This base can be incorporated as an homogeneous hydroxyl ions generator, but better results were measured if they come from solid hydrotalcites. Not only Mg spinels are promising supports for Ru oxidation catalysts operating in base-free liquid aqueous solutions of HMF, but also others such as the Mn containing ones. A better activity was found for the  $\text{MnCo}_2\text{O}_4$  supported catalyst than when  $\text{MnCo}_2\text{CO}_3$  was used.<sup>180</sup> This could be explained as due to a higher surface Brønsted acidity of the  $\text{MnCo}_2\text{O}_4$  spinel.  $\text{MnO}_2$  and  $\text{CoO}_2$  solids were also used as supports and their poor results proved the importance of the spinel structure, if high activity and selectivity towards FDCA were desired. Catalyst recycling studies proved that after 5 uses under kinetics-controlled regime the activity of  $\text{Ru}/\text{MnCo}_2\text{O}_4$  catalyst remained constant.

Pt-based catalysts have also been evaluated in the selective oxidation of HMF to FDCA. Some of the studies were carried out in high pH media (Table 6, entries 15-20) and others tried to avoid the use of basic aqueous solutions (Table 6, entries 21-22). In all cases, both the size of Pt particles deposited and the interaction with the support of the HMF and intermediates were important features to achieve good activity and selectivity results. The reaction mechanisms reported are the same as the ones investigated using other active metals as catalysts and they do not depend on the

pH.<sup>186</sup> Similar supports as those used for Ru and Au catalysts have been studied. For example,  $\text{TiO}_2$  and  $\text{ZrO}_2$  in alkaline aqueous solutions were tested using air as oxidant.<sup>63</sup> The catalyst supported on titania proved to be a slightly more active than that supported on zirconia, and doping zirconia with lanthana or yttria did not generate any advantage.

Other possible supports are different carbonaceous materials. Pt nanoparticles were deposited on iron oxide-carbon microspheres.<sup>182</sup> The iron oxide core allowed magnetic separation and the carbon supported very active Pt nanoparticles, originating promising and stable oxidation catalysts in aqueous media. Using carbon-based supports, different researchers demonstrated that Bi-promoted Pt catalysts show similar activities, but better stability in the HMF oxidation. Two alternatives have been considered: the impregnation of both Pt and Bi on the carbon support,<sup>181,183</sup> or the incorporation of Bi to a ceria support.<sup>184,185</sup> The role of Bi in ceria is facilitating the oxygen interchange, not only increasing the number of vacancies, but also modifying their environment. Comparable results have been attained operating in base-free aqueous solutions, where efficient HMF oxidation can be performed using Pt nanoparticles deposited on a low surface area zirconia,<sup>187</sup> or on other supports such as carbon nanotubes,<sup>200</sup> or on more sophisticated supports like nitrogen-doped-carbon decorated ceria.<sup>188</sup> This latter catalytic system showed high activity, selectivity and productivity (Table 4, entry 22). Even a higher productivity was measured using a magnetic graphene oxide-iron oxide as support.<sup>201</sup> Other promising supports investigated were N-doped carbon<sup>202</sup> or C-O-Mg solid containing very stable basic sites.<sup>203</sup> Even Pt nanoparticles, stabilized by polyvinylpyrrolidone (PVP), were tested in this reaction, but high activity and selectivity implied a quiet poor Pt productivity.<sup>204</sup>

Pd-based catalysts can also be used for the selective HMF oxidation to FDCA. In most cases, the process is carried out at high pH conditions, where different supports have been tested. When using metallic oxides, such as titania, alumina, zirconia or lanthana, a mixture of the last two oxides generated the most active catalyst.<sup>189</sup> Magnetic iron oxides decorated by carbon,<sup>190</sup> or hydroxyapatite,<sup>191</sup> allowed the preparation of Pd-based catalysts that can be magnetically recovered, but they showed low FDCA productivities. Pd PVP stabilized nanoparticles were also evaluated,<sup>192</sup> and their most interesting characteristic is the stability if used and preserved under basic conditions.

Moreover, bimetallic systems have also been studied in this oxidation reaction. For example, Pt-Ni on activated carbon showed, under base-free conditions, higher activities than the corresponding monometallic catalysts.<sup>205</sup> The alloying of Au with Pd proved to be a suitable strategy to improve the catalyst stability when using activated carbon,<sup>206</sup> or carbon nanotubes,<sup>207</sup> as support. This improved behavior is the result of the electronic interaction between Au and Pd when a solid alloy is formed.<sup>208</sup>

### 3.3.2. Base metal containing catalysts.

The high cost of precious metals has boosted the research on catalytic systems containing base metals. Pioneering work used a mixed metal ( $\text{Mn}_x\text{Fe}_y$ ) oxide catalyst together with 4 equivalents of

NaOH for the oxidation of FFCA into FDCA.<sup>209</sup> The catalytic activity was related to a synergetic cooperation among Mn(III), Mn(IV) and a hematite phase. The presence of the  $Mn_xFe_y$  catalyst in the first step of the reaction (oxidation of HMF into FFCA) promoted the formation of humins, which also deactivated the catalyst. In the case of mixed  $MnO_x-CeO_2$  oxides, the catalytic cycle involves the dissociative HMF adsorption onto  $Mn^{4+}$ , forming a metal-alkoxide and an adsorbed hydrogen.<sup>195</sup> The subsequent redox reaction consists in the oxidation of the alkoxide into the aldehyde and the reduction of  $Ce^{4+}$  to  $Ce^{3+}$ . In this step, a hydroxyl group from a base is required for the elimination of the  $\beta$ -hydrogen. The role of  $O_2$  is to close the catalytic cycle by transforming  $Ce^{3+}$  to  $Ce^{4+}$  and by reacting with the adsorbed hydrogen. As the reaction takes place in water, the aldehyde readily hydrates to form a geminal diol intermediate, which is transformed to FDCA by dehydrogenation. In order to get rid of the base, Ventura *et al.* added a third metal oxide to form a  $CuO-MnO_2-CeO_2$  material.<sup>196</sup> Moderate FDCA yields (i.e. 70.8%) were achieved with this catalyst; nonetheless, it deactivated due to the partial reduction of  $Cu^{2+}$  to  $Cu^0$  during the reaction. However, the activity was restored after a calcination step.

Two other research groups have studied the base-free HMF oxidation into FDCA in the absence of precious metals. Saha *et al.* synthesized a  $Fe^{III}$ -porous organic polymer ( $Fe^{III}$ -POP-1) containing basic porphyrin subunits and iron metal centers.<sup>193</sup> The proposed reaction mechanism involves the initial thermal autoxidation of HMF into peroxides, and next, a Fenton-type homolytic cleavage of the RO-OH bond over iron sites. Nguyen *et al.* reported a metal-free nitrogen containing nanoporous carbon (NNC) materials as an efficient catalyst for the HMF oxidation.<sup>194</sup> Quaternary N species, i.e. graphitic N, were the active catalytic sites. As observed in Table 4, entries 27-30, the activity of these species is significantly lower than that of precious metals, but noteworthy, the activity tests were carried out under base-free conditions. The amount of graphitic N in the catalyst could be increased by raising the calcination temperature to 1173 K. However, the catalyst lost activity upon reuse, which was related to the decrease in graphitic N in the spent sample. A Fe-Zr-O catalyst yielded a 61% FDCA under base-free conditions, but utilizing ionic liquids.<sup>210,211</sup>

### 3.3.3. Alternative reactants to 5-hydroxymethylfurfural.

It is well known that HMF production faces some relevant issues that makes its transition to industrial scale complicated: difficult extraction from the aqueous media in which is usually produced, not stable under the acidic conditions in which is produced and high HMF yields are only reported from fructose. Moreover, HMF oxidation reactions have to be performed in dilute solutions (< 2 wt%), as previously noted.<sup>212</sup> However, it must be taken into account that 5 wt% is the minimum reactant concentration recommended for viable industrial applications.<sup>152</sup> Recently, the acetalization of HMF with 1,3-propanediol was proposed to stabilize the reactive formyl group.<sup>213</sup> A 10 wt% aqueous solution of this acetal could be selectively converted to FDCA (94% yield) using an Au/ $CeO_2$  catalyst and  $Na_2CO_3$  as a base. When HMF was used as reactant in the same concentration, the FDCA was as low as 28%.

5-(Chloromethyl)furfural (CMF) is a functionally equivalent alternative to HMF. However, due to its lipophilicity and stability under acidic conditions, it is easier to isolate,<sup>214</sup> and it can be obtained in higher yields from raw biomass.<sup>215</sup> The simple heating of CMF in DMSO at 150 °C for 18 h gives DFF in 81% yield.<sup>216</sup> Lower DFF yields (i.e. 54) were obtained when using a  $Cu/SiO_2$  catalyst and pyridine N-oxide as the oxidant.<sup>217</sup> Mascal *et al.* proposed furan-2,5-dicarbonyl chloride (FDCC), that can be obtained from DFF by heating in tert-butyl hypochlorite, as an alternative to FDCA. Compared to FDCA, FDCC is soluble in common organic solvents and can be also used as starting material to produce polyethylene furanoate (PEF).<sup>218</sup>

## 4. Oxidation of furfural

The importance of furfural (FUR) in the context of valorisation of biomass was already recognised more than ten years ago when DOE named it, like some other molecules described above, one of the top 10 biomass-derived platform molecules from which biorefineries could be deployed.<sup>219</sup> At that time, FUR was already a commodity with important applications in the chemical industry. The relevance of FUR has continued to grow and holds the promise of a better future: annual world market amounted to 300 kTon in 2013 and it is forecasted to increase to over 625 kTon in 2020 (worth over 1,200 million USD). Its production technology relies on the acid-catalysed dehydration of the pentoses present in lignocellulosic agroresidues (like sugar cane bagasse, corncobs and grain hulls).<sup>220</sup> Furfuryl alcohol accounts for most of its production (83 % in 2013), but a wide variety of other interesting transformations to chemicals and biofuels have been demonstrated at laboratory scale.<sup>10</sup> Some advancements in the production of FUR may result in more cost-effective technologies,<sup>221</sup> what will boost the viability of all FUR derivatives.

Especially relevant are the products derived from FUR oxidation: maleic acid (MAC), maleic anhydride (MA), succinic acid (SAC), furanones, furan-2-acrolein (F2A), furoic acid and furoate esters. Although these transformations are not commercial yet, in some cases, directly drop-in products currently derived from oil can be obtained.

The right selection of the reaction conditions (i.e. type of oxidant and catalyst, reaction temperature and pressure, time of reaction, reaction media, among others) is a key issue when selectively targeting one of the multiple different products that can be obtained by oxidation of furfural. The challenge is the selective production of one of the derivatives that calls for the correct selection of the oxidant ( $O_2$  and  $H_2O_2$ ) and, especially, the catalytic technologies (gas phase, liquid phase, chemocatalysis, electrocatalysis and photochemistry). A summary of the different technological approaches for the oxidation of furfural and of their most relevant aspects are summarised beneath.

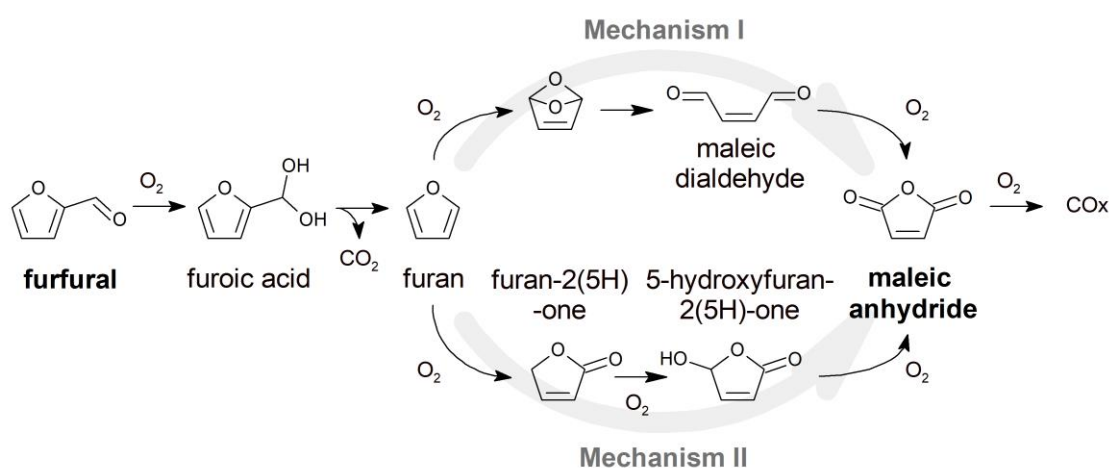
### 4.1 Production of C4 diacids and furanones

#### 4.1.1 Production of maleic anhydride in gas phase using $O_2$ as oxidant

The global production of maleic anhydride (MA) in 2012 reached 1,780 Kton with a trade worth over 314 million USD<sup>220</sup>. Important

derivatives of MA are, among others, unsaturated polyester resins, agrochemicals, food additives, lubricating oil additives, pharmaceuticals. Especially relevant are succinic acid,  $\gamma$ -butyrolactone (GBL), 1,4-butanediol (1,4-BDO) and tetrahydrofuran (THF) which are obtained by hydrogenation processes.<sup>222</sup> MA is a petrochemical,<sup>223</sup> which is obtained mainly by butane and benzene oxidation, although the latter accounts for a minor part. Several routes have been proposed for turning MA into a renewable product via oxidation of biomass-derived platform molecule, such as levulinic acid (LA), butanol or HMF.<sup>224</sup> The attractiveness of the FUR route relies on the fact that FUR is easily accessible in chemical industry.

The gas phase oxidation of FUR to produce maleic anhydride (see Figure 6 for a description of the most likely reaction pathways) was known at the beginning of 20<sup>th</sup> century.<sup>225,226</sup> The reaction is conducted at atmospheric pressure. Later in the 70s, some investigation of the kinetics and reaction mechanism was reported.<sup>227–231</sup> Surprisingly, despite these early reports, there is a remarkable lack of systematic studies to develop more efficient catalytic technologies and to unveil important practical and fundamental issues, such as the effect of contact time, reaction temperature, concentration of FUR and O<sub>2</sub>, deactivation phenomena, and catalytic surface species involved in the reaction mechanism.



**Figure 6.** Reaction mechanism proposed for the oxidation of furfural with O<sub>2</sub>. Mechanism I and II from references <sup>232</sup> and <sup>233</sup>, respectively.

Regarding the solid catalysts that have been used for this reaction, systems like alumina supported mixed V-Mo-Fe-P oxide,<sup>225–228</sup> and mixed Sn-V oxide,<sup>230</sup> were used in the early investigations; more recently the catalytic behaviour of alumina-supported vanadium oxide<sup>224,234</sup> and unsupported vanadium phosphates<sup>235</sup> have been explored.

Table 7 gathers a summary of catalytic properties and reaction conditions. No other transition metal oxides have been explored. In the case of vanadium oxide, besides Al<sub>2</sub>O<sub>3</sub>, other supports like SiO<sub>2</sub>, ZrO<sub>2</sub>, anatase and rutile TiO<sub>2</sub>, and CeO<sub>2</sub> have also been studied, but their MA yield were lower than that obtained with the VO<sub>x</sub>/Al<sub>2</sub>O<sub>3</sub> system.<sup>236</sup> In VO<sub>x</sub>/Al<sub>2</sub>O<sub>3</sub> systems, polyvanadate species dispersed over the alumina surface present higher intrinsic reaction rates for MA formation than highly dispersed isolated monovanadates, or crystalline V<sub>2</sub>O<sub>5</sub> species. Consequently, the best alumina-supported VO<sub>x</sub> catalyst is that with the largest amount of well-dispersed polyvanadate species, which is accomplished with 8–10 atoms of V per nm<sup>2</sup> of alumina support.<sup>234</sup>

Kinetics investigations conducted on alumina supported mixed V-Mo-Fe-P oxide,<sup>228</sup> and mixed Sn-V oxide,<sup>230</sup> revealed that the reaction proceeds via a redox Mars-van Krevelen mechanism in which FUR is oxidised by the active site, and the consequently so-formed reduced V active sites are re-oxidised by gaseous O<sub>2</sub>.<sup>228–230</sup> The re-oxidation of the reduced vanadium sites was identified as

the rate-determining step. Reaction orders for FUR and O<sub>2</sub> were found to be equal to 1. Between 493 and 553 K, FUR was oxidised in two parallel competitive reactions, yielding MA or CO<sub>x</sub>, whereas at higher temperatures MA can also be deeply oxidized to carbon oxides.

Besides the products depicted in Figure 6, heavy products, frequently referred to as resins, are formed via the condensation of FUR with itself or with intermediates (or by-products). Resins can be cumulatively deposited over the catalyst surface or migrates downstream the reactor if the melting point allows it. Along with the CO<sub>x</sub> formation, resins constitute one of the major non-selective side-products of the reaction; yields to other products (like furoic acid, furan and furanones) are frequently low or negligible. Resins can inadvertently be overlooked because of the difficulty to analyse them by conventional analytic methods. The lack of carbon balance is an unequivocal signal of the formation of resins.

**Table 7.** Selective oxidation of furfural into maleic anhydride (MA) in gas phase, using O<sub>2</sub> as oxidant

Catalyst	Operating conditions			Catalytic properties		Ref	
	[FUR] (wt%)	O <sub>2</sub> /FUR molar ratio	GHSV (h <sup>-1</sup> )	Temp. (K)	X <sub>FUR</sub> (%)		Y <sub>MA</sub> (%)
VO <sub>x</sub> /Al <sub>2</sub> O <sub>3</sub>	0.25	40	1720	583	100	86	224,234
MoO <sub>3</sub> -V <sub>2</sub> O <sub>5</sub>	0.31	67	2160	543	>95	75	225
V <sub>2</sub> O <sub>5</sub>	0.12	180	600-1000	593	>95	25	228
VMoPO <sub>x</sub>	0.31-0.64	n. r.	15700-18000	573	n. r.	60 <sup>a</sup>	226
V-Mo-P/α-Al <sub>2</sub> O <sub>3</sub>	0.76	3	8000-36000	575-623	n. r.	n. r.	227
VPO	10	2	2400	633	100	90	235

n. r.: not reported; <sup>a</sup> MA selectivity

Long term deactivation studies have only been conducted on VO<sub>x</sub>/Al<sub>2</sub>O<sub>3</sub>,<sup>224</sup> VPO,<sup>235</sup> and MoO<sub>3</sub>-V<sub>2</sub>O<sub>5</sub><sup>225</sup> catalysts. In the latter case, a conditioning of the catalyst was observed along the period of study (60 weeks), that resulted in a continuous increase in the MA yield. In the case of VPO system, no deactivation was observed after 25 h of time-on-stream.<sup>235</sup> Remarkably, furan resins were not reported to be formed and very high MA yield was obtained in these systems under optimum conditions. On the contrary, the VO<sub>x</sub>/Al<sub>2</sub>O<sub>3</sub> unavoidably deactivates by deposition of maleates and resins over the catalyst surface.<sup>224</sup> Burning these deposits off at 773 K resulted in the full recovery of the catalytic activity. The rates of maleate and resin deposition and, consequently, the deactivation rate could be retarded by contacting the catalyst with the reaction mixture at high oxidizing potential (high reaction temperatures and/or high O<sub>2</sub>/FUR molar ratio).<sup>224</sup>

Thus, initially contacting the catalyst at 573 K with the reaction mixture (1 vol% FUR and 20 vol% O<sub>2</sub>), MA yield was initially close to 75% and around 60% after 15 h on stream. On the contrary, by starting the contact at low temperature (523 K), and then increasing the temperature, the yield of MA yield never exceeded 30% (under these experimental conditions, the catalyst was deactivated).

#### 4.1.2. Production of maleic acid in liquid phase using O<sub>2</sub> as oxidant

The liquid phase oxidation of furfural to MAc using O<sub>2</sub> is another alternative catalytic technology. The reaction requires moderate O<sub>2</sub> pressure (1-2 MPa), but the main advantage of this approach is that the reaction proceeds at lower temperatures than those required

for the gas phase O<sub>2</sub>-driven oxidation (363-373 K vs. 523-573 K). Further details of the investigation conducted so far are given below, but the main challenges of this process are the identification of robust solid reusable catalysts in aqueous solution, or in green solvents (chelating nature of the diacids can give rise to leaching concerns),<sup>237</sup> and preventing the undesirable and unselective formation of resins (O<sub>2</sub> triggers the oligomerization of FUR to resins). Besides the selectivity issue associated to the formation of resins, their deposition over the catalyst surface can also cause deactivation.

Table 8 lists the highest MAc yield obtained from oxidation of FUR and HMF with several catalysts. Homogeneous catalysts have been tested in this reaction and, so far, the best results were achieved using H<sub>5</sub>PV<sub>2</sub>Mo<sub>10</sub>O<sub>40</sub> polyoxometalate acid as catalyst and Cu(CF<sub>3</sub>SO<sub>3</sub>)<sub>2</sub> as co-catalyst, resulting in a yield of maleic anhydride of 54 % at ca. 100% conversion (at 383 K, 14 h and 2 MPa O<sub>2</sub> in acetic acid).<sup>238-240</sup> However, the use of solid catalysts looks a better option because it can easily be reused or, provided that the stability of the catalyst is reasonably good, implemented in a continuous flow operation.<sup>241-246</sup> It is worth stressing that in organic medium (usually acetic acid) higher yield is obtained and both maleic acid and anhydride can be produced (the sum of MA and MAc is tabulated). Thus, the highest yield so far reported was achieved with a Mo-V-O catalyst (Mo<sub>4</sub>VO<sub>14</sub>), that attained a combined MA and MAc yield of 65 %, after 16 h of reaction (393 K and 20 bar of O<sub>2</sub>).<sup>241</sup> A catalyst based on vanadium-oxo species immobilised over graphene oxide (modified with a Schiff base) rendered 62 % of

combined MAc-MA yield at lower temperatures (383 K and 8 h of reaction, although with double loading of catalyst).<sup>242</sup> When other solvents like acetonitrile, MIBK, ethanol, DMSO or toluene were

used, the yield was severely lowered. Other systems, like vanadium oxide nanosheets deposited over graphene oxide,<sup>245</sup> attained quite similar yield in acetic acid.<sup>241</sup>

**Table 8.** Liquid-phase oxidation of furfural and HMF to maleic anhydride (MA) and acid (MAc), driven by O<sub>2</sub> (batch reactor)

Catalyst	Operating conditions					Catalytic properties				Ref.
	Substr. (wt%) (solvent)	Temp. (K)	Pressure (MPa)	time (h)	O <sub>2</sub> /subst. molar ratio	Cat/substr. (wt%)	X <sub>S</sub> (%)	Main Product (MP)	Y <sub>MP</sub> (%)	
<b>Oxidation of furfural with homogeneous catalysts</b>										
H <sub>3</sub> PMo <sub>12</sub> O <sub>40</sub>	7.0 (H <sub>2</sub> O/C <sub>2</sub> H <sub>2</sub> Cl <sub>4</sub> )	383	2.0	14	12	190.0	50	MAc	35	238
H <sub>3</sub> PMo <sub>12</sub> O <sub>40</sub> Cu(NO <sub>3</sub> ) <sub>2</sub>	+ 17.4 (H <sub>2</sub> O)	371	2.0	14	4.5	210.0	95	MAc	49	239
H <sub>5</sub> PV <sub>2</sub> Mo <sub>10</sub> O <sub>40</sub>	+ 7.8 (MeCN/FA)	383	2.0	14	10	15.0	99	MA	54	240
<b>Oxidation of furfural with heterogeneous catalysts</b>										
Mo <sub>4</sub> VO <sub>14</sub>	1.8(FA)	393	2.0	16	n. r.	15.6	100	MAc/MA	65	241
VO-NH <sub>2</sub> -GO	1.8 (FA)	363	2.0	8	n. r.	5.2	82	MAc/MA	62	242
CaCu <sub>2</sub> P <sub>2</sub> O <sub>7</sub>	5.0 (H <sub>2</sub> O)	388	0.8	18	4.8	20.0	68	MAc	37	243
FeT(p-Cl)PPCI	6.3 (H <sub>2</sub> O)	363	1.2	10	14	16.7	96	MAc	44	244
VON-GO	1.8 (FA)	363	2.0	10	30	5.2	86	MAc/MA	60	245
FeT(p-Br) PPCI/SBA15	4.8 (H <sub>2</sub> O)	373	1.0	6	10	20.8	76	MAc	56	246
<b>Oxidation of HMF with heterogeneous catalysts</b>										
VO-NH <sub>2</sub> -GO	2.4 (FA)	363	2.0	4	n. r.	4.0	100	MAc/MA	95	242
VON-GO	2.4 (FA)	363	2.0	4	30	4.0	100	MAc/MA	91	245
VO(acac) <sub>2</sub>	8.0 (MeCN)	363	1.0	4	n. r.	10.6	99	MAc	52	247
H <sub>5</sub> PV <sub>2</sub> Mo <sub>10</sub> O <sub>40</sub>	9.2 (MeCN/FA)	363	1.0	8	6.3	9.2	100	MAc/MA	64	248
V <sub>2</sub> O <sub>5</sub> /SiO <sub>2</sub>	2.4 (FA)	373	0.5	4	7.5	14.3	99	MAc/MA	75	249
Fe <sub>3</sub> O <sub>4</sub> @SiO <sub>2</sub> -CoO <sub>x</sub>	1.0 (H <sub>2</sub> O)	383	1.0	8	8	50.0	79	SAC <sup>a</sup>	73	250

Substrate (S): FUR or HMF; n. r.: not reported; FA: formic acid, MeCN: acetonitrile; <sup>a</sup> Addition of NaOH results in the selective conversion of HMF to SAC instead to MAc.

Other catalytic systems based on Cu phosphate,<sup>243</sup> or Fe-metalloporphyrin, reached a lower MAc yield,<sup>244,246</sup> but they have been tested in aqueous medium. In principle, conducting the reaction in water is greener than in organic solvents, but it led to a lower MAc yield.<sup>241,242,245</sup> Remarkably, an iron-metalloporphyrin supported on SBA-15 yielded 56 % of MAc in aqueous solution, in 6

h of reaction, a value slightly lower than that mentioned above using vanadium-oxo species immobilised over graphene oxide, but in acetic acid medium (62 %). The iron-metalloporphyrin system also showed a better stability. Unfortunately, no study is available so far in organic solvents for these latter catalysts. In this context, other noteworthy strategy to overcome the problem of the

unselective oxidation of FUR to resins is the use of immiscible mixtures of organic solvents and water. This approach has been shown to improve the yield, but it has only been investigated with a homogeneous system (phosphomolybdic acid).<sup>238</sup> The organic solvent (tetrachloromethane, nitrobenzene, toluene, cyclohexane among others) allows the extraction of furfural from the aqueous phase, lowering its concentration. Oxidation takes place in aqueous phase, where the homogeneous catalyst is, FUR is continuously transferred to the aqueous phase as reaction proceeds (furfural apparently cannot polymerise in the organic solvent). Maleic acid remains principally concentrated in the aqueous phase, so product separation and reutilisation could in principle be feasible: the extraction of maleic acid from the aqueous layer would allow catalyst reutilisation and the organic solvent could also be recycled for further reaction runs. Maleic acid (and/or anhydride) can also be obtained from the liquid phase oxidation of HMF with  $O_2$ .<sup>242,247–251</sup> The oxidation of HMF to chemicals other than maleic acid (like 2,5-furandicarboxylic, 5-formyl-2-furancarboxylic acid and 2,5-diformylfuran) has already been reviewed in previous sections. Although, apparently, the oxidation of HMF to MAc should be more difficult than with FUR because, in practice, it involves the loss of two carbon atoms (cleavage of two C-C bonds), the experimental results show that it proceeds faster and more selectively than the oxidation of FUR. Table 6 also gathers the information so far obtained for HMF oxidation and the most active catalyst reported in mentioned references.

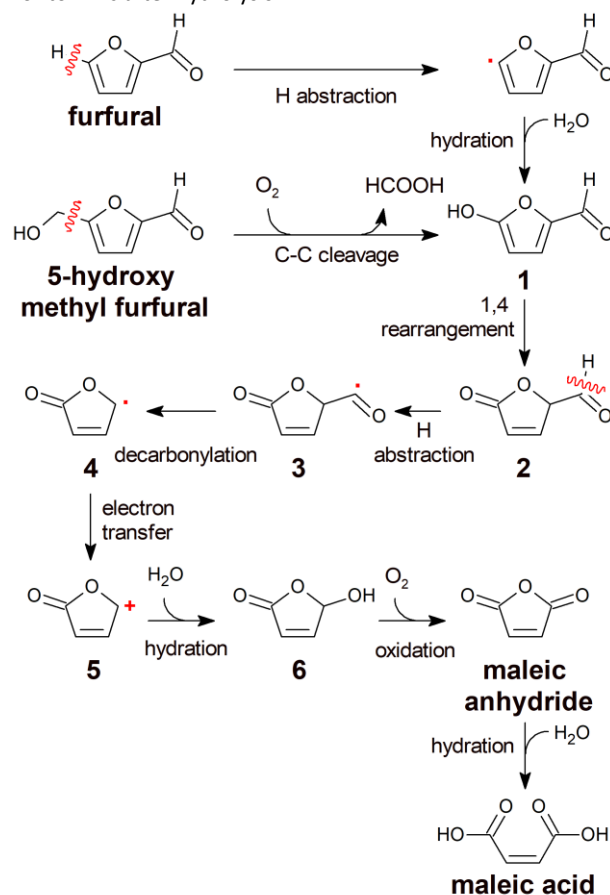
All the studied catalytic systems studied incorporate vanadium in its formulation, except a system based on cobalt oxide. Among the vanadium-based catalysts, the highest yield was also obtained, like for the furfural case, with vanadium-oxo species immobilised over graphene oxide (modified with a Schiff base), in acetic medium (in water, the yield was much lower).<sup>242</sup> In the case of cobalt oxide systems, magnetic separable Co oxide deposited on  $SiO_2$  covered  $Fe_3O_4$  nanoparticles ( $Fe_3O_4@SiO_2$ ) was investigated.<sup>250</sup> In the latter system, the maximum MAc yield reported was 59% at complete conversion (10 % of succinic acid was also observed). The reaction was conducted in aqueous phase, though no information was disclosed about the effect of solvent on the catalytic performance. Remarkably, the addition of NaOH to the reaction medium resulted in an exceptionally high succinic acid yield (73%).

A major issue requiring further experiments is the robustness of catalysts in the oxidation of either FUR or HMF. The catalyst stability has been evaluated conducting consecutive runs in batch mode, equivalent to few tens of hours in operation (Table 6). However, there is a lack of data about the catalyst stability under continuous long-term operation (at least for few days), a key aspect to reveal the long-term impact of any cause of deactivation. In the case of FUR, deactivation was observed in batch mode, not very pronounced, but persistent and evident after few runs (the experiments were conducted in acetic acid, or in water).<sup>242–246,252</sup> In the case of HMF, deactivation was also observed for the catalysts investigated in acetic acid.<sup>242,245,249</sup> Remarkably, the  $Fe_3O_4@SiO_2-CoO_x$  system was reused for 9 runs in aqueous medium, a less harsh medium than acetic acid, without significant deactivation.<sup>250</sup>

Leaching of active sites and deposition of heavy products are pointed as probable causes of deactivation with medium impact, although more research is needed to confirm it and to discriminate their real impact on deactivation.

Regarding the reaction pathway, it has been proposed that the oxidation involves free-radical species, since the reaction is severely suppressed by the incorporation of free radical inhibitors.<sup>240,245</sup> Another experimental fact is that formic acid and CO and  $CO_2$  have been observed as by-products of the reaction.<sup>240,245</sup>

Figure 7 schematized the routes proposed for vanadium-based systems. For HMF, the reaction would begin with scission of the C-C bond between the furan ring and hydroxymethyl group, catalysed by simultaneous electron and oxygen transfer processes that require the reduction of  $V^{5+}-O$  to  $V^{4+}-O$  species. This step leads to the formation of formic acid and species [1], the latter subsequently suffers a 1,4- rearrangement yielding species [2]. The H radical abstraction from [2] results in the formation of radical [3], whose decarbonylation gives rise to species 4 ( $CO_x$  are released), which is oxidized to cation [5]. This latter is attacked by  $H_2O$  to form 5-hydroxy-furan-2(5H)-one (species 6) that can be further oxidized to MA or to MAc after hydrolysis.

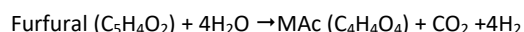


**Figure 7.** Proposed mechanism for the oxidation of FUR with  $O_2$  in liquid phase (adapted from reference <sup>253</sup>)

In the case of furfural, formic acid is not formed (there is no hydroxymethyl group to be released). The reaction starts by the homolytic abstraction of an H radical to form a furfural radical. The

latter is attacked by water to render the species [1], and the rest of steps are common to HMF oxidation. The pathways presented in Figure 7 are far from being fully disclosed and still require further experimental and/or theoretical chemistry support.

On the other hand, the electrochemical oxidation of furfural using a PbO<sub>2</sub> anode rendered a maximum yield of 65 % of MAC, using a 0.1 wt% of FUR in 0.1 M H<sub>2</sub>SO<sub>4</sub> solution (in basic medium, furfural is oxidised to furoic acid) and at 2.0 V vs. RHE.<sup>254</sup> It was proposed that the overall reaction in the cell was:



H<sub>2</sub>O oxidation competes with furfural selective oxidation and the faradaic efficiency was 46 %. Other anodes resistant to acid environment like Pt or MnO<sub>2</sub> gave lower MAC yields and faradaic efficiency. A reaction pathway is proposed where FUR is oxidised to 2-furanol (that must be at equilibrium with the corresponding 2- and 5-furanones) and furanol is then oxidised to MAC. Furoic acid was also proposed to be involved as an intermediate between FUR and 2-furanol.<sup>254</sup> Earlier investigations also reported the formation of β-formylacrylic acid as precursor of MAC.<sup>255,256</sup>

#### 4.1.3 Production of succinic acid and/or maleic acid in liquid phase using H<sub>2</sub>O<sub>2</sub> as oxidant

The oxidation of FUR can also be carried out with aqueous H<sub>2</sub>O<sub>2</sub>. The reaction is conducted under very mild reaction conditions (between close to room temperature up to 343-363 K, and under autogenous pressure). Several products can be formed, but the highest yields were for succinic acid (SAC), maleic acid, furan-2(5H)-one (also known as 2(5H)-furanone or 5-furanone), and 5-hydroxy-2(5H)-furanone (also known as 5-hydroxyfuranone) (Figure 8, in bold). Besides these products, fumaric acid (FumAc), malic acid (MalAc), tartaric acid (TarAc), formic acid (FA) and furan-2(3H)-one are also detected, although at much lower yields (Figure 8, in italic). The selectivity to the different acids and furanones is strongly affected by the experimental parameters, i.e. temperature and time of reaction, type of solvent, H<sub>2</sub>O<sub>2</sub> concentration, and type and amount of catalyst. Furanones are intermediates of the diacids, so they are formed at shorter reaction times and/or lower H<sub>2</sub>O<sub>2</sub>/furfural molar ratio than those required for diacids. Fumaric acid is the *trans* isomer of maleic acid, whereas malic and tartaric acids result from the addition of H<sub>2</sub>O or H<sub>2</sub>O<sub>2</sub> to the maleic C=C double bond, being favoured at longer reaction time and the former at very high H<sub>2</sub>O<sub>2</sub>/furfural molar ratio. Formic acid can be the result from a deeper oxidation of diacids. FAc is also present in the reaction medium because furfural must lose one carbon atom to go from a C<sub>5</sub> to a C<sub>4</sub> compound. This carbon atom comes from the carbonyl group that is lost as formic acid, and the mechanism of reaction will be discussed below. This formic acid is actually the most important product of the reaction, and it cannot be mixed up with that resulting from a deep oxidation of furfural.

The catalysts and reaction conditions needed to produce succinic acid will be first summarised, afterwards those for maleic acid. This section will end with 5-furanone and 5-hydroxyfuranone, the latter

can also be produced by photo-oxidation of furfural, besides oxidation with aqueous H<sub>2</sub>O<sub>2</sub>.

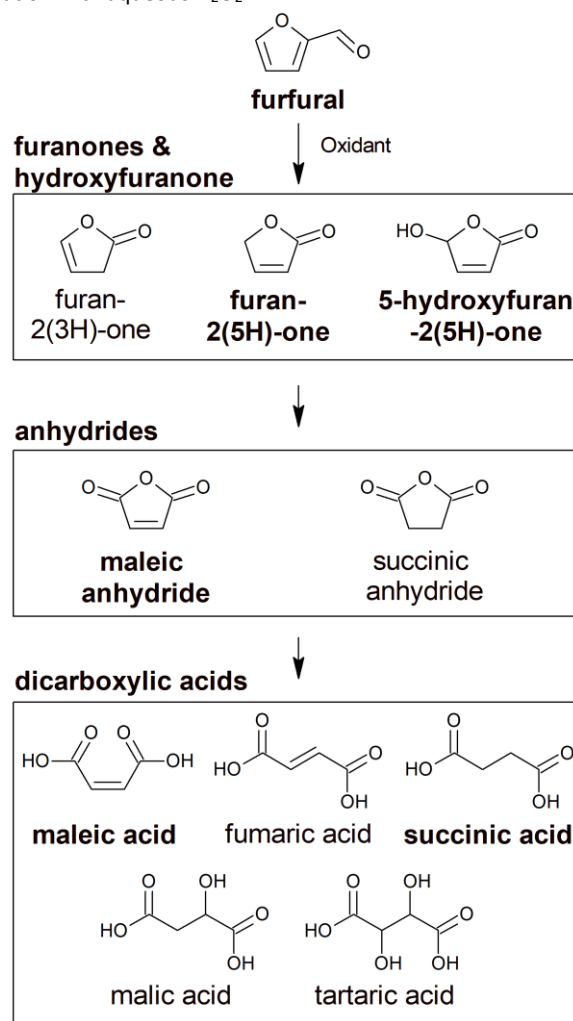
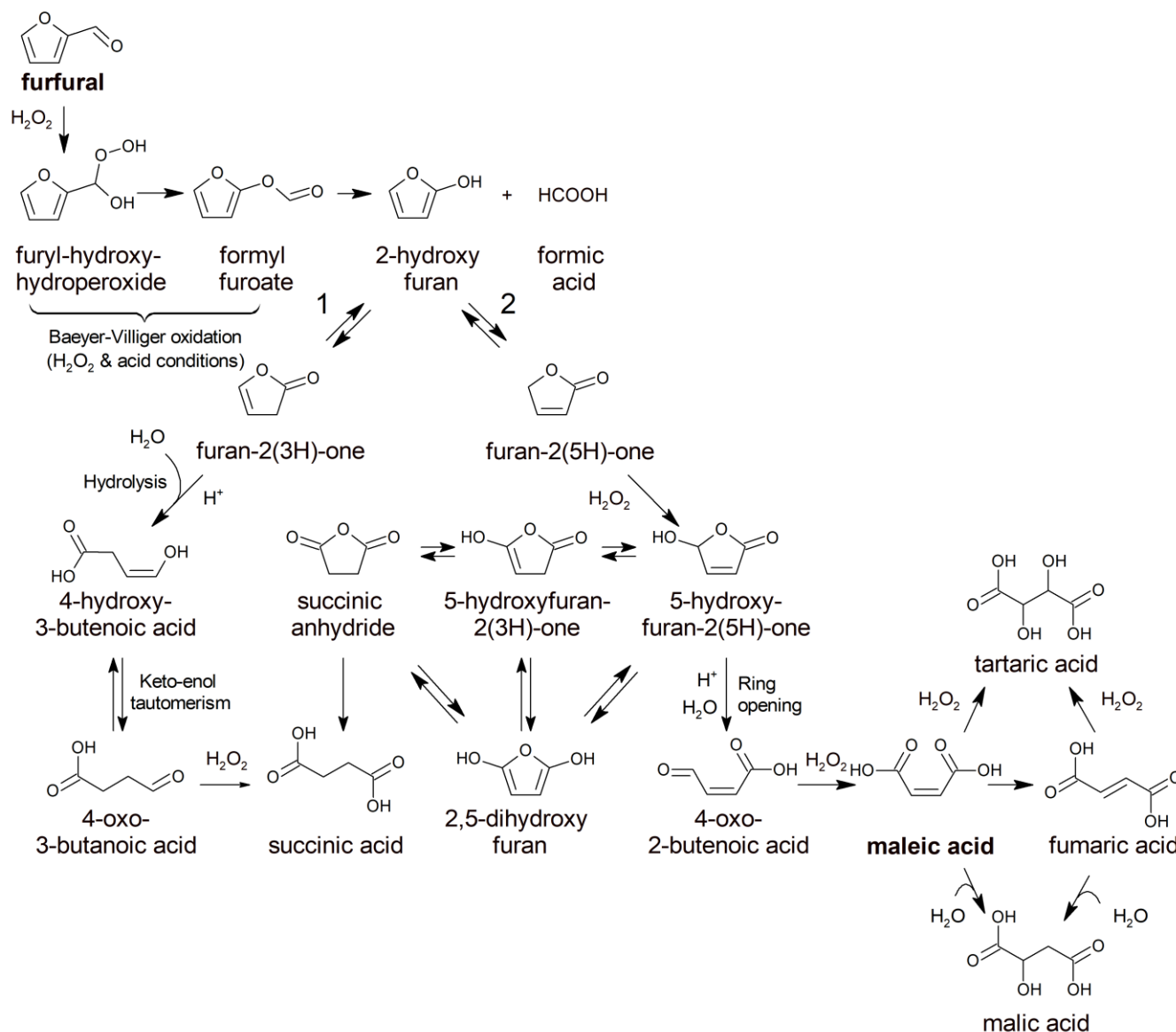


Figure 8. Main products of furfural oxidation with H<sub>2</sub>O<sub>2</sub>

##### 4.1.3.1. Production of succinic acid

Figure 9 exhibits the mechanism proposed by Ebitani *et al.* for the oxidation of furfural to succinic acid with aqueous H<sub>2</sub>O<sub>2</sub>.<sup>257</sup> The reaction initiates with the Baeyer-Villiger oxidation of the aldehyde group of FUR, rendering formylformate ester (also known as formylxyfuran ester) that is rapidly hydrolysed in aqueous solution to 2-hydroxyfuran, releasing formic acid. This step represents in fact the loss of a carbon atom of FUR (C<sub>5</sub> compound) to form a C<sub>4</sub> alcohol. 2-hydroxyfuran is at keto-enol tautomeric equilibrium with two different furanones: 3- and 5-furanones. 3-furanone is hydrolysed to 4-hydroxy-3-butenoic acid, in practice at equilibrium with the most stable 4-oxobutanoic acid. The latter is further oxidised with H<sub>2</sub>O<sub>2</sub> to SAC. On the other hand, 5-furanone can be oxidised with H<sub>2</sub>O<sub>2</sub> to 5-hydroxyfuranone, which is at equilibrium with 4-oxo-2-butenoic acid (also known as 4-oxocrotonic acid or *cis*-β-formylacrylic acid); the latter is then further oxidised to MAC (which can be isomerized to fumaric acid). Malic and tartaric acids, formed at much smaller yields, are derived from the addition of H<sub>2</sub>O and H<sub>2</sub>O<sub>2</sub>, respectively, to the double C=C bond of MAC (or fumaric acid).



**Figure 9.** Mechanism proposed for the oxidation of furfural to succinic acid.

A slightly different mechanism was earlier proposed by Badovskaya *et al.*, in which 2-hydroxyfuran is directly oxidised to 5-hydroxyfuranone with  $\text{H}_2\text{O}_2$ , the latter is at equilibrium with 4-oxo-2-butenic acid, that is subsequently oxidised to maleic acid.<sup>258</sup> It has also been proposed that SAc could derive from 5-hydroxyfuranone via tautomeric equilibrium of either 2,5-dihydroxyfuran or 5-hydroxyfuran-2(3H)-one.<sup>259</sup> The stoichiometric

amount of  $\text{H}_2\text{O}_2$  required for converting FUR to SAc is 2, although a higher amount is needed to accelerate the reaction rate, as well as to compensate the unselective decomposition of  $\text{H}_2\text{O}_2$ , or its consumption in other unselective reactions like deep oxidation to FAc. Thus  $\text{H}_2\text{O}_2/\text{FUR}$  mol ratio between 3-4 is frequently used, but reaction time must also be considered because short reaction times rendered 3-furanone rather than SAc. Nevertheless, it is also



important to bear in mind that the problem with this complex mechanism is the control of selectivity, since besides SAc formation, 5-furanone, 5-hydroxyfuranone or MAC production is unavoidable, irrespective the H<sub>2</sub>O<sub>2</sub>/FUR molar ratio used. Consequently, the right experimental conditions and catalyst must be selected to achieve a high selectivity to SAc.

A first family of catalysts that complies with this mechanism encompasses those that possess Brønsted acid sites. In general, acid catalysts are quite selective to the formation of SAc, with relatively low yields of 5-furanone, 5-hydroxyfuranone and MAC. The following have been studied: H<sub>2</sub>SO<sub>4</sub> and HCl,<sup>257,260,261</sup> organic acids like acetic acid,<sup>257,260,261</sup> formic acid,<sup>262,263</sup> p-toluenesulphonic acid,<sup>257,260,261</sup> poly-(styrene sulphonic acid),<sup>264</sup> betaine hydrochloride<sup>265</sup> and 1-(alkylsulfonic)-3-methylimidazolium chloride ionic liquid.<sup>266</sup> The latter are dissolved in the reaction medium (homogeneous catalysts). The reaction can actually progress without the addition of a catalyst,<sup>267</sup> being initially the reaction rate slow, but, upon formation of SAc, MAC and FAC (all Brønsted organic acids), the reaction accelerates.

Other non-soluble solids with Brønsted acid sites have also been tested, such as sulfonic resins (Amberlyst-15,<sup>257,260,261</sup> Nafion NR50<sup>257,260,261</sup> and Smopex 101)<sup>268</sup>, sulphonated β-cyclodextrin-derived carbon,<sup>269</sup> Nafion-silica composite (Nafion SAC13),<sup>257,260,261</sup> sulphonated graphene oxide,<sup>270</sup> and vanadyl or zirconium pyrophosphate and zirconium pyrophosphate supported on well-ordered mesoporous KIT-6.<sup>271</sup> Table 9 summarizes only the results obtained with heterogeneous catalysts, which are easier to reuse because they can be separated from the reaction medium by simple

filtration. Moreover, when considering an industrial application, they can be easily implemented in a more productive fixed bed continuous reactor. Betaine hydrochloride<sup>265</sup> and 1-(alkylsulfonic)-3-methylimidazolium chloride ionic liquid<sup>266</sup> (homogeneous) have shown interesting recyclability properties for few runs, but the reusing protocol of these homogeneous catalysts involved the use of organic solvents and evaporation steps to extract the product, which limit their industrial application. Amberlyst-15<sup>261</sup>, Smopex<sup>268</sup>, sulphonated carbon,<sup>269</sup> and sulphonated graphene oxide (GO)<sup>270</sup> gave quite high yield of SAc (74, 79, 81 and 88 %, respectively). The first three showed poor recyclability due to fouling by deposits and leaching of sulphonic groups, but sulphonated GO was recycled for six runs, exhibiting only a slight deactivation<sup>270</sup>.

A similar mechanism has been claimed to occur with catalysts with Brønsted basic sites (NaOH, Mg(OH)<sub>2</sub>, Ca(OH)<sub>2</sub>, Sr(OH)<sub>2</sub> and Ba(OH)<sub>2</sub>).<sup>272</sup> The problem is that the selectivity toward SAc was lower than that of acid catalysts. Thus, the highest SAc yield (33%) was achieved with Mg(OH)<sub>2</sub>, but the product with the highest yield corresponded actually to the formation of 5-furanone. Besides, the practical interest of these systems is more limited because of the formation of carboxylate salts by the neutralization of organic acids formed in the course of the reaction (formic, succinic, maleic, etc.), that unavoidably must result in catalyst deactivation. It has also been reported that a basic pH can give rise to the formation of other compounds different to that previously described, like 2-hydroxy-5-oxotetrahydrofuran-2-carboxylic acid.<sup>273</sup>

**Table 9.** Selective oxidation of furfural into succinic acid (SAc) in liquid phase using H<sub>2</sub>O<sub>2</sub> as oxidant

Catalyst	Operating conditions				Catalytic properties			Ref
	FUR (wt%)	H <sub>2</sub> O <sub>2</sub> /FUR molar ratio	Cat/FUR (wt%)	Temp. (K)	time (h)	X <sub>FUR</sub> (%)	Y <sub>SAc</sub> (%)	
Amberlyst-15	3.2	4	52	353	24	100	74	257,260,261
Nafion NR50	3.2	4	52	353	24	100	41	257,260,261
Nafion SAC13	3.2	4	52	353	24	100	28	257,260,261
Smopex 101	10.6	4	n. r.	353	24	100	65	268
C-SO <sub>3</sub> H	9.6	4.5	37.5	333	1	100	81	269
GO-SO <sub>3</sub> H	3.2	6	10.4	343	24	99.8	88	270
VZPK1	20 <sup>a</sup>	3	6.3	343	1	81.2	29	271

n. r.: not reported; solvent: water; <sup>a</sup> solvent: acetonitrile

Finally, regarding other oxidation processes with H<sub>2</sub>O<sub>2</sub> of other platform molecules different from furfural, it is worth mentioning that SAc can also be obtained from LA.<sup>274</sup> In this sense, tungstic acid has been used as catalyst, though a rather modest SAc yield (36%) was reached after 6 h at 363 K. Besides SAc, 3-hydroxypropanoic (3-HPA) was also produced with a yield of 7 % (among other minor products). Baeyer-Villiger oxidation of the ketone group can proceed in both sides of the carbonyl group

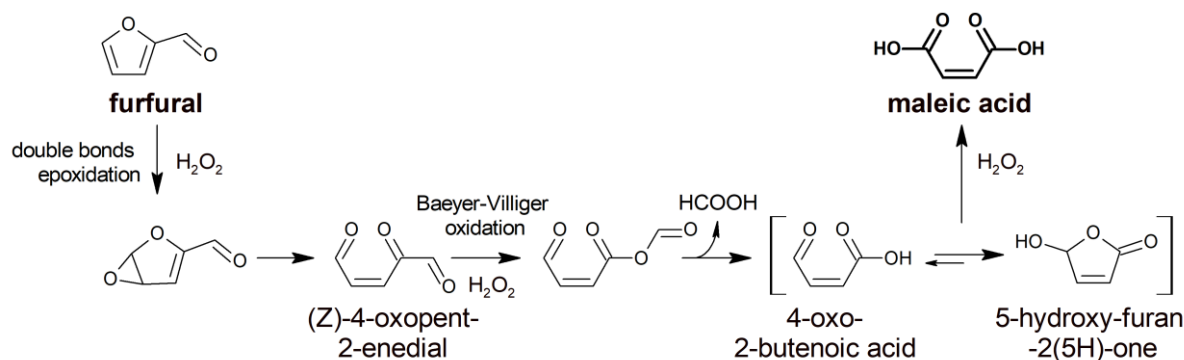
rendering methyl succinate, the precursor of SAc, and 3-acetoxypropanoic, the precursor of 3-HPA.

#### 4.1.3.2. Production of maleic acid

The stoichiometric amount of H<sub>2</sub>O<sub>2</sub> required for converting FUR to MAC is 3, but as in the case of SAc, a higher H<sub>2</sub>O<sub>2</sub>:FUR molar ratio is also needed to compensate the unselective reactions of H<sub>2</sub>O<sub>2</sub>. The selective formation of MAC using Brønsted acid or basic catalysts

previously mentioned is not feasible, even using H<sub>2</sub>O<sub>2</sub>/FUR molar ratio much higher than 3.<sup>264</sup> The experiments so far reported show that SAC is also formed at quite similar yields of MAc (besides other minor compounds such as 5-furanone and fumaric and malic acids). Brønsted acid or basic catalysts are better used for producing SAC. Interestingly, a titanium silicalite zeolite (TS-1) has been reported to catalyse the H<sub>2</sub>O<sub>2</sub>-oxidation of FUR with high MAc yields, attaining a 78% with a 5 wt% aqueous solution of FUR, a H<sub>2</sub>O<sub>2</sub>/FUR molar ratio of 7.5, at 323 K and after 24 h of reaction.<sup>275</sup> Minor yields of 5-hydroxy-furan-2(5H)-one (<10%), FAc (<5%), malic acid (<2%), furanones (<2%), and SAC (<2%) were also observed. Leaching of Ti and deposition of insoluble heavy by-products were identified as probable causes of deactivation. Catalytic activity was significantly recovered by removal of deposits by burning them off at 773 K. Ti leaching has a much lower impact, but threatens the very long term catalyst stability because it is irreversible.<sup>276</sup> It is noteworthy that the incorporation of  $\gamma$ -valerolactone (GVL) as co-solvent resulted in a better MAc yield than in only-water reaction. GVL also prevents the catalyst deactivation by suppressing the deposition of insoluble heavy by-products over the surface and cavities of TS-1 (it was reused for 17 runs without noticeable deactivation).<sup>277</sup> GVL also facilitates the final purification of MAc by precipitation of sodium maleate with NaOH addition due to its low solubility in GVL.<sup>277</sup> In addition, GVL is a renewable solvent, which has been used for the

production of FUR from biomass at high yield,<sup>221</sup> thus making it a suitable solvent to obtain MAc from biomass. Remarkably, the reutilization was performed with furfural directly obtained from corn cobs using GVL-H<sub>2</sub>O mixtures as solvent.<sup>277</sup> Finally, it has also been demonstrated that the post-synthesis treatment of TS-1 with tetrapropylammonium hydroxide also improved the MAc yield (82% at 343 K, 5 wt% FUR, H<sub>2</sub>O<sub>2</sub>/FUR molar ratio= 7.5, catalyst/FUR weight ratio= 1, 34 wt% of H<sub>2</sub>O and 42.5 wt% of GVL) because of the generation of mesoporosity within the zeolite primary particles and the increase in hydrophobicity of zeolitic channels and cavities.<sup>278</sup> The mechanism involved in the reaction with TS-1 must be different to that proposed for Brønsted acid/basic catalysts because of the low SAC yield attained. A different reaction mechanism (Figure 10) to that presented in Figure 9 depicts the reaction pathways proposed so far for this specific case.<sup>275</sup> Reaction begins with the epoxidation of the C=C bond at the farthest position of the aldehyde group of furfural (and not with its Baeyer-Villiger oxidation). The epoxide is subsequently isomerised to (Z)-4-oxopent-2-enedial, which undergoes a Baeyer-Villiger oxidation yielding the corresponding ester, whose subsequent hydrolysis releases formic acid and gives rise to 4-oxo-butenoic acid (also known cis- $\beta$ -formylacrylic acid). The latter C<sub>4</sub> compound is at equilibrium with 5-hydroxyfuranone. Further oxidation of one of these compounds renders MAc.



**Figure 10.** Mechanism via epoxidation of the furan ring using TS-1 as solid catalyst

Methyltrioxorhenium in solution, or polystyrene-supported, has also showed to render high MAc yields, with a 70% after 24 h at 293 K, using 5 wt% catalyst, and 5 equivalents H<sub>2</sub>O<sub>2</sub>. The incorporation of 1% HBF<sub>4</sub> is required as a co-catalyst. Succinic and furoic acids were also formed as minor products. The catalyst was reused for four additional runs, under similar experimental conditions, and the MAc yield did not decrease in successive runs.<sup>279</sup>

#### 4.1.4. Production of furanones in liquid phase

5-hydroxyfuranone finds applications for the synthesis of pharmaceuticals, insecticides and fungicides.<sup>280</sup> The interest in the synthesis of 5-furanone family of compounds is justified by their biological activity,<sup>263,281,282</sup> and possible applications as plant growth regulator, antiulcer and fish growth promoter.<sup>283</sup> The synthesis of

surfactants has also been proposed. More recently, it has been showed that 5-furanone can be readily converted to  $\gamma$ -butyrolactone (GBL) by hydrogenation, which is currently a petrochemical with multiple applications.<sup>284,285</sup>

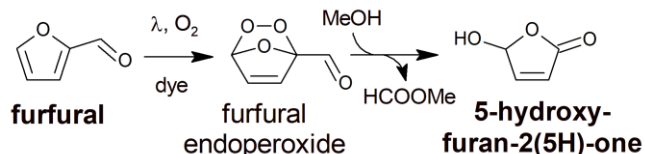
In principle, 5-furanone and 5-hydroxyfuranone are intermediates in the oxidation of FUR to diacids. Therefore, an optimization of the reaction conditions, especially of both H<sub>2</sub>O<sub>2</sub>/FUR molar ratio and reaction time, can stop the progress of the reaction to attain high yields of these furanones. Thus, the highest yield of 5-furanone close to 90% was reached after 1 h of reaction, at 298 K, from a 10 wt% FUR in a formic acid-water-methanol (10/10/80) solution, using a H<sub>2</sub>O<sub>2</sub>/FUR molar ratio of 1.8,<sup>286</sup> using a Pt(1wt%)/TiO<sub>2</sub>-ZrO<sub>2</sub> catalyst. A yield of 60–62% of 5-furanone was also obtained after 1.5 h of reaction, at 333 K, using ca. 17 wt% FUR in a biphasic

aqueous/organic system (1,2-dichloroethane or ethyl acetate, as organic solvents) and only formic acid as catalyst.<sup>263</sup> Regarding the 5-hydroxyfuranone, ca. 52 % of yield was obtained after only 0.5 h of reaction, at 343 K, using TS-1 as catalyst, a H<sub>2</sub>O<sub>2</sub>/FUR molar ratio of 7.5 and a 5 wt% FUR in a biphasic GVL-H<sub>2</sub>O system.<sup>277</sup>

The salts and oxides of transition metals of Groups V-VI (V, Nb, Cr, Mo) also catalyse the oxidation of FUR with H<sub>2</sub>O<sub>2</sub>. Thus, NaVO<sub>3</sub> preferentially led to 5-hydroxyfuranone and 4-oxo-2-butenic (totalling 33%), whereas NaCr<sub>2</sub>O<sub>7</sub> gave rise to 5-hydroxyfuranone (22%) and 5-furanone (25%), with a niobium acetate, a 34% 5-furanone and Na<sub>2</sub>MoO<sub>4</sub> yielded 5-hydroxyfuranone (30%) and 5-furanone (20 %). Other acids, such as maleic, malic, tartaric and fumaric acids, are also formed, but at lower yields. These catalysts are soluble in water, but insoluble metal oxide solids have also been studied, like Nb<sub>2</sub>O<sub>5</sub> and V<sub>2</sub>O<sub>5</sub>. Nb<sub>2</sub>O<sub>5</sub> yielded preferentially 5-furanone (29%) and 17 % (SAC),<sup>287</sup> whereas V<sub>2</sub>O<sub>5</sub> produced 5-hydroxyfuranone (55%) and MAc (25 % ).<sup>288</sup> Unfortunately, there is no study of stability of these V and Nb oxides.

Regarding the mechanism of reaction using these transition metal salts and oxides, it is well documented their capacity of forming very reactive metal peroxy complexes when reacting with H<sub>2</sub>O<sub>2</sub>. Consequently, it has been proposed that, instead of the formation of furyl-hydroxyhydroperoxide intermediate (Figure 10), the initial intermediates are ozonide-type adducts between furfural and these metal peroxy complexes.<sup>287</sup> These are further decomposed to the corresponding 2-furyl-formate, which evolves to furyl endoperoxides and subsequently to different oxidation products depending on both the type of metals and experimental conditions (see details of the mechanism in reference <sup>287</sup>).

Photochemical oxidation of FUR rendering 5-hydroxyfuranone has also been technically demonstrated (Figure 11). Photosensitizer dyes, like rose Bengal or methylene blue, are required to absorb in the visible region.<sup>280,289</sup> The reaction of FUR with the singlet oxygen generated during the photochemical sensitisation of O<sub>2</sub> results in the formation of an endo-peroxide, which is decarbonylated to afford the 5-hydroxyfuranone. Methanol was selected as the solvent and consequently methyl formate is formed through its reaction with the formic acid released by the decarbonylation.<sup>289</sup> Unfortunately, long-term operation studies of the very expensive sensitizer dyes were not presented.



**Figure 11.** Simplified scheme of the photo-oxidation of furfural to 5-hydroxy-furan-2(5H)-one.

The two main challenges in the oxidation processes of furfural are selectivity to the target product and catalyst stability. Thus, in the case of gas-phase oxidation of furfural with O<sub>2</sub>, the deactivation of the catalyst and the formation of heavy resins, that lowers the maleic acid yield, are the main drawbacks. Sensitivity analysis conducted in a recent techno-economic evaluation has concluded

that the process seems economically competitive. The price of furfural and the selectivity to maleic acid at full conversion (it must be above 80 %) are the factors with the highest impact on the final price.<sup>290</sup> At this respect, the results with VPO catalysts are very interesting and require further confirmation.<sup>235</sup>

The economic assessment has not been reported so far in the case of liquid phase O<sub>2</sub>-oxidation. It is conducted at lower temperatures so it may be possible that the selectivity requirements are not as high as those required for gas phase. Robustness of the reusable catalysts is also critical, especially the leaching of active phase. Consequently the results with Fe<sub>3</sub>O<sub>4</sub>@SiO<sub>2</sub>-CoO<sub>x</sub> system described in the reference are very promising.<sup>250</sup>

Regarding the liquid phase oxidation with H<sub>2</sub>O<sub>2</sub>, the techno-economic analysis mentioned above indicated that the high cost of H<sub>2</sub>O<sub>2</sub> makes unaffordable the commercialization of the maleic acid so obtained when confronted with petrochemical maleic acid, unless a much cheaper route to produce H<sub>2</sub>O<sub>2</sub> is identified.<sup>290</sup> The analysis was not extended to succinic acid, but considering its current price, this factor also threatens this application. Selectivity is also a real problem, because different products are formed depending on the time of reaction and H<sub>2</sub>O<sub>2</sub> concentration. Consequently, purification costs also complicate practical application.

#### 4.2. Production of furoic acid and furoates

The oxidation of the aldehyde group of furfural gives rise to furoic acid, a chemical with interesting applications in agrochemical, pharmaceutical, flavor and fragrances fields.<sup>291</sup>

The direct oxidation for furfural to obtain furoic acid is industrially produced *via* Cannizzaro reaction using NaOH as homogeneous catalyst,<sup>291,292</sup> which attacks to the carbon of the carbonyl group. The resulting tetrahedral intermediate collapses, re-forming the carbonyl and transferring a hydride to attack another carbonyl. In the final reaction step, the acid and alkoxide ions formed exchange a proton (Figure 12). In the presence of a very high concentration of base, the aldehyde first forms a doubly charged anion, from which a hydride ion is transferred to the second molecule of aldehyde to form carboxylate and alkoxide ions. Under ideal experimental conditions, the reaction produces only 50% of the alcohol and the carboxylic acid (two aldehydes disproportionate into one acid and one alcohol). To avoid low yields, it is more common to conduct the crossed Cannizzaro reaction, in which a sacrificial aldehyde, as formaldehyde, is used in combination with a more valuable chemical. Several strong oxidant agents have been used for the FUR oxidation to furoic acid, such as chromium,<sup>292-294</sup> and chlorite species.<sup>295,296</sup> However, none of them can be considered as green oxidants, since these are strongly harmful to health. Nowadays, the challenge is focused on selective oxidation of FUR to FurAc using less toxic reagents, such as H<sub>2</sub>O<sub>2</sub> or O<sub>2</sub>, and cheaper processes.

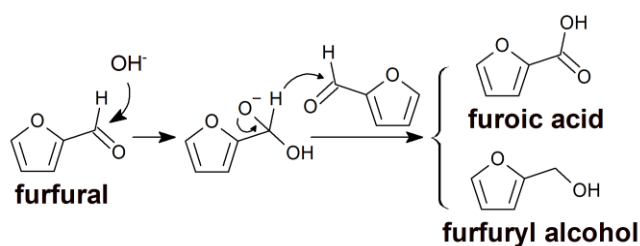


Figure 12. Mechanism of the Cannizzaro reaction.

In the last decades, different heterogeneous catalysts have been proposed for this oxidation process, although the competitive reactions generate undesired side-products.<sup>291</sup> Several authors have previously reported the use of noble metals for FUR oxidation. Thus, Parpot *et al.* obtained a FurAc yield up to 80% by an electro-oxidation process, using Ni-metal as electrode, in the presence of NaOH.<sup>297</sup> Other strategy frequently employed is the oxidation of FUR with  $\text{O}_2$  using noble metals, such as Pd, Pt, Au or Ag, supported on a large variety of metal oxides ( $\text{Fe}_2\text{O}_3$ , NiO,  $\text{Co}_3\text{O}_4$ , CuO,  $\text{CeO}_2$ ,  $\text{TiO}_2$ ,  $\text{Bi}_2\text{O}_3$  or  $\text{Sb}_2\text{O}_5$ ). In earlier studies, Gaset *et al.* optimized the experimental conditions to reach high selectivities toward FurAc in the presence of bimetallic PbPt catalysts.<sup>298,299</sup> They suggested that  $\text{Pb}^{2+}$  species interact with the  $\pi$ -electrons of the furan ring, while Pt is involved in the oxidation of FUR to furoic acid.<sup>299</sup> More recently, Tian *et al.* have obtained a high selectivity to FurAc using  $\text{Ag}_2\text{O}/\text{CuO}$  catalysts, with a maximum yield of 92%.<sup>300</sup> Douthwaite *et al.* have carried out the controlled catalytic oxidation of furfural to furoic acid, taking advantage of the synergetic effect of Au and Pd particles dispersed on  $\text{Mg}(\text{OH})_2$ , under mild conditions (303 K and  $\text{O}_2$  pressure of 0.3 MPa).<sup>301</sup> In all cases, the catalyst is susceptible to deactivate by the strong interaction of furoate with the active sites. This deactivation can be minimized by the co-feed of strong bases, but these exhibit environmental disadvantages and can also favor polymerization side-reactions.

In the last years, the use of metal-free catalysts has emerged in many organic processes as the selective oxidation of aldehyde to carboxylic groups. In this sense, a N-heterocyclic carbene (NHC) catalyst has shown an excellent catalytic behavior in the oxidation of furfural to furoic acid because, in the metal-free reaction, carbon atom bridged with two quaternary-N atoms in NHCs stabilizes carbene in air by the synergy of resonance and inductive effects.<sup>302</sup> The nucleophilic properties of NHCs can activate various aldehyde compounds and form highly reactive Breslow intermediates, which are involved in the oxidation process to yield carboxylic acids with molecular  $\text{O}_2$  at relatively low temperatures (Figure 13).

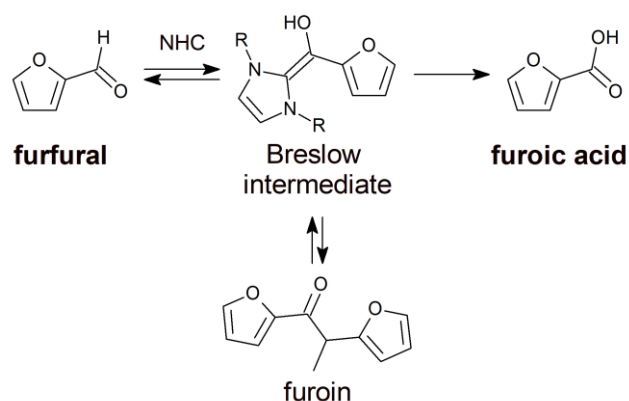


Figure 13. Synthesis of furoic acid from the Breslow intermediate

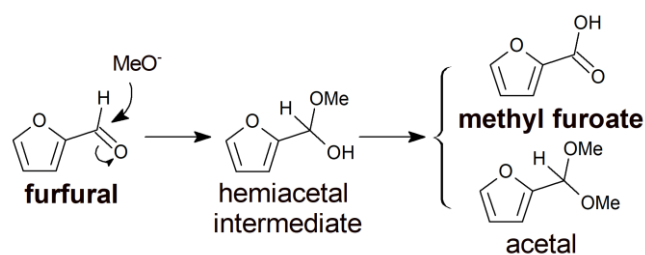
The oxidation of FUR to FurAc can also be carried out in aqueous medium. However, if an alcohol is used, this can be involved in the reaction, giving rise to cascade reactions such as oxidative esterification, forming alkyl furoates, or oxidative condensation leading to furan-2-acrolein (F2A). Alkyl furoates possess interesting applications for flavors and fragrances, as well as in the fine chemical industry. Traditionally, these are synthesized from FUR, using  $\text{KMnO}_4$  as oxidant and acetone as solvent, to form the FurAc, which reacts with an alkyl alcohol in the presence of  $\text{H}_2\text{SO}_4$ .<sup>291</sup> This process achieves high alkyl furoate yields, although the use of mineral acids, and especially the oxidant, has a negative environmental impact. In the last years, several heterogeneous catalysts have been reported to synthesize alkyl furoate, mainly Au-based catalysts (Table 10).<sup>303–306</sup>

In later studies, it was established that the choice of support plays a very important role in oxidative esterification. Thus, the group of Menegazzo pointed out that  $\text{Au}/\text{ZrO}_2$  exhibited an excellent catalytic behavior, even better than that of  $\text{Au}/\text{TiO}_2$  due to electronic effects and a high dispersion of small Au particles on  $\text{ZrO}_2$ .<sup>307–310</sup> This group also evaluated the incorporation of sulphate ions as donor species, which retard the crystallization and increase the surface area of  $\text{ZrO}_2$ , increasing the dispersion of Au particles.<sup>311</sup>  $\text{CeO}_2$  is another support that has shown a high potential in the oxidative esterification due to its ability to store and release oxygen, as well as its capacity to favor the formation of small Au particles, which has a direct influence on the amount of available active sites, although hardly influences on the selectivity pattern.<sup>312</sup> The oxygen mobility capacity can be increased if a small proportion of  $\text{Zr}^{4+}$  is incorporated into the  $\text{CeO}_2$  lattice, improving the catalytic activity in the oxidative esterification of FUR.<sup>313</sup> However, other authors have reported that a support without oxygen mobility like  $\text{MgO}$  also displays an excellent catalytic behavior in the oxidative esterification of aldehydes.<sup>314</sup>

As it has been previously indicated, the tailoring of the Au particle size is a key parameter in determining the catalytic activity. Thus, Menegazzo *et al.* compared the morphology of Au particles supported on  $\text{CeO}_2$  obtained by two methods: sol-immobilized and deposited-precipitated. They reported a full FUR conversion with Au particles synthesized by sol-immobilized due to its high

dispersion.<sup>315</sup> Calcination conditions and the interaction Au-support can also influence on the particle size.<sup>313,316,317</sup>

Generally, the aldehyde oxidation in the presence of an alcohol to give rise an ester takes place via a hemiacetal intermediate (Figure 14).<sup>318</sup> According to Casanova *et al.*, the hemiacetal is oxidized into ester or converted in its acetal, which is favored by the presence of Lewis acid sites.<sup>318,319</sup> Traditionally, supported Au catalysts led to the methyl furoate via hemiacetal, although the use of ZrO<sub>2</sub> can modify the selectivity pattern.<sup>309,318</sup> In this sense, the study of bimetallic AuPd and AuAg supported on hydroxyapatite nanorods has demonstrated that the incorporation of Pd and Ag favors remarkably the acetal formation. This process is even enhanced when the reaction temperature increases.<sup>320</sup>



**Figure 14.** Formation of methyl furoate using CH<sub>3</sub>OH as solvent, in basic medium under O<sub>2</sub> pressure

**Table 10.** Catalytic data and experimental conditions in the oxidative esterification of FUR

Catalyst	Operating conditions			Catalytic properties		Ref.	
	Catalyst loading (wt%)	Pressure (oxidant) (MPa)	Temp. (K)	time (h)	X <sub>FUR</sub> (%)		Y <sub>MFur</sub> (%)
Au/ZrO <sub>2</sub>	1.5	6 (O <sub>2</sub> )	393	3	99	98	308
Au/ZrO <sub>2</sub>	1.0	6 (O <sub>2</sub> )	393	3	82	72	309
Au/CeO <sub>2</sub>	2.2	6 (O <sub>2</sub> )	393	3	65	45	309
Au/TiO <sub>2</sub>	1.2	6 (O <sub>2</sub> )	393	3	20	18	309
Au/ZrO <sub>2</sub>	0.4	6 (O <sub>2</sub> )	393	3	99	97	310
Au/CeO <sub>2</sub>	1.5	6 (O <sub>2</sub> )	393	3	74	52	321
Au/ZrO <sub>2</sub>	1.0	6 (O <sub>2</sub> )	393	1	n. r.	28	313
Au/CeO <sub>2</sub>	1.5	6 (O <sub>2</sub> )	393	2	99	86	315
Au/HAP	5	t-butyl hydroperoxide <sup>a</sup>	393	3	76	71	320
Au <sub>0.8</sub> Pd <sub>0.2</sub> /HPA	5	t-butyl hydroperoxide <sup>a</sup>	393	3	94	93	320
Au <sub>0.8</sub> Ag <sub>0.2</sub> /HPA	5	t-butyl hydroperoxide <sup>a</sup>	393	3	89	88	320
Pd/HAP	5	t-butyl hydroperoxide <sup>a</sup>	393	3	86	2	320
Ag/HAP	5	t-butyl hydroperoxide <sup>a</sup>	393	3	72	18	320
Au/C	5	t-butyl hydroperoxide <sup>a</sup>	393	3	78	75	322
Pd/C	5	t-butyl hydroperoxide <sup>a</sup>	393	3	80	73	322
Pt/C	5	t-butyl hydroperoxide <sup>a</sup>	393	3	60	52	322
Ni/C	5	t-butyl hydroperoxide <sup>a</sup>	393	3	21	21	322
Co-N-C/MgO <sup>b</sup>	4	0.5 (O <sub>2</sub> )	373	3	93	90	323

n. r.: not reported; solvent: methanol; base: NaOH; <sup>a</sup> oxidant/furfural molar ratio = 3, <sup>a</sup> base: K<sub>2</sub>CO<sub>3</sub>

Other active phases have been less explored in the oxidative esterification of FUR. In this sense, studies carried out with different noble metals supported on a mesoporous carbon have revealed that the catalytic activity of Pd is in the same range as that shown by the Au-based catalyst, while the Pt-based ones displays a catalytic activity slightly lower.<sup>322</sup> These data are in agreement with those reported by Ampelli *et al.*, where, besides Au-based catalysts, the most active sites were Pd, Pt and Pd-Pt.<sup>313</sup>

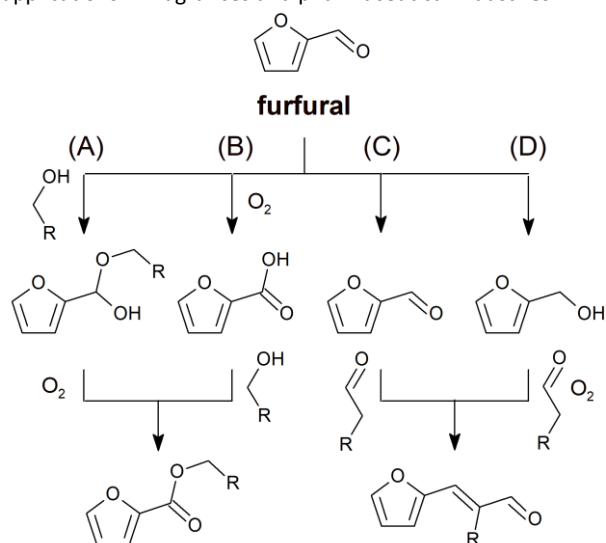
The new perspectives must be focused on the development of inexpensive and environmentally friendly catalysts, which provide

efficient catalytic behavior in the oxidative esterification of FUR. In this sense, metal containing N-doped carbon catalyst has emerged as alternative to precious metals, reaching a MFur yield of 95%.<sup>324</sup>

### 4.3. Production of furan-2-acrolein by oxidative-condensation of furfural

The condensation of FUR and an aldehyde or ketone, coming from the oxidation of primary and secondary alcohols, in the presence of O<sub>2</sub> or H<sub>2</sub>O<sub>2</sub>, is a feasible process to increase the length of the hydrocarbon chain.<sup>304</sup> The obtained product is a low volatile liquid,

which can be used as fuel. In addition, this product finds applications in fragrances and pharmaceutical industries.



**Figure 15.** Competitive mechanism between oxidative esterification and oxidative condensation.

When the aliphatic alcohol displays H in the C- $\alpha$ , the oxidative esterification competes with the oxidative condensation. Thus, the oxidation of FUR in aliphatic alcohols can proceed by different routes (Figure 15):<sup>325–327</sup>

*Route (A):* FUR reacts with the aliphatic alcohol to form a hemiacetal. Then, hemiacetal is oxidized to methyl furoate.

*Route (B):* FUR is oxidized to furoic acid, which esterifies with the aliphatic alcohol to form alkyl furoate.

*Route (C):* Aliphatic alcohol is oxidized to aldehyde. Then, aldehyde reacts with FUR to give rise to the furan-based acrolein through an aldol condensation.

*Route (D):* A hydrogen transferring process takes place between FUR and the aliphatic alcohol. Then, the formed aldehyde reacts with another FUR molecule to produce the furan-based acrolein, and furfuryl alcohol can be oxidized to FUR by the oxidant medium ( $O_2$ ) to close the cycle.

Both routes (A) and (B) are involved in the oxidative esterification, while routes (C) and (D) coexist in the condensation esterification.

Several parameters can influence on the route followed in the oxidation process. Thus, short-chain alcohols, with H in C- $\alpha$  positions, favor the formation of oxidative condensation products, while alcohols with longer chain diminish this selectivity. These authors have pointed out that the selectivity towards oxidative condensation follows the next trend: ethanol = *n*-propanol > *i*-propanol > *n*-butanol > *n*-hexanol.<sup>328</sup> The support acidity also plays a key role in this process, being reported that weak acid sites favors condensations products.<sup>327</sup> In addition, the promoting effect of the base is other important parameter influencing selectivity. These authors have established that an increase in basicity also favors the formation of oxidative condensation products.<sup>327</sup> However, this basicity must be tuned, since too strong bases can cause a uncontrolled polymerization.<sup>301</sup>

**Table 11.** Main catalytic systems and experimental conditions used in the oxidative condensation of FUR

Catalyst	Operating conditions					Catalytic properties			Ref
	Catalyst Loading (wt%)	Pressure (MPa)	Solvent	Base	Temp. (K)	time (h)	X <sub>FUR</sub> (%)	Y <sub>F2A</sub> (%)	
Au/Al <sub>2</sub> O <sub>3</sub>	5	3 (O <sub>2</sub> )	ethanol	K <sub>2</sub> CO <sub>3</sub>	413	4	85	68	327
Au/Fe <sub>3</sub> O <sub>4</sub>	5	3 (O <sub>2</sub> )	ethanol	K <sub>2</sub> CO <sub>3</sub>	413	4	68	61	327
Au/Co <sub>3</sub> O <sub>4</sub>	5	3 (O <sub>2</sub> )	ethanol	K <sub>2</sub> CO <sub>3</sub>	413	4	86	66	327
Au/CeO <sub>2</sub>	5	3 (O <sub>2</sub> )	ethanol	K <sub>2</sub> CO <sub>3</sub>	413	4	97	53	327
Au/Nb <sub>2</sub> O <sub>5</sub>	5	3 (O <sub>2</sub> )	ethanol	K <sub>2</sub> CO <sub>3</sub>	413	4	39	35	327
Co <sub>x</sub> O <sub>y</sub> -N@-Kaolin	5	3 (O <sub>2</sub> )	<i>n</i> -propanol	Cs <sub>2</sub> CO <sub>3</sub>	413	4	75 <sup>a</sup>	69	328
Pt/FH	5	3 (O <sub>2</sub> )	ethanol	K <sub>2</sub> CO <sub>3</sub>	413	4	94	64	303
Pt/HTc	5	3 (O <sub>2</sub> )	ethanol	K <sub>2</sub> CO <sub>3</sub>	413	4	97	67	303
Pt/Fe <sub>3</sub> O <sub>4</sub>	5	3 (O <sub>2</sub> )	ethanol	K <sub>2</sub> CO <sub>3</sub>	413	4	94	67	303
Pt/Al <sub>2</sub> O <sub>3</sub>	5	3 (O <sub>2</sub> )	ethanol	K <sub>2</sub> CO <sub>3</sub>	413	4	97	67	303
Pt/ZrO <sub>2</sub>	5	3 (O <sub>2</sub> )	ethanol	K <sub>2</sub> CO <sub>3</sub>	413	4	59	48	303
CuO/CeO <sub>2</sub>	15	3 (O <sub>2</sub> )	<i>n</i> -propanol	K <sub>2</sub> CO <sub>3</sub>	413	10	85 <sup>a</sup>	81	329

<sup>a</sup> Yield of 3-(furan-2-yl)-2-methylacrylaldehyde

Regarding the active phases used in the oxidative condensation of FUR, a large variety of catalysts has been studied compared to oxidative esterification studies (Table 11). Taking into account that the Au is one of the most studied active phase in oxidation reactions, earlier studies evaluated the influence of the support and the base to modulate the yield towards the furan-based acrolein, obtaining the best results for an Au/Fe<sub>x</sub>O<sub>y</sub>-hydroxyapatite catalyst, using K<sub>2</sub>CO<sub>3</sub> as base.<sup>326,327</sup>

In later studies, the catalytic behavior of Au supported on a metal-organic framework (MOF) was evaluated, with an excellent catalytic behavior, with high selectivity towards furan-based acrolein, by using ethanol.<sup>325</sup> Similarly, Pt has been supported on metal oxides with acid and/or basic sites,<sup>303</sup> and the catalytic data show that Pt dispersed on an acidic support like ZrO<sub>2</sub> increases the catalytic activity, reaching the maximum conversion when K<sub>2</sub>CO<sub>3</sub> is used as base.<sup>303</sup>

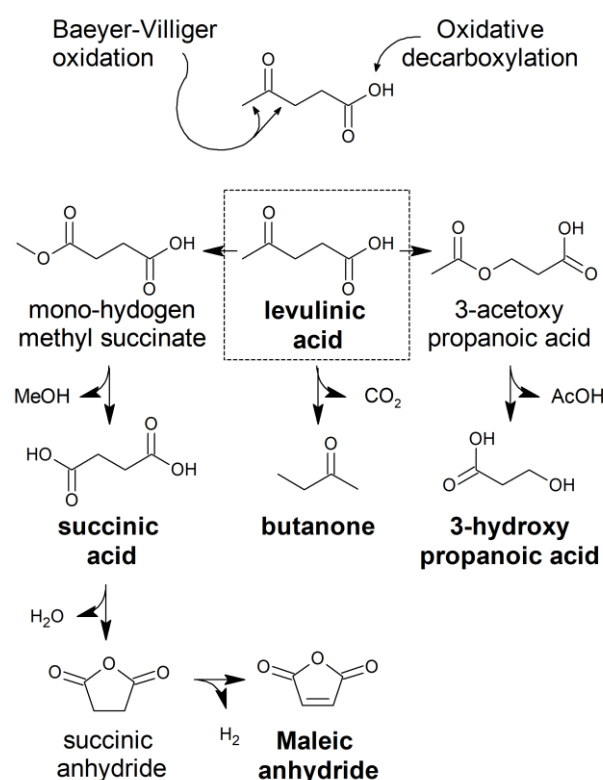
As precious metals render expensive catalysts due to a low availability, much attention is being paid to the development of new catalytic systems based on non-precious and abundant metal. Thus, CuO-CeO<sub>2</sub> systems show an interesting behavior in the oxidative condensation of FUR, mainly with catalysts with a low Cu/Ce molar ratio.<sup>329</sup> These authors also reported an efficient tandem process formed by a copper/azodicarboxylate system, reaching a furfural conversion of 82.5% conversion with 87.7% selectivity toward F2A.<sup>330</sup> On the other hand, Co<sub>x</sub>O<sub>y</sub> catalysts have also exhibited an excellent catalytic performance in the oxidative condensation of furfural, with a FUR conversion of 75% with a selectivity towards F2A close to 93%.<sup>328</sup>

### 5. Oxidation of levulinic acid

Levulinic acid (4-keto pentanoic acid) is one of the most versatile platform molecules directly associated to biomass. Its production takes place by acid treatment of saccharide-rich feedstock, including lignocellulosic biomass or the hydrolysates thereof. Several patented industrial procedures, such as Biofine,<sup>331</sup> Dibanet,<sup>332</sup> or Waleva,<sup>333</sup> among others, have made possible the cost-effective production of this building block in large quantities, and its use as starting point for the chemical production of a large variety of chemicals is now feasible.<sup>334</sup>

The chemical versatility of levulinic acid (LA) comes from the existence of ketone and acid functionalities within the same molecule. These have been modified through a variety of reaction pathways, involving hydrogenation, esterification, and, more recently, oxidation routes. The selective oxidation of LA has been reported to occur in three different locations of the molecule, leading to distinct useful levulinic acid oxidation-derived

products,<sup>335</sup> as depicted in Figure 16 and Table 12. Thus, the oxidation of the ketone group through a Baeyer-Villiger mechanism can lead to two different products, depending on which side of the carbonyl group the oxygen atom is inserted.<sup>336</sup> This type of oxidation gives rise to the formation of either the di-acid derivative (succinic acid, SAC), or the acetate derivative (3-hydroxy propanoic acid, 3-HPA), being both of them valuable chemicals for the synthesis of technical bio-based polymers. A different approach is the oxidation of LA on the other end of the molecule, on the carboxylic acid moiety. This alternative, due to the maximum oxidation state of this terminal carbon, necessarily favors the decarboxylation of the molecule, with the consequent evolution of carbon dioxide. In this case, the main reaction product is 2-butanone. Another alternative is the oxidation of another carbon, not those at the extremes of the molecule, but the β position of levulinic acid throughout the Riley oxidation.<sup>337</sup> Nevertheless, this last alternative requires of quite toxic selenium dioxide, so it has not been widely reported.



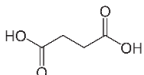

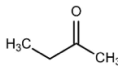
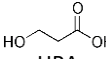
**Figure 16.** Reported reactions for levulinic acid valorisation through selective oxidation pathways.

### 5.1. Production of succinic acid

Among the oxidation products of LA, succinic acid (butane 1,4-dicarboxylic acid) has become a chemical of significance in recent years.<sup>78,338</sup> Nowadays, it is an attractive feedstock as C<sub>4</sub> building block, fuel additive, solvent, food, cosmetics, pharmaceuticals, polyesters, polyurethane, plasticizers, and fine chemicals.<sup>261,339</sup> It is traditionally produced through the fermentation of saccharides (mainly mono- and di-saccharides) by *A. succinogenes*,<sup>340</sup> though it can also be synthesized from the light naphtha C<sub>4</sub> stream from petroleum refineries. However, with the increasing demand for SAC, its synthesis from a renewable feedstock like LA, considering the high structure similarity to SAC, is gaining increasing attention. Thus,

several attempts have been made in the selective oxidation of LA into SAC. The first report of this process backs to a 1954 patent describing V<sub>2</sub>O<sub>5</sub> as catalyst to produce succinic anhydride and succinic acid from gas-phase LA/oxygen admixtures at high temperature (473-673 K).<sup>341</sup> A process, also based on the use of V<sub>2</sub>O<sub>5</sub> as catalyst, was also patented, this time treating levulinic acid in liquid phase, but using nitric acid as oxidant, instead of oxygen. The high oxidizing power of nitric acid makes unnecessary high temperature conditions, being 313-333 K enough to yield 38-52% of the starting levulinic acid as SAC.<sup>342</sup>

**Table 12.** Reported reactions for levulinic acid valorisation through selective oxidation pathways.

Product	Subst. <sup>a</sup>	Catalyst	Operating Conditions				Catalytic properties		Ref.
			Oxid. <sup>b</sup>	Medium	time (h)	Temp. (K)	X <sub>s</sub> <sup>d</sup> (%)	Y <sup>e</sup> (%)	
 Succinic acid (or anhydride)	LA	Supported V <sub>2</sub> O <sub>5</sub>	O <sub>2</sub>	gas phase		473-673	-	81	341
	LA	V <sub>2</sub> O <sub>5</sub>	HNO <sub>3</sub> (12.4:1)	nitric acid	1-4	313-333	-	38-52	342
	LA	Ru-NMP	O <sub>2</sub> (1 MPa)	water	6	423	53.8	51.7	343
	LA	Mn(OAc) <sub>3</sub> ·2H <sub>2</sub> O	O <sub>2</sub> (0.5 MPa)	acetic anhydride	20	363	97.9	9.4	344
	LA	TFA	H <sub>2</sub> O <sub>2</sub> (5.7:1)	TFA	2	363	~100	62	345
	LA	Tungstic acid	H <sub>2</sub> O <sub>2</sub> (5:1)	water	6	363	48	36	346
	ML	Mn(OAc) <sub>3</sub> ·2H <sub>2</sub> O	O <sub>2</sub> (0.5 MPa)	acetic anhydride	10	363	95	58.6	347
	ML	Amberlyst-15	H <sub>2</sub> O <sub>2</sub> (2:1)	methanol	6	353	67	41	348
	ML	Hg(OTf) <sub>2</sub>	H <sub>2</sub> O <sub>2</sub> (2:1)	methanol	6	353	40	19	348
 Maleic anhydride	LA	Mn(OAc) <sub>3</sub> ·2H <sub>2</sub> O	O <sub>2</sub> (0.5 MPa)	acetic anhydride	20	363	97.9	26.0	344
	LA	VO <sub>x</sub> /SiO <sub>2</sub>	O <sub>2</sub>	gas phase	3.9 <sup>c</sup>	573	100	71	349
	LA	VO <sub>x</sub> /TiO <sub>2</sub>	O <sub>2</sub>	gas phase	0.39 <sup>c</sup>	548	93	26	349
	LA	VO <sub>x</sub> /Al <sub>2</sub> O <sub>3</sub>	O <sub>2</sub>	gas phase	78 <sup>c</sup>	548	98	33	349
 Butanone (MEK)	LA	CuO	--	KH <sub>2</sub> PO <sub>4</sub> -NaOH solution	3	573	99.1	57.2	350
	LA	AgNO <sub>3</sub>	S <sub>2</sub> O <sub>8</sub> <sup>2-</sup>	KH <sub>2</sub> PO <sub>4</sub> -NaOH solution, pH 5	0.5	433	71	44.2	350
 HPA	LA	TFA	H <sub>2</sub> O <sub>2</sub> (5.7:1)	TFA	2	263	~100	9	345
	LA	KOH	H <sub>2</sub> O <sub>2</sub> (5.7:1)	30% aq. H <sub>2</sub> O <sub>2</sub>		388	~100	47	351,352
	AL	Enzyme (BVMO)	Air O <sub>2</sub>	LB medium	24	297	60-90	60-90	353

<sup>a</sup> Substrate for the oxidation: LA, levulinic acid; ML, methyl levulinate; AL, alkyl levulinates; <sup>b</sup> Oxidant, in brackets when available: pressure for O<sub>2</sub>-based processes; oxidant:substrate molar ratio for other oxidants; <sup>c</sup> Contact time in min; <sup>d</sup> Substrate conversion; <sup>e</sup> Yield of product.

On the other hand, Podolean *et al.* opted for using a highly active Ru-based magnetite-supported catalyst as the main strategy to moderate the requiring reaction conditions, using O<sub>2</sub> or H<sub>2</sub>O<sub>2</sub> as oxidant, and operating at mild temperature, 423 K.<sup>343</sup> Under these conditions, more than 50% of the starting levulinic acid was transformed into SAC. In another work, Mn(OAc)<sub>3</sub>·2H<sub>2</sub>O was reported as an effective catalyst for the oxidative C–C cleavage of

methyl levulinate into methyl succinate, employing O<sub>2</sub> as oxidant.<sup>347</sup> Succinate yield was shown to rise up to 58.6% under the proper reaction conditions (363 K, 0.5 MPa O<sub>2</sub>). The involvement of a free radical process was suggested, providing Mn(OAc)<sub>3</sub>·2H<sub>2</sub>O a particular selectivity for the oxidative C–C cleavage of levulinate at the terminal methyl-carbonyl position. Although this study was focused on the use of a homogeneous catalyst, further studies



performed by the same authors evidenced that this catalytic system is highly interesting, allowing to control the selectivity towards the formation of different organic acids from LA. Thus, the reaction pathway promoted by this catalytic system differs when using LA or methyl levulinate (under the same experimental conditions). The former directly provides SAc as main reaction product, whereas the second leads to a preferential production of maleic anhydride,<sup>344</sup> being this behaviour unique among the studies reported in the oxidation of levulinic acid (or its ester derivatives).

Despite manganese-based catalysts displayed poor catalytic activity when used in the presence of H<sub>2</sub>O<sub>2</sub>, some other catalytic systems act the opposite. Thus, Dutta *et al.* described the synthesis of SAc from LA using H<sub>2</sub>O<sub>2</sub> as oxidant.<sup>345</sup> Catalysed by trifluoroacetic acid (TFA), the yield of SAc could reach 62% (isolated yield) at 363 K after a reaction time of 2 h. The formation of SAc from LAC was considered to proceed through a Baeyer-Villiger type mechanism. This work, although conducted in the presence of a homogeneous catalyst such as TFA, opened a new synthesis strategy for SAc production, based on the use of both strong Brønsted and Lewis acid catalysts, in combination with hydrogen peroxide as oxidant.

Román-Leshkov *et al.* reported the use of this strategy in the oxidation of methyl levulinate into dimethyl succinate, using hydrogen peroxide and *tert*-butyl hydroperoxide as oxidants, and applying mild conditions in the presence of both Brønsted and Lewis acid catalysts.<sup>348</sup> Despite the oxidation is described to follow a Baeyer-Villiger pathway, the oxidation of methyl levulinate through the insertion of an oxygen atom in between the methyl and the carbonyl groups was predominant. The opposite behaviour to the expected one, which is the formation of the acetate ester, was attributed to the influence of the solvent in the Criegee intermediate adduct, which was deformed in the presence of protic solvents such as alcohols, evolving towards the migration of the methyl group. Selectivities to succinate and acetate derivatives of approx. 60 and 40%, respectively, were obtained with strong Brønsted acids in methanol. However, switching the solvent from methanol to heptane produced dramatic changes in the selectivity pattern, and the succinate/acetate ratio in products could be tuned from 1.6 to 0.3. As for the comparison between the different tested catalysts, Brønsted acids provided higher substrate conversion values and selectivity towards the formation of dimethyl succinate than Lewis acids. Acid strength also seemed to play an important role in the enhancement of the catalytic activity. Finally, comparing the catalytic performance of Amberlyst-15 with its homogeneous counterpart (*p*-tosyl acid) revealed the higher activity of the latter, probably because the absence of mass transfer hindrances in this case. However, both types of catalysts provided similar product distributions. Using LAC instead of levulinate, the benefits of using tungstic acid as catalyst, with H<sub>2</sub>O<sub>2</sub> as oxidant, in the absence of any organic solvent, has been proved.<sup>274</sup> Tungstic acid, though soluble in the presence of H<sub>2</sub>O<sub>2</sub> by formation of pertungstic acid, readily precipitates at high conversion values, being easily recovered through a simple filtration. This catalytic system provided a maximum SAc selectivity of 75% for 48% LA conversion. The proposed mechanism followed an interaction of the catalyst with

the substrate through the carboxyl group, forming a cyclic species, and thus introducing steric hindrance that makes difficult the migration of the largest substituent of the carbonyl group. Under these circumstances, the migration of the methyl group is favoured, thus favouring the formation of the methyl ester versus the acetate to yield 3-HPA.

## 5.2. Production of maleic anhydride

Maleic anhydride (MA) is an important intermediate in the production of value-added chemicals, such as polymers and surfactants.<sup>354,355</sup> MA is industrially produced via oxidation from petroleum-based hydrocarbons (e.g. butane) under high temperatures (> 623 K). As a renewable alternative, besides the production via FUR oxidation, as above described, LAC has been also proposed as starting point to produce MA, in this case through the oxidative cleavage of the methyl ketone group. Chatzidimitriou *et al.* developed a novel catalytic route for MA synthesis from LAC using supported vanadates.<sup>349</sup> The proposed catalytic strategy involved a continuous flow packed-bed reactor, based on VO<sub>x</sub>/SiO<sub>2</sub> as catalyst, which allows achieving single-pass MA yields of 71% at 573 K. In the catalytic cycle, the C<sub>4</sub>-C<sub>5</sub> bond in LA was firstly cleaved to form succinic acid and formaldehyde; subsequently, succinic acid was converted to succinic anhydride by dehydration, and finally, MA was generated through the oxidative dehydrogenation of succinic anhydride. The same authors extended the catalytic study of oxidative ketone scissions to different vanadate supports (SiO<sub>2</sub>,  $\gamma$ -Al<sub>2</sub>O<sub>3</sub>, TiO<sub>2</sub>, and CeO<sub>2</sub>) using 2-pentanone as representative substrate.<sup>356</sup> The study revealed that the intrinsic activity of supported vanadates is sensitive to both vanadium oxide structure and support nature.

## 5.3. Production of butanone

Butanone (methyl-ethyl-ketone, MEK) usually finds use as solvent in organic synthesis, though it can also serve as precursor for other industrial commodities such as ethyl acetate (through the Baeyer-Villiger oxidation), or butanol (via hydrogenation), which has great potential as renewable fuel. Thus, decarboxylation of levulinic acid to produce butanone gains importance as one of the key conversion steps from biomass-derived platform molecules to advanced biofuels. Gong *et al.* studied the decarboxylation of LA to MEK using CuO as catalyst, transformation assigned as an oxidation reaction, achieving a yield as high as 57.2%. However, the reaction conditions were relatively extreme (573 K, 3 h). When LA was oxidized by a combination of silver ion and persulfate, Ag(I)/S<sub>2</sub>O<sub>8</sub><sup>2-</sup>, the reaction conditions were much more moderate (413 K, 30 min), although in this case the yield to butanone is lower (44.2%) and the cost of the catalyst is much higher.<sup>350,357,358</sup>

## 5.4. Production of 3-hydroxypropanoic acid

3-hydroxypropanoic acid (HPA) can be considered as a versatile C<sub>3</sub> intermediate for the synthesis of 1,3-propanediol, acrylates, and the like, being also employed in the formulation of polymer coatings and as an additive for textiles, rendering them with anti-static properties.<sup>359</sup> 3-Hydroxypropanoic acid can be produced by

several different routes (hydration of acrylic acid, propanediol or allylic alcohol oxidation, glucose or glycerol fermentation, etc.), however, the synthesis of succinic acid from LA has opened a new promising way for the production of 3-HPA via selective oxidation of LA. In fact, the Baeyer-Villiger oxidation of levulinic acid should theoretically provide, as previously stated, the acetate ester of 3-hydroxypropanoic acid as main product. Thus, Wu *et al.* have found that LA could be converted, as happened with the SAC, into HPA using H<sub>2</sub>O<sub>2</sub> as oxidant.<sup>351,352</sup> These authors reported 3-HPA and 3-(hydroperoxy)propanoic acid, which could be subsequently hydrogenated to 3-HPA, as the main oxidation products when using basic reaction conditions. Indeed, while running the reaction under acidic conditions favours the methyl group migration to give SAC in good yield, switching the medium to basic pH allows controlling the selectivity of the migration to increase the production of HPA. Thus, using KOH as catalyst at 388 K, a yield to HPA up to 47% could be achieved. Enzymatic catalysis has also been applied for the production of HPA derivatives via oxidation of levulinates over Baeyer-Villiger monooxygenases using atmospheric oxygen as oxidant.<sup>353</sup>

## 6. Conclusions and prospects

This review focus on those heterogeneous catalysts reported to be active and selective in the oxidation of the most relevant biomass-derived platform molecules – glucose, furfural, 5-hydroxymethylfurfural and levulinic acid – using benign oxidants, to yield a large spectrum of target products. Most of the works reported in the literature deal with the conversion of high-purity commercial molecules, using different types of catalysts, whose nature depend on the active sites needed to drive the required transformations, so that the number and variety of investigations is huge. Their choice was based on their relevance for current and potential applications in important fields, such as the synthesis of drugs and pharmaceuticals, or the production of fuels, among others.

Despite of the high effort invested in this field, there are still important challenges to face. These include developing catalytic systems to drive the transformation of complex feedstocks, robust and stable under long-term operation, highly active under mild temperature and pressure conditions, and being formulate from non-essential components.

Developing efficient and sustainable catalytic technologies for the conversion of complex carbohydrates, like polysaccharides – cellulose, cellobiose, sucrose, starch, inulin, xylans–, or even lignocellulosic raw materials is of major importance, because of the reduced price of these feedstock compared to processed sugars and their derivatives. For this purpose, new insights, not only in the development of advanced catalytic technologies for oxidation processes would be required, but also in their integration into emerging processes devoted to the transformation of lignocellulosic biomass will have to be tackled. Selective oxidation of biomass-derived polysaccharides has been shown to be a major challenge, requiring the development of bifunctional catalysts able to promote the hydrolysis of polysaccharides and the oxidation of the evolving monosaccharides. Nevertheless, these studies are still quite few,

and major challenges will consist on treating solid biomass feedstocks. For this purpose, the development of additional technologies like biomass conditioning treatments, will be required. The objective will be developing efficient fractionation processes, able to separate the different fractions of biomass to be subsequently depolymerized into their building units, and derivatives, that can be used as raw materials for oxidation processes. The application of advanced biomass treatment technologies will be necessary, such as mechanochemistry procedures to facilitate the breakdown of lignocellulose, or selective extraction for an appropriate fractionation of the different components of biomass, and the separation of impurities. Together with these developments to facilitate treating solid biomass, designing robust and stable catalytic systems together with innovative operation and regeneration modes will be of major importance.

The impact of advanced oxidation catalytic technology on a future biorefinery will require of long-term stable systems, requiring these studies for the most outstanding catalytic systems under development. It is still necessary to deepen in the search of catalysts showing high catalytic activity and stability under mild experimental conditions – the milder the better –. These investigation will need to count on realistic life cycle and techno-economic analysis to evaluate the economic and environmental feasibility of a particular catalytic technology, as identifying its bottlenecks and weaknesses during their development is the most straight way to find appropriate solutions and developing catalytic systems able to be applied at industrial scale.

Finally, the search of active catalytic phases based on non-essential, most-abundant, low-cost non-noble metals should be investigated to get highly efficient heterogeneous catalytic systems. In addition, new combinations of different active species will have to be addressed to get multifunctional catalysts able to promote cascades of reactions in an efficient manner –especially if starting from complex carbohydrates–, in a sort of process intensification through the catalyst.

Last, electrochemical and photochemical oxidation processes, and the use of non-conventional solvents (deep eutectic solvents, ionic liquids, supercritical fluids, among others) must be envisaged, as much as the resulting process could be more sustainable and greener than those already proposed.

## 7. List of abbreviations

AL	alkyl levulinates
DFF	2,5-diformylfuran
DMF	N,N-dimethylformamide
DMSO	dimethylsulfoxide
DR	deposition-reduction
FAc	Formic acid
FDCA	2,5-furandicarboxylic acid
FDCC	furan-2,5-dicarbonyl chloride
FFCA	5-formyl-2-furancarboxylic acid
FumAc	fumaric acid
FurAc	furoic acid
FUR	furfural
F2A	furan-2-acrolein

- GHSV Gas Hourly Space Velocity 16 H. Kobayashi and A. Fukuoka, *Green Chem.*, 2013, **15**, 1740–1763.
- GLU glucose 17 A. Liu, Z. Huang and X. Wang, *Catal. Letters*, 2018, **148**, 2019–2029.
- GO graphene oxide 18 H. Zhang and N. Toshima, *Catal. Sci. Technol.*, 2013, **3**, 268–278.
- GVL  $\gamma$ -valerolactone 19 P. A. and L. C. Ramachandran Sumitra, Fontanille Pierre, *Food Technol. Biotechnol.*, 2006, **44**, 185–195.
- HMF 5-hydroxymethylfurfural 20 B. P. Lawson, E. Golikova, A. M. Sulman, B. D. Stein, D. G. Morgan, N. V. Lakina, A. Y. Karpenkov, E. M. Sulman, V. G. Matveeva and L. M. Bronstein, *ACS Sustain. Chem. Eng.*, 2018, **6**, 9845–9853.
- HMFCA 5-hydroxymethyl-2-furancarboxylic acid 21 S. Ramachandran, S. Nair, C. Larroche and A. Pandey, in *Current Developments in Biotechnology and Bioengineering: Production, Isolation and Purification of Industrial Products*, 2016.
- HPA 3-hydroxypropanoic acid 22 N. N. Lichtin and M. H. Saxe, *J. Am. Chem. Soc.*, 1955, **77**, 1875–1880.
- HT hydrotalcite 23 B. N. Grgur, D. L. Žugić, M. M. Gvozdenović and T. L. Trišović, *Carbohydr. Res.*, 2006, **341**, 1779–1787.
- LA levulinic acid 24 K. Fischer and H. P. Bipp, *Bioresour. Technol.*, 2005, **96**, 831–842.
- MA maleic anhydride 25 D. Bin, H. Wang, J. Li, H. Wang, Z. Yin, J. Kang, B. He and Z. Li, *Electrochim. Acta*, 2014, **130**, 170–178.
- MalAc maleic acid 26 T. Rafaïdeen, S. Baranton and C. Coutanceau, *Appl. Catal. B Environ.*, 2019, **243**, 641–656.
- MAc maleic acid 27 A. Mirescu and U. Prüße, *Appl. Catal. B Environ.*, 2007, **70**, 644–652.
- MeCN acetonitrile 28 D. An, A. Ye, W. Deng, Q. Zhang and Y. Wang, *Chem. - Eur. J.*, 2012, **18**, 2938–2947.
- MFur methyl furoate 29 P. N. Amaniampong, X. Jia, B. Wang, S. H. Mushrif, A. Borgna and Y. Yang, *Catal. Sci. Technol.*, 2015, **5**, 2393–2405.
- ML methyl levulinate 30 M. Hernández, E. Lima, A. Guzmán, M. Vera, O. Novelo and V. Lara, *Appl. Catal. B Environ.*, 2014, **144**, 528–537.
- NP nanoparticle 31 H. Zhang, N. Li, X. Pan, S. Wu and J. Xie, *ACS Sustain. Chem. Eng.*, 2017, **5**, 4066–4072.
- SAc succinic acid 32 W. Hou, M. Zhang and J. Bao, *Bioresour. Technol.*, 2018, **264**, 395–399.
- SG solid grinding 33 X. Han, G. Liu, W. Song and Y. Qu, *Bioresour. Technol.*, 2018, **248**, 248–257.
- TarAc tartaric acid 34 X. Zhou, X. Zhou, L. Huang, R. Cao and Y. Xu, *Bioresour. Technol.*, 2017, **243**, 855–859.
- TFA trifluoroacetic acid 35 A. Abbadi and H. van Bekkum, *J. Mol. Catal.*, 1995, **97**, 111–118.
- X mol% conversion 36 A. Tathod, T. Kane, E. S. Sanil and P. L. Dhepe, *J. Mol. Catal. A Chem.*, 2014, **388–389**, 90–99.
- Y mol% yield 37 I. V. Delidovich, O. P. Taran, L. G. Matvienko, A. N. Simonov, I. L. Simakova, A. N. Bobrovskaya and V. N. Parmon, *Catal. Letters*, 2010, **140**, 14–21.
- 38 T. Haynes, V. Dubois and S. Hermans, *Appl. Catal. A Gen.*, 2017, **542**, 47–54.
- 39 M. Besson, *J. Catal.*, 1995, **152**, 116–121.
- 40 S. Karski, *J. Mol. Catal. A Chem.*, 2003, **191**, 87–92.
- 41 S. Karski, *J. Mol. Catal. A Chem.*, 2006, **253**, 147–154.
- 42 M. Wenkin, M. Devillers, P. Ruiz and B. Delmon, in *Studies in Surface Science and Catalysis*, 2001, pp. 295–302.
- 43 M. Wenkin, R. Touillaux, P. Ruiz, B. Delmon and M. Devillers, *Appl. Catal. A Gen.*, 1996, **148**, 181–199.
- 44 C. Megías-Sayago, J. L. Santos, F. Ammari, M. Chenouf, S. Ivanova, M. A. Centeno and J. A. Odriozola, *Catal. Today*, 2018, **306**, 183–190.

### Conflicts of interest

There are no conflicts to declare.

### Acknowledgements

This research was funded by the Spanish Ministry of Economy and Competitiveness (RTI2018-94918) and FEDER (European Union) funds. J.A.C. thanks University of Malaga for contracts of PhD incorporation.

### References

- 1 S. G. Wettstein, D. Martin Alonso, E. I. Gürbüz and J. A. Dumesic, *Curr. Opin. Chem. Eng.*, 2012, **1**, 218–224.
- 2 A. Corma, S. Iborra, A. Velty, A. Corma Canos, S. Iborra and A. Velty, *Chem. Rev.*, 2007, **107**, 2411–2502.
- 3 L. T. Mika, E. Cséfalvay and Á. Németh, *Chem. Rev.*, 2018, **118**, 505–613.
- 4 S. Dutta, S. De, B. Saha and M. I. Alam, *Catal. Sci. Technol.*, 2012, **2**, 2025.
- 5 T. Wang, M. W. Nolte and B. H. Shanks, *Green Chem.*, 2014, **16**, 548–572.
- 6 I. Agirrezabal-Telleria, I. Gandarias and P. L. Arias, *Catal. Today*, 2014, **234**, 42–58.
- 7 M. Besson, P. Gallezot and C. Pinel, *Chem. Rev.*, 2014, **114**, 1827–1870.
- 8 K. Gupta, R. K. Rai and S. K. Singh, *ChemCatChem*, 2018, **10**, 2326–2349.
- 9 Z. Zhang and G. W. Huber, *Chem. Soc. Rev.*, 2018, **47**, 1351–1390.
- 10 R. Mariscal, P. Maireles-Torres, M. Ojeda, I. Sádaba and M. López Granados, *Energy Environ. Sci.*, 2016, **9**, 1144–1189.
- 11 R. Ma, Y. Xu and X. Zhang, *ChemSusChem*, 2015, **8**, 24–51.
- 12 C. Liu, S. Wu, H. Zhang and R. Xiao, *Fuel Process. Technol.*, 2019, **191**, 181–201.
- 13 F. W. Lichtenthaler, *Acc. Chem. Res.*, 2002, **35**, 728–737.
- 14 S. Anastassiadis and I. Morgunov, *Recent Pat. Biotechnol.*, 2007, **1**, 167–180.
- 15 L. P. S. Vandenberghe, S. G. Karp, P. Z. de Oliveira, J. C. de Carvalho, C. Rodrigues and C. R. Soccol, *Curr. Dev. Biotechnol. Bioeng.*, 2018, 415–434.

- 45 C. Liu, J. Zhang, J. Huang, C. Zhang, F. Hong, Y. Zhou, G. Li and M. Haruta, *ChemSusChem*, 2017, **10**, 1976–1980.
- 46 J. Zhang, Z. Li, J. Huang, C. Liu, F. Hong, K. Zheng and G. Li, *Nanoscale*, 2017, **9**, 16879–16886.
- 47 P. Qi, S. Chen, J. Chen, J. Zheng, X. Zheng and Y. Yuan, *ACS Catal.*, 2015, **5**, 2659–2670.
- 48 A. Mirescu, H. Berndt, A. Martin and U. Prütze, *Appl. Catal. A Gen.*, 2007, **317**, 204–209.
- 49 Y. Cao, X. Liu, S. Iqbal, P. J. Miedziak, J. K. Edwards, R. D. Armstrong, D. J. Morgan, J. Wang and G. J. Hutchings, *Catal. Sci. Technol.*, 2016, **6**, 107–117.
- 50 M. Signoretto, F. Menegazzo, A. Di Michele and E. Fioriniello, *Catalysts*, 2016, **6**, 87.
- 51 C. Megías-Sayago, S. Ivanova, C. López-Cartes, M. A. Centeno and J. A. Odriozola, *Catal. Today*, 2017, **279**, 148–154.
- 52 P. J. Miedziak, H. Alshammari, S. A. Kondrat, T. J. Clarke, T. E. Davies, M. Morad, D. J. Morgan, D. J. Willock, D. W. Knight, S. H. Taylor and G. J. Hutchings, *Green Chem.*, 2014, **16**, 3132–3141.
- 53 S. Biella, L. Prati and M. Rossi, *J. Catal.*, 2002, **206**, 242–247.
- 54 I. Nikov and K. Paev, *Catal. Today*, 1995, **24**, 41–47.
- 55 M. Wenkin, C. Renard, P. Ruiz, B. Delmon and M. Devillers, in *Studies in Surface Science and Catalysis*, 1997, pp. 517–526.
- 56 M. Wenkin, P. Ruiz, B. Delmon and M. Devillers, *J. Mol. Catal. A Chem.*, 2002, **180**, 141–159.
- 57 M. Haruta, T. Kobayashi, H. Sano and N. Yamada, *Chem. Lett.*, 1987, **16**, 405–408.
- 58 M. Comotti, C. Della Pina, R. Matarrese and M. Rossi, *Angew. Chemie Int. Ed.*, 2004, **43**, 5812–5815.
- 59 P. Beltrame, M. Comotti, C. Della Pina and M. Rossi, *Appl. Catal. A Gen.*, 2006, **297**, 1–7.
- 60 T. Ishida, H. Watanabe, T. Bebeko, T. Akita and M. Haruta, *Appl. Catal. A Gen.*, 2010, **377**, 42–46.
- 61 T. Ishida, N. Kinoshita, H. Okatsu, T. Akita, T. Takei and M. Haruta, *Angew. Chemie Int. Ed.*, 2008, **47**, 9265–9268.
- 62 H. Okatsu, N. Kinoshita, T. Akita, T. Ishida and M. Haruta, *Appl. Catal. A Gen.*, 2009, **369**, 8–14.
- 63 T. Ishida, S. Okamoto, R. Makiyama and M. Haruta, *Appl. Catal. A Gen.*, 2009, **353**, 243–248.
- 64 N. Thielecke, M. Aytemir and U. Prütze, *Catal. Today*, 2007, **121**, 115–120.
- 65 H. Zhang, M. Haba, M. Okumura, T. Akita, S. Hashimoto and N. Toshima, *Langmuir*, 2013, **29**, 10330–10339.
- 66 N. Toshima and H. Zhang, *Macromol. Symp.*, 2012, **317–318**, 149–159.
- 67 H. Zhang and N. Toshima, *J. Colloid Interface Sci.*, 2013, **394**, 166–176.
- 68 H. Zhang, K. Kawashima, M. Okumura and N. Toshima, *J. Mater. Chem. A*, 2014, **2**, 13498–13508.
- 69 H. Zhang, L. Lu, Y. Cao, S. Du, Z. Cheng and S. Zhang, *Mater. Res. Bull.*, 2014, **49**, 393–398.
- 70 H. Zhang and N. Toshima, *Appl. Catal. A Gen.*, 2011, **400**, 9–13.
- 71 H. Zhang, M. Okumura and N. Toshima, *J. Phys. Chem. C*, 2011, **115**, 14883–14891.
- 72 R. Rinaldi and F. Schüth, *Energy Environ. Sci.*, 2009, **2**, 610.
- 73 J. Zhang, X. Liu, M. N. Hedhili, Y. Zhu and Y. Han, *ChemCatChem*, 2011, **3**, 1294–1298.
- 74 P. N. Amaniampong, K. Li, X. Jia, B. Wang, A. Borgna and Y. Yang, *ChemCatChem*, 2014, **6**, 2105–2114.
- 75 K. Morawa Eblagon, M. F. R. Pereira and J. L. Figueiredo, *Appl. Catal. B Environ.*, 2016, **184**, 381–396.
- 76 X. Tan, W. Deng, M. Liu, Q. Zhang and Y. Wang, *Chem. Commun.*, 2009, **0**, 7179.
- 77 P. N. Amaniampong, A. Y. Booshehri, X. Jia, Y. Dai, B. Wang, S. H. Mushrif, A. Borgna and Y. Yang, *Appl. Catal. A Gen.*, 2015, **505**, 16–27.
- 78 T. Werpy and G. Petersen, *Top Value Added Chemicals from Biomass: Volume I – Results of Screening for Potential Candidates from Sugars and Synthesis Gas*, Golden, CO (United States), 2004.
- 79 Glucaric Acid Market Size & Share | Global Industry Report, 2018-2025.
- 80 P. J. M. Dijkgraaf, M. E. C. G. Verkuylen and K. van der Wiele, *Carbohydr. Res.*, 1987, **163**, 127–131.
- 81 Y. Wu, Y. Enomoto, H. Masaki and T. Iwata, *J. Appl. Polym. Sci.*, 2019, **136**, 47255.
- 82 Y. Wu, Y. Enomoto-Rogers, H. Masaki and T. Iwata, *ACS Sustain. Chem. Eng.*, 2016, **4**, 3812–3819.
- 83 S. Li, W. Deng, S. Wang, P. Wang, D. An, Y. Li, Q. Zhang and Y. Wang, *ChemSusChem*, 2018, **11**, 1995–2028.
- 84 Z. Walaszek, J. Szemraj, M. Hanausek, A. K. Adams and U. Sherman, *Nutr. Res.*, 1996, **16**, 673–681.
- 85 Z. Walaszek, *Cancer Lett.*, 1990, **54**, 1–8.
- 86 T. N. Smith, K. Hash, C.-L. Davey, H. Mills, H. Williams and D. E. Kiely, *Carbohydr. Res.*, 2012, **350**, 6–13.
- 87 S. Donen and K. Jensen, *US Pat. 0275622*.
- 88 J. M. H. Dirx, H. S. van der Baan and J. M. A. J. van den Broen, *Carbohydr. Res.*, 1977, **59**, 63–72.
- 89 M. Besson, G. Flèche, P. Fuertes, P. Gallezot and F. Lahmer, *Recl. des Trav. Chim. des Pays-Bas*, 2010, **115**, 217–221.
- 90 S. Solmi, C. Morreale, F. Ospitali, S. Agnoli and F. Cavani, *ChemCatChem*, 2017, **9**, 2797–2806.
- 91 X. Jin, M. Zhao, J. Shen, W. Yan, L. He, P. S. Thapa, S. Ren, B. Subramaniam and R. V. Chaudhari, *J. Catal.*, 2015, **330**, 323–329.
- 92 X. Jin, M. Zhao, M. Vora, J. Shen, C. Zeng, W. Yan, P. S. Thapa, B. Subramaniam and R. V. Chaudhari, *Ind. Eng. Chem. Res.*, 2016, **55**, 2932–2945.
- 93 J. Lee, B. Saha and D. G. Vlachos, *Green Chem.*, 2016, **18**, 3815–3822.
- 94 E. Derrien, M. Mounquengui-Diallo, N. Perret, P. Marion, C. Pinel and M. Besson, *Ind. Eng. Chem. Res.*, 2017, **56**, 13175–13189.
- 95 E. Derrien, P. Marion, C. Pinel and M. Besson, *Org. Process Res. Dev.*, 2016, **20**, 1265–1275.
- 96 X. Liu, S. Li, Y. Liu and Y. Cao, *Cuihua Xuebao/Chinese J. Catal.*, 2015, **36**, 1461–1475.
- 97 P. Preuster and J. Albert, *Energy Technol.*, 2018, **6**, 501–509.
- 98 J. Hietala, A. Vuori, P. Johnsson, I. Pollari, W. Reutemann and H. Kieczka, in *Ullmann's Encyclopedia of Industrial Chemistry*, Wiley-VCH Verlag GmbH & Co. KGaA, Weinheim, Germany, 2016, pp. 1–22.
- 99 US4218568, 1980, 1–3.
- 100 N. Yan and K. Philippot, *Curr. Opin. Chem. Eng.*, 2018, **20**, 86–92.
- 101 D. M. Weekes, D. A. Salvatore, A. Reyes, A. Huang, C. P. Berlinguette and S. Blusson, *Acc. Chem. Res.*, 2018, **51**, 39.
- 102 H. S. Isbell and R. G. Naves, *Carbohydr. Res.*, 1974, **36**, C1–C4.

- 103 D. A. Bulushev and J. R. H. H. Ross, *ChemSusChem*, 2018, **11**, 821–836.
- 104 J. Yun, G. Li, H. Enomoto and F. Jin, in *AIP Conference Proceedings*, 2007, vol. 898, pp. 143–146.
- 105 N. Zargari, Y. Kim and K. W. Jung, *Green Chem.*, 2015, **17**, 2736–2740.
- 106 T. Lu, Y. Hou, W. Wu, M. Niu, S. Ren, Z. Lin and V. K. Ramani, *Fuel*, 2018, **216**, 572–578.
- 107 M. Niu, Y. Hou, S. Ren, W. Wu and K. N. Marsh, *Green Chem.*, 2015, **17**, 453–459.
- 108 M. Watanabe, T. M. Aida, R. L. Smith and H. Inomata, *J. Japan Pet. Inst.*, 2012, **55**, 219–228.
- 109 J. Yun, G. Yao, F. Jin, H. Zhong, A. Kishita, K. Tohji, H. Enomoto and L. Wang, *AIChE J.*, 2016, **62**, 3657–3663.
- 110 J. Albert, J. Mehler, J. Tucher, K. Kastner and C. Streb, *ChemistrySelect*, 2016, **1**, 2889–2894.
- 111 N. V. Gromov, O. P. Taran, I. V. Delidovich, A. V. Pestunov, Y. A. Rodikova, D. A. Yatsenko, E. G. Zhizhina and V. N. Parmon, *Catal. Today*, 2016, **278**, 74–81.
- 112 Y. Nakagawa, D. Sekine, N. Obara, M. Tamura and K. Tomishige, *ChemCatChem*, 2017, **9**, 3412–3419.
- 113 L. Cheng, H. Liu, Y. Cui, N. Xue and W. Ding, *J. Energy Chem.*, 2014, **23**, 43–49.
- 114 H. Choudhary, S. Nishimura and K. Ebitani, *Appl. Catal. B Environ.*, 2015, **162**, 1–10.
- 115 R. Sato, H. Choudhary, S. Nishimura and K. Ebitani, *Org. Process Res. Dev.*, 2015, **19**, 449–453.
- 116 M. Bellardita, E. I. García-López, G. Marci, B. Megna, F. R. Pomilla and L. Palmisano, *RSC Adv.*, 2015, **5**, 59037–59047.
- 117 B. Jin, G. Yao, X. Wang, K. Ding and F. Jin, *ACS Sustain. Chem. Eng.*, 2017, **5**, 6377–6381.
- 118 B. Zhou, J. Song, H. Zhou, T. Wu and B. Han, *Chem. Sci.*, 2015, **7**, 463–468.
- 119 L. Da Vià, C. Recchi, T. E. Davies, N. Greeves and J. A. Lopez-Sanchez, *ChemCatChem*, 2016, **8**, 3475–3483.
- 120 R. J. Van Putten, J. C. Van Der Waal, E. De Jong, C. B. Rasrendra, H. J. Heeres and J. G. De Vries, *Chem. Rev.*, 2013, **113**, 1499–1597.
- 121 P. Pal and S. Saravanamurugan, *ChemSusChem*, 2019, **12**, 145–163.
- 122 M. Ventura, A. Dibenedetto and M. Aresta, *Inorganica Chim. Acta*, 2018, **470**, 11–21.
- 123 X. Tong, Y. Ma and Y. Li, *Appl. Catal. A Gen.*, 2010, **385**, 1–13.
- 124 A. A. Rosatella, S. P. Simeonov, R. F. M. Frade and C. A. M. Afonso, *Green Chem.*, 2011, **13**, 754–793.
- 125 M. Ventura, M. Aresta and A. Dibenedetto, *ChemSusChem*, 2016, **9**, 1096–1100.
- 126 O. R. Schade, K. F. Kalz, D. Neukum, W. Kleist and J. D. Grunwaldt, *Green Chem.*, 2018, **20**, 3530–3541.
- 127 A. S. Amarasekara, D. Green and L. T. D. Williams, *Eur. Polym. J.*, 2009, **45**, 595–598.
- 128 Z. Hui and A. Gandini, *Eur. Polym. J.*, 1992, **28**, 1461–1469.
- 129 K. T. Hopkins, W. D. Wilson, B. C. Bender, D. R. McCurdy, J. E. Hall, R. R. Tidwell, A. Kumar, M. Bajic and D. W. Boykin, *J. Med. Chem.*, 1998, **41**, 3872–3878.
- 130 H. Adams, R. Bastida, A. De Blas, M. Carnota, D. E. Fenton, A. Macías, A. Rodriguez and T. Rodriguez-Blas, *Polyhedron*, 1997, **16**, 567–572.
- 131 J. Ma, M. Wang, Z. Du, C. Chen, J. Gao and J. Xu, *Polym. Chem.*, 2012, **3**, 2346–2349.
- 132 J. L. H. Nie Junfang; Xie, *J. Catal.*, 2013, **301**, 83–91.
- 133 A. Takagaki, M. Takahashi, S. Nishimura and K. Ebitani, *ACS Catal.*, 2011, **1**, 1562–1565.
- 134 Y. Wang, B. Liu, K. Huang and Z. Zhang, *Ind. Eng. Chem. Res.*, 2014, **53**, 1313–1319.
- 135 I. Gandarias, E. Nowicka, B. J. May, S. Alghareed, R. D. Armstrong, P. J. Miedziak and S. H. Taylor, *Catal. Sci. Technol.*, 2016, **6**, 4201–4209.
- 136 J. Chen, Y. Guo, J. Chen, L. Song and L. Chen, *ChemCatChem*, 2014, **6**, 3174–3181.
- 137 Z. Yang, W. Qi, R. Su and Z. He, *Energy and Fuels*, 2017, **31**, 533–541.
- 138 Z. Zhang, Z. Yuan, D. Tang, Y. Ren, K. Lv and B. Liu, *ChemSusChem*, 2014, **7**, 3496–3504.
- 139 C. A. Antonyraj, J. Jeong, B. Kim, S. Shin, S. Kim, K. Y. Lee and J. K. Cho, *J. Ind. Eng. Chem.*, 2013, **19**, 1056–1059.
- 140 WO 03/02494 7A1, 2003.
- 141 G. A. Halliday, R. J. Young and V. V. Grushin, *Org. Lett.*, 2003, **5**, 2003–2005.
- 142 C. Carlini, P. Patrono, A. M. R. Galletti, G. Sbrana and V. Zima, *Appl. Catal. A Gen.*, 2005, **289**, 197–204.
- 143 I. Sádaba, Y. Y. Gorbanev, S. Kegnes, S. S. R. Putluru, R. W. Berg and A. Riisager, *ChemCatChem*, 2013, **5**, 284–293.
- 144 J. Nie and H. Liu, *Pure Appl. Chem.*, 2011, **84**, 765–777.
- 145 F. Xu and Z. Zhang, *ChemCatChem*, 2015, **7**, 1470–1477.
- 146 N. T. Le, P. Lakshmanan, K. Cho, Y. Han and H. Kim, *Appl. Catal. A Gen.*, 2013, **464–465**, 305–312.
- 147 G. D. Yadav and R. V. Sharma, *Appl. Catal. B Environ.*, 2014, **147**, 293–301.
- 148 F. Neațu, N. Petrea, R. Petre, V. Somoghi, M. Florea and V. I. Parvulescu, *Catal. Today*, 2016, **278**, 66–73.
- 149 J. Chen, J. Zhong, Y. Guo and L. Chen, *RSC Adv.*, 2015, **5**, 5933–5940.
- 150 M. Ventura, F. Lobefaro, E. de Giglio, M. Distaso, F. Nocito and A. Dibenedetto, *ChemSusChem*, 2018, **11**, 1305–1315.
- 151 D. Gupta, K. K. Pant and B. Saha, *Mol. Catal.*, 2017, **435**, 182–188.
- 152 J.-P. Lange, *Catal. Sci. Technol.*, 2016, **6**, 4759–4767.
- 153 R. R. Sever and T. W. Root, *J. Phys. Chem. B*, 2003, **107**, 4080–4089.
- 154 F. L. Grasset, B. Katryniok, S. Paul, V. Nardello-Rataj, M. Pera-Titus, J. M. Clacens, F. De Campo and F. Dumeignil, *RSC Adv.*, 2013, **3**, 9942–9948.
- 155 Z. Z. Yang, J. Deng, T. Pan, Q. X. Guo and Y. Fu, *Green Chem.*, 2012, **14**, 2986–2989.
- 156 X. Xiang, L. He, Y. Yang, B. Guo, D. Tong and C. Hu, *Catal. Letters*, 2011, **141**, 735–741.
- 157 G. Lv, H. Wang, Y. Yang, T. Deng, C. Chen, Y. Zhu and X. Hou, *Green Chem.*, 2016, **18**, 2302–2307.
- 158 W. Ghezali, K. De Oliveira Vigier, R. Kessas and F. Jérôme, *Green Chem.*, 2015, **17**, 4459–4464.
- 159 J. Zhao, J. Anjali, Y. Yan and J. M. Lee, *ChemCatChem*, 2017, **9**, 1187–1191.
- 160 J. Zhao, A. Jayakumar, Z. T. Hu, Y. Yan, Y. Yang and J. M. Lee, *ACS Sustain. Chem. Eng.*, 2018, **6**, 284–291.
- 161 Y. Liu, L. Zhu, J. Tang, M. Liu, R. Cheng and C. Hu, *ChemSusChem*, 2014, **7**, 3541–3547.
- 162 Z. Hu, B. Liu, Z. Zhang and L. Chen, *Ind. Crops Prod.*, 2013, **50**, 264–269.
- 163 A. S. Amarasekara, L. T. D. Williams and C. C. Ebede, *Carbohydr. Res.*, 2008, **343**, 3021–3024.
- 164 T. A. Werypy, J. E. Holladay and J. F. White, *Top Value Added Chemicals From Biomass: I. Results of Screening for*

- 165 *Potential Candidates from Sugars and Synthesis Gas*, 2004. E. de Jong, M. A. Dam, L. Sipos and G. J. M. Gruter, in *Biobased Monomers, Polymers, and Materials*, eds. P. Smith and R. Gross, American Chemical Society, ACS Symposium Series, Washington, DC, 2012, pp. 1–13.
- 166 S. E. Davis, B. N. Zope and R. J. Davis, *Green Chem.*, 2012, **14**, 143–147.
- 167 O. Casanova, S. Iborra and A. Corma, *ChemSusChem*, 2009, **2**, 1138–1144.
- 168 S. Albonetti, A. Lolli, V. Morandi, A. Migliori, C. Lucarelli and F. Cavani, *Appl. Catal. B Environ.*, 2015, **163**, 520–530.
- 169 C. Megías-Sayago, A. Lolli, S. Ivanova, S. Albonetti, F. Cavani and J. A. Odriozola, *Catal. Today*, 2018, 0–1.
- 170 N. Masoud, B. Donoeva and P. E. de Jongh, *Appl. Catal. A Gen.*, 2018, **561**, 150–157.
- 171 A. Lolli, R. Amadori, C. Lucarelli, M. G. Cutrufello, E. Rombi, F. Cavani and S. Albonetti, *Microporous Mesoporous Mater.*, 2016, **226**, 466–475.
- 172 B. Donoeva, N. Masoud and P. E. De Jongh, *ACS Catal.*, 2017, **7**, 4581–4591.
- 173 J. Cai, H. Ma, J. Zhang, Q. Song, Z. Du, Y. Huang and J. Xu, *Chem. - A Eur. J.*, 2013, **19**, 14215–14223.
- 174 Y. Y. Gorbanev, S. Kegnæs and A. Riisager, *Top. Catal.*, 2011, **54**, 1318–1324.
- 175 Y. Y. Gorbanev, S. Kegnæs and A. Riisager, *Catal. Letters*, 2011, **141**, 1752–1760.
- 176 C. M. Pichler, M. G. Al-Shaal, D. Gu, H. Joshi, W. Ciptonugroho and F. Schüth, *ChemSusChem*, 2018, **11**, 2083–2090.
- 177 F. Wang, Z. Yuan, B. Liu, S. Chen and Z. Zhang, *J. Ind. Eng. Chem.*, 2016, **38**, 181–185.
- 178 F. Kerdi, H. Ait Rass, C. Pinel, M. Besson, G. Peru, B. Leger, S. Rio, E. Monflier and A. Ponchel, *Appl. Catal. A Gen.*, 2015, **506**, 206–219.
- 179 J. Xie, J. Nie and H. Liu, *Chinese J. Catal.*, 2014, **35**, 937–944.
- 180 D. K. Mishra, H. J. Lee, J. Kim, H. S. Lee, J. K. Cho, Y. W. Suh, Y. Yi and Y. J. Kim, *Green Chem.*, 2017, **19**, 1619–1623.
- 181 H. Ait Rass, N. Essayem and M. Besson, *ChemSusChem*, 2015, **8**, 1206–1217.
- 182 Y. Zhang, Z. Xue, J. Wang, X. Zhao, Y. Deng, W. Zhao and T. Mu, *RSC Adv.*, 2016, **6**, 51229–51237.
- 183 H. Ait Rass, N. Essayem and M. Besson, *Green Chem.*, 2013, **15**, 2240–2251.
- 184 Z. Miao, T. Wu, J. Li, T. Yi, Y. Zhang and X. Yang, *RSC Adv.*, 2015, **5**, 19823–19829.
- 185 K. Yu, D. Lei, Y. Feng, H. Yu, Y. Chang, Y. Wang, Y. Liu, G. C. Wang, L. L. Lou, S. Liu and W. Zhou, *J. Catal.*, 2018, **365**, 292–302.
- 186 S. E. Davis, A. D. Benavidez, R. W. Gosselink, J. H. Bitter, K. P. De Jong, A. K. Datye and R. J. Davis, *J. Mol. Catal. A Chem.*, 2014, **388–389**, 123–132.
- 187 H. Chen, J. Shen, K. Chen, Y. Qin, X. Lu, P. Ouyang and J. Fu, *Appl. Catal. A Gen.*, 2018, **555**, 98–107.
- 188 C. Ke, M. Li, G. Fan, L. Yang and F. Li, *Chem. - An Asian J.*, 2018, **13**, 2714–2722.
- 189 B. Siyo, M. Schneider, J. Radnik, M. M. Pohl, P. Langer and N. Steinfeldt, *Appl. Catal. A Gen.*, 2014, **478**, 107–116.
- 190 N. Mei, B. Liu, J. Zheng, K. Lv, D. Tang and Z. Zhang, *Catal. Sci. Technol.*, 2015, **5**, 3194–3202.
- 191 Z. Zhang, J. Zhen, B. Liu, K. Lv and K. Deng, *Green Chem.*, 2015, **17**, 1308–1317.
- 192 B. Siyo, M. Schneider, M. M. Pohl, P. Langer and N. Steinfeldt, *Catal. Letters*, 2014, **144**, 498–506.
- 193 B. Saha, D. Gupta, M. M. Abu-Omar, A. Modak and A. Bhaumik, *J. Catal.*, 2013, **299**, 316–320.
- 194 C. Van Nguyen, Y. Te Liao, T. C. Kang, J. E. Chen, T. Yoshikawa, Y. Nakasaka, T. Masuda and K. C. W. Wu, *Green Chem.*, 2016, **18**, 5957–5961.
- 195 X. Han, C. Li, X. Liu, Q. Xia and Y. Wang, *Green Chem.*, 2017, **19**, 996–1004.
- 196 M. Ventura, F. Nocito, E. De Giglio, S. Cometa, A. Altomare and A. Dibenedetto, *Green Chem.*, 2018, **20**, 3921–3926.
- 197 B. N. Zope, S. E. Davis and R. J. Davis, *Top. Catal.*, 2012, **55**, 24–32.
- 198 N. K. Gupta, S. Nishimura, A. Takagaki and K. Ebitani, *Green Chem.*, 2011, **13**, 824–827.
- 199 C. Ferraz, M. Zielinski, M. Pietrowski, S. Heyte, F. Dumeignil, L. M. Rossi and R. Wojcieszak, *ACS Sustain. Chem. Eng.*, 2018, **6**, 16332–16340.
- 200 C. Zhou, W. Deng, X. Wan, Q. Zhang, Y. Yang and Y. Wang, *ChemCatChem*, 2015, **7**, 2853–2863.
- 201 C. Zhou, W. Shi, X. Wan, Y. Meng, Y. Yao, Z. Guo, Y. Dai, C. Wang and Y. Yang, *Catal. Today*, 2019, **330**, 92–100.
- 202 X. Han, C. Li, Y. Guo, X. Liu, Y. Zhang and Y. Wang, *Appl. Catal. A Gen.*, 2016, **526**, 1–8.
- 203 X. Han, L. Geng, Y. Guo, R. Jia, X. Liu, Y. Zhang and Y. Wang, *Green Chem.*, 2016, **18**, 1597–1604.
- 204 S. Siankevich, G. Savoglidis, Z. Fei, G. Laurenczy, D. T. L. Alexander, N. Yan and P. J. Dyson, *J. Catal.*, 2014, **315**, 67–74.
- 205 J. Shen, H. Chen, K. Chen, Y. Qin, X. Lu, P. Ouyang and J. Fu, *Ind. Eng. Chem. Res.*, 2018, **57**, 2811–2818.
- 206 A. Villa, M. Schiavoni, S. Campisi, G. M. Veith and L. Prati, *ChemSusChem*, 2013, **6**, 609–612.
- 207 X. Wan, C. Zhou, J. Chen, W. Deng, Q. Zhang, Y. Yang and Y. Wang, *ACS Catal.*, 2014, **4**, 2175–2185.
- 208 H. Xia, J. An, M. Hong, S. Xu, L. Zhang and S. Zuo, *Catal. Today*, 2018, **319**, 113–120.
- 209 F. Neațu, R. S. Marin, M. Florea, N. Petrea, O. D. Pavel and V. I. Pârvulescu, *Appl. Catal. B Environ.*, 2016, **180**, 751–757.
- 210 D. Yan, J. Xin, Q. Zhao, K. Gao, X. Lu, G. Wang and S. Zhang, *Catal. Sci. Technol.*, 2018, **8**, 164–175.
- 211 D. Yan, J. Xin, C. Shi, X. Lu, L. Ni, G. Wang and S. Zhang, *Chem. Eng. J.*, 2017, **323**, 473–482.
- 212 K. I. Galkin, E. A. Krivodaeva, L. V. Romashov, S. S. Zalesskiy, V. V. Kachala, J. V. Burykina and V. P. Ananikov, *Angew. Chemie - Int. Ed.*, 2016, **55**, 8338–8342.
- 213 M. Kim, Y. Su, A. Fukuoka, E. J. M. Hensen and K. Nakajima, *Angew. Chemie - Int. Ed.*, 2018, **57**, 8235–8239.
- 214 M. Mascal, *ChemSusChem*, 2015, **8**, 3391–3395.
- 215 M. Mascal and E. B. Nikitin, *Green Chem.*, 2010, **12**, 370–373.
- 216 C. Laugel, B. Estrine, J. Le Bras, N. Hoffmann, S. Marinkovic and J. Muzart, *ChemCatChem*, 2014, **6**, 1195–1198.
- 217 A. I. Vicente, J. A. S. Coelho, S. P. Simeonov, H. I. Lazarova, M. D. Popova and C. A. M. Afonso, *Molecules*, 2017, **22**, 1–14.
- 218 M. Gomes, A. Gandini, A. J. D. Silvestre and B. Reis, *J. Polym. Sci. Part A Polym. Chem.*, 2011, **49**, 3759–3768.
- 219 J. J. Bozell and G. R. Petersen, *Green Chem.*, 2010, **12**, 539–554.
- 220 <https://mcgroup.co.uk/news/20131213/global-maleic>

- anhydride-consumption-registered-35-yoy-increase.html.
- 221 D. M. Alonso, S. H. Hakim, S. Zhou, W. Won, O. Hosseinaei, J. Tao, V. Garcia-Negron, A. H. Motagamwala, M. A. Mellmer, K. Huang, C. J. Houtman, N. Labbé, D. P. Harper, C. T. Maravelias, T. Runge and J. A. Dumesic, *Sci. Adv.*, 2017, **3**, e1603301.
- 222 M. L. Granados, in *Furfural: An Entry Point of Lignocellulose in Biorefineries to Produce Renewable Chemicals, Polymers, and Biofuels*, 2018, pp. 239–261.
- 223 R. Wojcieszak, F. Santarelli, S. Paul, F. Dumeignil, F. Cavani and R. V. Gonçalves, *Sustain. Chem. Process.*, 2015, **3**, 9.
- 224 N. Alonso-Fagúndez, M. Ojeda, R. Mariscal, J. L. G. Fierro and M. López Granados, *J. Catal.*, 2017, **348**, 265–275.
- 225 W. V. Nielsen, *Ind. Eng. Chem.*, 1949, **41**, 365–368.
- 226 N. A. Milas and W. L. Walsh, *J. Am. Chem. Soc.*, 1935, **57**, 1389–1393.
- 227 D. R. Kreile, V. A. Slavinskaya, M. V. Shimanskaya and E. Y. Lukevits, *Chem. Heterocycl. Compd.*, 1969, **5**, 429–430.
- 228 M. S. Murthy and K. Rajamani, *Chem. Eng. Sci.*, 1974, **29**, 601–609.
- 229 M. S. Murthy, K. Rajamani and P. Subramanian, *Chem. Eng. Sci.*, 1975, **30**, 1529.
- 230 K. Rajamani, P. Subramanian and M. S. Murthy, *Ind. Eng. Chem. Process Des. Dev.*, 1976, **15**, 232–234.
- 231 V. A. Slavinskaya, D. R. Kreile, e. E. Dzilyuma and D. e. Sile, *Chem. Heterocycl. Compd.*, 1977, **7**, 881–894.
- 232 N. A. Milas and W. L. Walsh, *J. Am. Chem. Soc.*, 1935, **57**, 1389–1393.
- 233 V. A. Slavinskaya, D. R. Kreile, e. E. Dzilyuma and D. e. Sile, *Chem. Heterocycl. Compd.*, 1978, **13**, 710–721.
- 234 N. Alonso-Fagúndez, M. L. Granados, R. Mariscal and M. Ojeda, *ChemSusChem*, 2012, **5**, 1984–1990.
- 235 X. Li, J. Ko and Y. Zhang, *ChemSusChem*, 2018, **11**, 612–618.
- 236 R. M. and M. L. G. N. Alonso-Fagúndez, *Unpubl. results*.
- 237 I. Sádaba, M. López Granados, A. Riisager and E. Taarning, *Green Chem.*, 2015, **17**, 4133–4145.
- 238 H. Guo and G. Yin, *J. Phys. Chem. C*, 2011, **115**, 17516–17522.
- 239 S. Shi, H. Guo and G. Yin, *Catal. Commun.*, 2011, **12**, 731–733.
- 240 J. Lan, Z. Chen, J. Lin and G. Yin, *Green Chem.*, 2014, **16**, 4351–4358.
- 241 X. Li, B. Ho and Y. Zhang, *Green Chem.*, 2016, **18**, 2976–2980.
- 242 G. Lv, C. Chen, B. Lu, J. Li, Y. Yang, C. Chen, T. Deng, Y. Zhu and X. Hou, *RSC Adv.*, 2016, **6**, 101277–101282.
- 243 M. Gál, T. Soták, J. Škriniarová, M. Hronec and E. Dobročka, *Catal. Letters*, 2017, **147**, 2714–2723.
- 244 Y. Huang, C. Wu, W. Yuan, Y. Xia, X. Liu, H. Yang and H. Wang, *J. Chinese Chem. Soc.*, 2017, **64**, 786–794.
- 245 G. Lv, S. Chen, H. Zhu, M. Li and Y. Yang, *J. Clean. Prod.*, 2018, **196**, 32–41.
- 246 Y. Xie, Y. Huang, C. Wu, W. Yuan, Y. Xia, X. Liu and H. Wang, *Mol. Catal.*, 2018, **452**, 20–27.
- 247 Z. Du, J. Ma, F. Wang, J. Liu and J. Xu, *Green Chem.*, 2011, **13**, 554–557.
- 248 J. Lan, J. Lin, Z. Chen and G. Yin, *ACS Catal.*, 2015, **5**, 2035–2041.
- 249 X. Li and Y. Zhang, *Green Chem.*, 2016, **18**, 643–647.
- 250 A. Tirsoaga, M. El Fergani, V. I. Parvulescu and S. M. Coman, *ACS Sustain. Chem. Eng.*, 2018, **6**, 14292–14301.
- 251 X. Kong, Y. Zhu, Z. Fang, J. A. Kozinski, I. S. Butler, L. Xu, H. Song and X. Wei, *Green Chem.*, 2018, **20**, 3657–3682.
- 252 J. R. García, L. Palmisano, E. Díaz, Z. Amghouz, G. Marci, I. Krivtsov, E. I. García-López and S. Ordóñez, *Appl. Catal. B Environ.*, 2016, **204**, 430–439.
- 253 G. Lv, C. Chen, B. Lu, J. Li, Y. Yang, T. Deng, Y. Zhu and X. Hou, *Rsc Adv.*, 2016, **6**, 101277–101282.
- 254 S. R. Kubota and K. S. Choi, *ACS Sustain. Chem. Eng.*, 2018, **6**, 9596–9600.
- 255 V. L. Mil'man and G. M. Sycheva, *Sov. Electrochem.*, 1986, **21**, 1133–1134.
- 256 V. L. Mil'man and G. M. Sycheva, *Sov. Electrochem.*, 1987, 1539–1540.
- 257 A. Takagaki, S. Nishimura and K. Ebitani, *Catal. Surv. from Asia*, 2012, **16**, 164–182.
- 258 G. F. Muzychenko, L. A. Badovskaya and V. G. Kul'nevich, *Chem. Heterocycl. Compd.*, 1972, **8**, 1311–1313.
- 259 V. V. Poskonin and L. A. Badovskaya, *Chem. Heterocycl. Compd.*, 2003, **39**, 594–597.
- 260 H. Choudhary, S. Nishimura and K. Ebitani, *Chem. Lett.*, 2012, **41**, 409–411.
- 261 H. Choudhary, S. Nishimura and K. Ebitani, *Appl. Catal. A Gen.*, 2013, **458**, 55–62.
- 262 X. Li, B. Ho, D. S. W. Lim and Y. Zhang, *Green Chem.*, 2017, **19**, 914–918.
- 263 X. Li, X. Lan and T. Wang, *Catal. Today*, 2016, **276**, 97–104.
- 264 V. Laserna, A. Heras, N. Alonso-Fagúndez, A. C. Alba-Rubio, R. Mariscal, M. L. Granados and M. Mengibar, *Catal. Today*, 2014, **234**, 285–294.
- 265 N. Araji, D. D. Madjinza, G. Chatel, A. Moores, F. Jérôme and K. De Oliveira Vigier, *Green Chem.*, 2017, **19**, 98–101.
- 266 A. S. Amarasekara and N. C. Okorie, *Catal. Commun.*, 2018, **108**, 108–112.
- 267 V. G. Kul'nevich, L. A. Badovskaya and G. F. Muzychenko, *Chem. Heterocycl. Compd.*, 1973, **6**, 535–537.
- 268 F. Saleem, P. Müller, K. Eränen, J. Warnå, D. Yu Murzin and T. Salmi, *J. Chem. Technol. Biotechnol.*, 2017, **92**, 2206–2220.
- 269 P. Maneechakr and S. Karnjanakom, *Energy Convers. Manag.*, 2017, **154**, 299–310.
- 270 W. Zhu, F. Tao, S. Chen, M. Li, Y. Yang and G. Lv, *ACS Sustain. Chem. Eng.*, 2019, **7**, 296–305.
- 271 M. Rezaei, A. Najafi Chermahini, H. A. Dabbagh, M. Saraji and A. Shahvar, *J. Environ. Chem. Eng.*, 2019, **7**, article number 102855.
- 272 B. Zhang, Y. Zhu, X. Xiang, H. Zheng, G. Ding and J. Cui, *Catal. Commun.*, 2016, **86**, 41–45.
- 273 V. V. Poskonin and L. A. Badovskaya, *Chem. Heterocycl. Compd.*, 1998, **34**, 646–650.
- 274 D. Carnevali, M. G. Rigamonti, T. Tabanelli, G. S. Patience and F. Cavani, *Appl. Catal. A Gen.*, 2018, **563**, 98–104.
- 275 N. Alonso-Fagúndez, I. Agirrezabal-Telleria, P. L. Arias, J. L. G. Fierro, R. Mariscal and M. L. Granados, *RSC Adv.*, 2014, **4**, 54960–54972.
- 276 A. C. Alba-Rubio, J. L. G. Fierro, L. León-Reina, R. Mariscal, J. A. Dumesic and M. López Granados, *Appl. Catal. B Environ.*, 2017, **202**, 269–280.
- 277 Y. Rodenas, R. Mariscal, J. L. G. Fierro, D. Martín Alonso, J. A. Dumesic and M. López Granados, *Green Chem.*, 2018, **20**, 2845–2856.
- 278 Y. Rodenas, J. L. G. Fierro, R. Mariscal, M. Retuerto and M. López Granados, *Top. Catal.*, 2019, **62**, 560–569.
- 279 US 6809895 B2, 2013.

- 280 P. Esser, B. Pohlmann and H. -D Scharf, *Angew. Chemie Int. Ed. English*, 1994, **33**, 2009–2023.
- 281 N. B. Carter, A. E. Nadany and J. B. Sweeney, *J. Chem. Soc. Perkin Trans. 1*, 2002, 2324–2342.
- 282 A. Hashem and E. Kleinpeter, in *Advances in Heterocyclic Chemistry*, 2001, vol. 81, pp. 107–165.
- 283 L. L. R. Cao, C. Liu, *Org. Prep. Proced.*, 1996, **28**, 215–216.
- 284 X. Li, X. Lan and T. Wang, *Green Chem.*, 2016, **18**, 638–642.
- 285 X. Li, W. Wan, S. Kattel, J. G. Chen and T. Wang, *J. Catal.*, 2016, **344**, 148–156.
- 286 T. Lu, Z. Huang, F. Li, G. Yuan and B. Chen, *Appl. Catal. A Gen.*, 2014, **478**, 252–258.
- 287 L. A. Badovskaya and V. V. Poskonin, *Kinet. Catal.*, 2015, **56**, 164–172.
- 288 V. V. Poskonin and L. A. Badovskaya, *Chem. Heterocycl. Compd.*, 1991, **27**, 1177–1182.
- 289 A. Gassama, C. Ernenwein and N. Hoffmann, *ChemSusChem*, 2009, **2**, 1130–1137.
- 290 I. Agirre, I. Gandarias, P. L. Arias and M. López Granados, *Biomass Convers. Biorefinery*.
- 291 K. J. J. Zeitsch, *Sugar Ser. Vol. 13, Elsevier, Netherlands*, 2001, **13**, 338–339.
- 292 C. D. Hurd, J. W. Garrett and E. N. Osborne, *J. Am. Chem. Soc.*, 1933, **55**, 1082–1084.
- 293 G. S. Chaubey, S. Das and M. K. Mahanti, *Bull. Chem. Soc. Jpn.*, 2002, **75**, 2215–2220.
- 294 T. K. Chakraborty and S. Chandrasekaran, *Synth. Commun.*, 1980, **10**, 951–956.
- 295 J. A. Moore and E. M. Partain III, *Org. Prep. Proced. Int. New J. Org. Synth.*, 1985, **17**, 203–205.
- 296 E. Dalcanale and F. Montanari, *Society*, 1986, **1**, 567–569.
- 297 P. Parpot, A. P. Bettencourt, G. Chamoulaud, K. B. Kokoh and E. M. Belgsir, *Electrochim. Acta*, 2004, **49**, 397–403.
- 298 P. Verdeguer, N. Merat and A. Gaset, *Appl. Catal. A Gen.*, 1994, **112**, 1–11.
- 299 P. Verdeguer, N. Merat, L. Rigal and A. Gaset, *J. Chem. Technol. Biotechnol.*, 1994, **61**, 97–102.
- 300 Q. Y. Tian, D. X. Shi and Y. W. Sha, *Molecules*, 2008, **13**, 948–957.
- 301 M. Douthwaite, X. Huang, S. Iqbal, P. J. Miedziank, G. L. Brett, S. A. Kondrat, J. K. Edwards, M. Sankar, D. W. Knight, D. Bethell and G. J. Hutchings, *Catal. Sci. Technol.*, 2017, **7**, 5284–5293.
- 302 N. K. Gupta, A. Fukuoka and K. Nakajima, *ACS Sustain. Chem. Eng.*, 2018, **6**, 3434–3442.
- 303 Z. Liu, X. Tong, J. Liu, S. Xue, C. Sci, Z. Liu, X. Tong, J. Liu and S. Xue, *Catal. Sci. Technol.*, 2016, **6**, 1214–1221.
- 304 T. Mallat and A. Baiker, *Chem. Rev.*, 2004, **104**, 3037–3058.
- 305 E. Taarning, I. S. Nielsen, K. Egeblad, R. Madsen and C. H. Christensen, *ChemSusChem*, 2008, **1**, 75–78.
- 306 S. Kegnæs, J. Mielby, U. V. Mentzel, T. Jensen, P. Fristrup and A. Riisager, *Chem. Commun.*, 2012, **48**, 2427–2429.
- 307 F. Pinna, A. Olivo, V. Trevisan, F. Menegazzo, M. Signoretto, M. Manzoli and F. Boccuzzi, *Catal. Today*, 2013, **203**, 196–201.
- 308 M. Signoretto, F. Menegazzo, L. Contessotto, F. Pinna, M. Manzoli and F. Boccuzzi, *Appl. Catal. B Environ.*, 2013, **129**, 287–293.
- 309 F. Menegazzo, M. Signoretto, F. Pinna, M. Manzoli, V. Aina, G. Cerrato and F. Boccuzzi, *J. Catal.*, 2014, **309**, 241–247.
- 310 C. Ampelli, K. Barbera, G. Centi, C. Genovese, G. Papanikolaou, S. Perathoner, K. J. Schouten and J. K. van der Waal, *Catal. Today*, 2016, **278**, 56–65.
- 311 M. Manzoli, F. Boccuzzi, V. Trevisan, F. Menegazzo, M. Signoretto and F. Pinna, *Appl. Catal. B Environ.*, 2010, **96**, 28–33.
- 312 M. Manzoli, F. Menegazzo, M. Signoretto, G. Cruciani and F. Pinna, *J. Catal.*, 2015, **330**, 465–473.
- 313 C. Ampelli, G. Centi, C. Genovese, G. Papanikolaou, R. Pizzi, S. Perathoner, R. J. van Putten, K. J. P. Schouten, A. C. Gluhoi and J. C. van der Waal, *Top. Catal.*, 2016, **59**, 1659–1667.
- 314 X. Wan, W. Deng, Q. Zhang and Y. Wang, *Catal. Today*, 2014, **233**, 147–154.
- 315 F. Menegazzo, M. Signoretto, T. Fantinel and M. Manzoli, *J. Chem. Technol. Biotechnol.*, 2017, **92**, 2196–2205.
- 316 F. Menegazzo, M. Signoretto, F. Pinna, M. Manzoli, V. Aina, G. Cerrato and F. Boccuzzi, *J. Catal.*, 2014, **309**, 241–247.
- 317 C. Ampelli, K. Barbera, G. Centi, C. Genovese, G. Papanikolaou, S. Perathoner, K. J. Schouten and J. K. van der Waal, *Catal. Today*, 2016, **278**, 56–65.
- 318 M. Manzoli, F. Menegazzo, M. Signoretto and D. Marchese, *Catalysts*, 2016, **6**, 107.
- 319 O. Casanova, S. Iborra and A. Corma, *J. Catal.*, 2009, **265**, 109–116.
- 320 R. Radhakrishnan, K. Kannan, S. Kumaravel and S. Thiripuranthagan, *RSC Adv.*, 2016, **6**, 45907–45922.
- 321 M. Manzoli, F. Menegazzo, M. Signoretto, G. Cruciani and F. Pinna, *J. Catal.*, 2015, **330**, 465–473.
- 322 R. Radhakrishnan, S. Thiripuranthagan, A. Devarajan, S. Kumaravel, E. Erusappan and K. Kannan, *Appl. Catal. A Gen.*, 2017, **545**, 33–43.
- 323 N. Huo, H. Ma, X. Wang, T. T. T. Wang, G. Wang, T. T. T. Wang, L. Hou, J. Gao and J. Xu, *Cuihua Xuebao/Chinese J. Catal.*, 2017, **38**, 1148–1154.
- 324 N. Huo, H. Ma, X. Wang, T. Wang, G. Wang, T. Wang, L. Hou, J. Gao and J. Xu, *Chinese J. Catal.*, 2017, **38**, 1148–1154.
- 325 L. Ning, S. Liao, X. Liu, P. Guo, Z. Zhang, H. Zhang and X. Tong, *J. Catal.*, 2018, **364**, 1–13.
- 326 X. Tong, Z. Liu, L. Yu and Y. Li, *Chem. Commun.*, 2015, **51**, 3674–3677.
- 327 X. Tong, Z. Liu, J. Hu and S. Liao, *Appl. Catal. A Gen.*, 2016, **510**, 196–203.
- 328 L. Yu, S. Liao, L. Ning, S. Xue, Z. Liu and X. Tong, *ACS Sustain. Chem. Eng.*, 2016, **4**, 1894–1898.
- 329 X. Tong, L. Yu, X. Luo, X. Zhuang, S. Liao and S. Xue, *Catal. Today*, 2017, **298**, 175–180.
- 330 H. Cui, X. Tong, L. Yu, M. Zhang, Y. Yan and X. Zhuang, *Catal. Today*, 2019, **319**, 100–104.
- 331 S. W. Fitzpatrick, in *ACS Symposium Series*, 2006, vol. 921, pp. 271–287.
- 332 D. Hayes, *Optimal Use of DIBANET Feedstocks and Technologies*, 2013.
- 333 J. Matías, A. Gil, V. López, L. Arribas and C. González, in *23rd European Biomass Conference and Exhibition*, Viena, 2015, pp. 1–3.
- 334 F. D. Pileidis and M.-M. Titirici, *ChemSusChem*, 2016, **9**, 562–582.
- 335 R. Saladino, T. Pagliaccia, D. S. Argyropoulos and C. Crestini, in *Materials, Chemicals, and Energy from Forest Biomass*, ed. D. S. (North C. S. U. Argyropoulos, American Chemical Society, 2007, pp. 262–279.
- 336 R. C. P. Cubbon and C. Hewlett, *J. Chem. Soc. C Org.*, 1968,



- 2983–2986.
- 337 B. V. Timokhin, V. A. Baransky and G. D. Eliseeva, *Russ. Chem. Rev.*, 1999, **68**, 73–84.
- 338 J. J. Bozell and G. R. Petersen, *Green Chem.*, 2010, **12**, 539–554.
- 339 C. Delhomme, D. Weuster-Botz and F. E. Kühn, *Green Chem.*, 2009, **11**, 13–26.
- 340 H. Almqvist, C. Pateraki, M. Alexandri, A. Koutinas and G. Lidén, *J. Ind. Microbiol. Biotechnol.*, 2016, **43**, 1117–1130.
- 341 US 2676186, 1954.
- 342 WO 2012/044168 A1, 2012.
- 343 I. Podolean, V. Kuncser, N. Gheorghe, D. MacOvei, V. I. Parvulescu and S. M. Coman, *Green Chem.*, 2013, **15**, 3077–3082.
- 344 F. Xia, Z. Du, J. Liu, Y. Ma and J. Xu, *RSC Adv.*, 2016, **6**, 72744–72749.
- 345 S. Dutta, L. Wu and M. Mascal, *Green Chem.*, 2015, **17**, 2335–2338.
- 346 D. Carnevali, M. G. Rigamonti, T. Tabanelli, G. S. Patience and F. Cavani, *Appl. Catal. A Gen.*, 2018, **563**, 98–104.
- 347 J. Liu, Z. Du, T. Lu and J. Xu, *ChemSusChem*, 2013, **6**, 2255–2258.
- 348 Y. Wang, F. Vogelgsang and Y. Román-Leshkov, *ChemCatChem*, 2015, **7**, 916–920.
- 349 A. Chatzidimitriou and J. Q. Bond, *Green Chem.*, 2015, **17**, 4367–4376.
- 350 Y. Gong, L. Lin and Z. Yan, *BioResources*, 2011, **6**, 686–699.
- 351 L. Wu, S. Dutta and M. Mascal, *ChemSusChem*, 2015, **8**, 1167–1169.
- 352 US2018/0029980, 2018.
- 353 M. J. Fink and M. D. Mihovilovic, *Chem. Commun.*, 2015, **51**, 2874–2877.
- 354 J. Cai, J. Zhu, L. Zuo, Y. Fu and J. Shen, *Catal. Commun.*, 2018, **110**, 93–96.
- 355 V. Thakur, S. Kumar and P. Das, *Catal. Sci. Technol.*, 2017, **7**, 3692–3697.
- 356 R. Zhu, A. Chatzidimitriou and J. Q. Bond, *J. Catal.*, 2018, **359**, 171–183.
- 357 Y. Gong, L. Lin, J. Shi and S. Liu, *Molecules*, 2010, **15**, 7946–7960.
- 358 Y. Gong and L. Lin, *Molecules*, 2011, **16**, 2714–2725.
- 359 C. Della Pina, E. Falletta and M. Rossi, *Green Chem.*, 2011, **13**, 1624.